UNIVERSITY COLLEGE LONDON

System Modelling and Optimisation Studies of Fuel Cell Based micro-CHP for Residential Energy Demand Reduction

Alexandros Adam

A thesis submitted in fulfillment of the degree of
Doctor of Philosophy

Department of Chemical Engineering

Declaration of Authorship

I, Alexandros Adam confirm that the work presented in this thesis is my own. Where information has been derived from other sources, I confirm that this has been indicated in the thesis.

Signed:

_____

Date:

_____

Acknowledgements

I would like to express my deepest gratitude for the help and guidance received by my supervisors Prof. Eric S. Fraga and Prof. Dan J.L Brett throughout my PhD: Eric for introducing me to the amazing world of mathematical modelling but especially for his approach of analysing situations. Dan for sharing his in depth knowledge of the theory of fuel cells and for all the fun times in the Christmas parties.

There is a number of people that I would like to thank that helped me in various ways. Maria-Christina, who is always close to me, encouraging me and supporting my decisions. My parents Michalis and Anna for providing the continuous support over the years of my studies. Also thank you to the people in the PPSE room, Cristian, Asif, Shade for having great times in and outside the office.

I would also like to thank Elisabeth Ness, a former Crest Nicholson employee, for the interest she showed in my work. She happily organised a site visit for me to witness a fuel cell micro-CHP system in operation in a Crest Nicholson test site in Epsom.

Finally, I would like to express my graditute to Georgios Mantas, a mathematics teacher who was an inspirational figure to me during my school times.

This research was made possible by EPSRC support for the London-Loughborough Centre for Doctoral Research in Energy Demand, grant number EP/H009612/1 and EPSRC funding support of the Electrochemical Innovation Lab via EP/G030995/1 and EP/I037024/1.

Abstract

Fuel cell combined heat and power (CHP) units used for domestic applications can provide significant cost and environmental benefits for end users and contribute to the UK's 2050 emissions target by reducing primary energy consumption in dwellings.

Recently there has been increased research interest in the use of modelling methods for the design of such systems and their smoother integration with domestic building services. Several models in the literature, whether they use a simulation or an optimisation approach, ignore the dwelling side of the system and optimise the efficiency or delivered power of the unit. However the design of the building services is linked to the choice of heating plant and its characteristics.

Adding the dwelling's energy demand and temperature constraints in a model can produce more general results that can optimise the whole system, not only the micro-CHP unit. The fuel cell has a number of heat streams that can be utilised to satisfy heat demand in a dwelling and the design can be different according to the heat used from each heat stream.

Firstly a mixed integer non-linear (MINLP) programming mathematical model was developed to provide all high level information for the design and sizing the plant of each configuration examined. Next, a MINLP model that can handle multiple heat sources and demands is presented. The model can provide a design that integrates the temperature and water flow constraints of a dwelling's heating system with the heat streams within the fuel cell processes while optimising total CO_2 emissions. The model is demonstrated through different case studies that attempt to capture the variability of the housing stock.

This research represents a significant step towards an integrated fuel cell micro-CHP and dwelling design.

Contents

List of Figures

List of Tables

Symbols

Model 1

This section presents the symbols used in the model presented in Chapter 6.

Indices	**Description**	**Units**
t (1...T)	Time Step	
j (fc,gb)	Plant type for model	
k (heat,ele)	Energy demand type for model	
p (1...n)	Breakpoints for linearisation	
Parameters		
Q_k^{req}(t)	Energy Demand at Timestep t	kW
ra	Fuel Cell Ramp Up Rate	kW/sec
f_g	Natural Gas Emission Factor	kg/kWh
f_e	Grid Electricity Emission Factor	Kg/kWh
cp	Specific Heat Capacity of Water	kJ/KgK
ϱ	Water Density	kg/m^3
T^{env}	Environment Temperature	^{o}C
Variables		
P_j	Maximum capacity of plant j	kW
$r_j(t)$	Load factor of plant	-
$Q_{j,k}(t)$	Energy Output k from plant j	kW
Q^{stout}(t)	Heat from TST to demand	kW
$\eta_{j,k}(t)$	Efficiency k of plant j	%
$E^g(t)$	Grid electricity input	kW
$E^{st}(t)$	Heat stored in TST	kJ

V^{st}	TST Volume	m^3
M^{fc}	CO_2 emissions caused by fuel cell	kg
M^{gb}	CO_2 emissions caused by gas boiler	kg
M^{el}	CO_2 emissions caused by grid electricity	kg
z	Total CO_2 emissions	kg

Binary Variables

$y_j(t)$	1 if plant j is on, 0 otherwise	-
$y_p(t)$	1 if interval $\left[\xi^p, \xi^{p+1}\right]$is activated	-

Model 2

This section presents the symbols used in the model presented in Chapter 7 .

Indices	**Description**	**Units**
s (CH_4, H_2, CO_2)	Species	-
t (1,...,288)	Timestep	-
g (h,l)	FC Heat Exchanger (FC Cooling Circuit or Afterburner)	-
j (Heat,dhw,sto,ele)	Type of Energy Demand	-
p (sup,ret)	Supply or Return position on pipework	-

Parameters

Q_j^{req}(t)	Dwelling Energy Demand	kW
T^{env}	Environment Reference Temperature	°C
E^{th}	Theoretical fuel cell voltage	V
ra	Fuel cell ramp up	kW/sec
q^{ref}	Heat required for the reforming process	kJ/mol
i_{H2}	Electrical current of fuel cell from hydrogen flow	kAsec/mol
MW^s	Molecular Weight of species s	kg/mol
HHV^s	Higher Heating Value of species s	kJ/mol
cp	Specific Heat Capacity of Water	kJ/kgK
f_e	Emissions factor for electricity grid	kg/kWh
n^{gb}	Boiler Efficiency	-

A_j^{gb}	Boiler Maximum Heat Output per demand j	kW
A_{gj}^{fc}	Fuel cell Maximum Heat Output per demand j per heat exchanger g	kW
B_j^{st}	Temperature constraint for demand j	°C
δt	Timestep	sec
Variables		-
$n_s^{fc}(t)$	Molar Flow Rate of species s in fuel cell at time t	mol/sec
$m_s^{fc}(t)$	Mass Flow Rate of species s in fuel cell at time t	mol/sec
$n_s^{gb}(t)$	Molar Flow rate of species s in gas boiler at time t	mol/sec
$m_s^{gb}(t)$	Mass Flow rate of species s in gas boiler at time t	mol/sec
V^{st}	Storage Tank Volume	m^3
$V^c(t)$	Fuel cell Voltage at time t	V
$U^{fc}(t)$	Hydrogen Utilisation at time t Factor	-
$FT_{p,j}(t)$	System Temperature at flow p, demand j at time t	°C
$T^{gb}(t)$	Boiler Temperature at time t	°C
$T_g(t)$	Heat Exchanger Temperature at grade g at time t	°C
$T^{st}(t)$	TST Temperature at time t	°C
$E^g(t)$	Grid Electricity	kW
$E^{fc}(t)$	Fuel Cell Electrical Output at time t	kW
$E^{exp}(t)$	Exported Electricity to the grid at time t	kW
$Q_j^{gb}(t)$	Boiler Output at time t and demand j	kW
$r^{gb}(t)$	Load factor of Gas Boiler	-
P^{gb}	Maximum capacity of Gas Boiler	kW
$Q_{g,j}(t)$	Fuel cell heat output of g heat	kW

	exchanger at time t and demand j	
$E^{st}(t)$	Heat stored in TST	kJ
$Q_j^{stout}(t)$	TST Heat Output at time t and demand j	kW
$Q^{bur}(t)$	Heat generated from hydrogen combustion at time t	kW
$Q^{ref}(t)$	Heat required for reforming at time t	kW
$m_j^{total}(t)$	Total System Water Flow rate at time t and demand j	kg/sec
$m_j^{stout}(t)$	TST Water Flow rate at time t and demand j	kg/sec
$m_j^{gb}(t)$	Boiler Flow rate at time t and demand j	kg/sec
$m_{gj}(t)$	Flow rate at fuel cell grade g at time t and demand j	kg/sec
M^{fc}	CO_2 emissions caused by fuel cell	kg
M^{gb}	CO_2 emissions caused by gas boiler	kg
M^{el}	CO_2 emissions caused by grid electricity	kg
M^{exp}	CO_2 emissions savings by exporting electricity to the grid	kg
z	Total CO_2emissions	kg
Binary Variables		
$y_j^s(t)$	1 if temperature constraint is activated for demand j, 0 otherwise	-
$y_{gj}(t)$	1 if fuel cell heat source g releases heat to demand j, 0 otherwise	-
$y_j^{gb}(t)$	1 if gas boiler releases heat to demand j, 0 otherwise	-
$y_j^{stout}(t)$	1 if TST releases heat to demand j, 0 otherwise	-

Chapter 1

Introduction

1.1 Introduction to the Project

Energy and environment are becoming key matters in the modern world. As world's population is increasing, cities are growing larger and energy demand is rising. The International Energy Outlook 2013 predicts that worldwide consumption of energy will rise 56% by 2040, a demand which will be caused primarily by developing countries [121]. As fossil fuels reserves are depleting and nuclear power imposes a safety risk, a sustainable way of producing energy is required to ensure that the predicted increase in energy demand can be satisfied.

Energy consumption in buildings is about 45% of total energy in the UK and contributes significantly to climate change [45]. Energy efficient technologies for microgeneration can reduce CO_2 emissions and satisfy energy demand in buildings. Renewable technologies that have been used in buildings include PVs, solar thermal panels, small scale wind turbines, ground source heat pumps, biomass boilers and others. A technology that is suitable for dwelling applications and has seen significant development in the recent years is Combined Heat and Power.

Combined Heat and Power (CHP) is the use of a single process to generate both electricity and heat. Cogeneration allows for primary energy savings to be made as the production of electricity (from power plants) and heat (from boilers) is separate. Many technologies can be used as prime movers for CHP systems such as internal combustion engines, micro-turbines and fuel cells. The EU and the UK government

consider CHP as an important technology: the potential of installing CHP in buildings is assessed in the EU Directive on the Energy performance of buildings, where it is stated that for any building above 1000 m^2 there is a requirement for the designers to evaluate the potential of installing a CHP system [60].

Energy demand in dwellings is usually covered by grid electricity and boilers. However, micro-CHP systems based on fuel cells can serve domestic demand efficiently. Fuel cells have higher electrical efficiencies than heat engines and different power to hear ratio. Fuel cell micro-CHPs can be an efficient way of satisfying residential energy demand on the basis that cost targets can be met. It can improve energy security and contribute towards reduced peak electricity demandsas energy will be generated and used locally [75]. The design of fuel cell based micro-CHP systems is a complicated problem as various subcomponents are involved that need to work together to meet energy demand efficiently. Residential energy demand fluctuates on a day by day and seasonal basis. Similarly the fuel cell has operational constraints such as longer start up times compared to conventional systems or specific ramp up rates. It is therefore crucial to determine the control method of the fuel cell micro-CHP to satisfy building energy demands.

1.2 Project Motivation

The aim of this PhD project is to investigate the environmental and technical benefits by optimising the design of a fuel cell based micro-CHP for dwelling microgeneration. A holistic approach is used in the process considering the energy source and demand as part of one wider system. The focus is to identify ways of integration of the fuel cell micro-CHP system with the building energy system. This is achieved by combining building energy modelling and implementing mathematical models to apply optimisation techniques. A variety of models have been developed as part of the project, some simple and some more complex. The modelling procedure investigates ways that fuel cell micro-CHPs can be integrated into dwellings. The existing building stock comprises of various energy systems, so this will identify which parameters are important when designing fuel cell micro-CHP systems and how energy savings can be achieved. The project aims to expand the understanding of building services and fuel cell micro-CHP design and operation, propose new methods to improve the integration of fuel cell micro-CHPs in dwellings to increase efficiency and reduce total energy demand.

1.3 Outline of the Thesis

The rest of the thesis is divided in 7 chapters. Chapter 2 introduces the context of the project, the basics of fuel cells and dwelling energy demand.

Chapter 3 discusses the body of literature and previous work in fuel cell micro-CHP, environmental assessment and design optimisation. An overview of the different methods, models and techniques is presented.

Chapter 4 discusses the heat recovery choices in a fuel cell and the potential for integration with building services. It addresses the point that multiple heat streams are available in a fuel cell and discusses the need for an optimisation tool that can maximise the utilisation of these streams in a domestic environment.

Chapter 5 presents the reference buildings against which the designs produced by the models will be compared to. The reference buildings are modelled with building modelling software and are served by conventional heating and electricity systems.

Chapter 6 describes the development of a mixed integer non-linear programming (MINLP) model for determining sizing and operational characteristics of a fuel cell micro-CHP. The model uses efficiency equations to describe plant operation and the results provided by the model can be used for the evaluation of proposed designs. Three case studies are presented in this chapter that illustrate the application of the model on different weather data.

In Chapter 7 a MINLP model is presented that integrates the design of a fuel cell micro-CHP along with the design of the building services in a dwelling. It is systematic design tool that can expand the understanding for fuel cell micro-CHP systems in houses by offering better knowledge of the temperature constraints in the plant-dwelling system. Four case studies are presented in this chapter examining different scenarios.

Finally, Chapter 8 summarises the main contributions of the thesis and provides suggestions for future work.

Chapter 2

Background

2.1 Overview of the UK Energy System

A short overview of the context of the project will help identify the drivers behind it. It will also show the relation of the presented work to the big picture of climate change and building energy demand.

In terms of primary energy the UK minimised energy imports following the development of the North Sea oil and natural gas reserves in the 70s and became an exporter of energy in the beginning of the 80s. By the end of the millennium, the UK became one of largest producers of natural gas in the world and exported oil. The production of gas and oil from the North Sea reserves peaked at the end of the previous millenium and then started declining, so the UK became an importer of energy in 2004. Figure 2.1.1 illustrates the production and consumption of primary fuels in 2013, whereas figure 2.1.2 shows the total energy consumption by fuel from 1970 to 2013. It can be seen that natural gas and petroleum fuels account for the largest proportion of fuel consumption in the UK. The depletion of oil and gas reserves in the North Sea therefore raises an energy security issue which additionally to climate change forces the UK to find alternative ways for energy generation [44] .

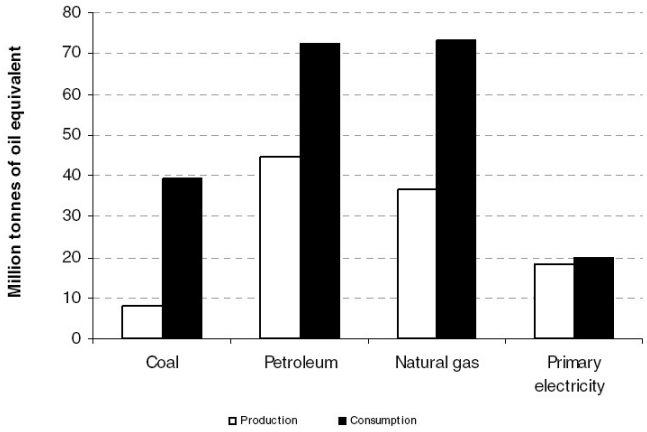

Figure 2.1.1: Production and Consumption of Primary Fuels in the UK in 2013 ([48])

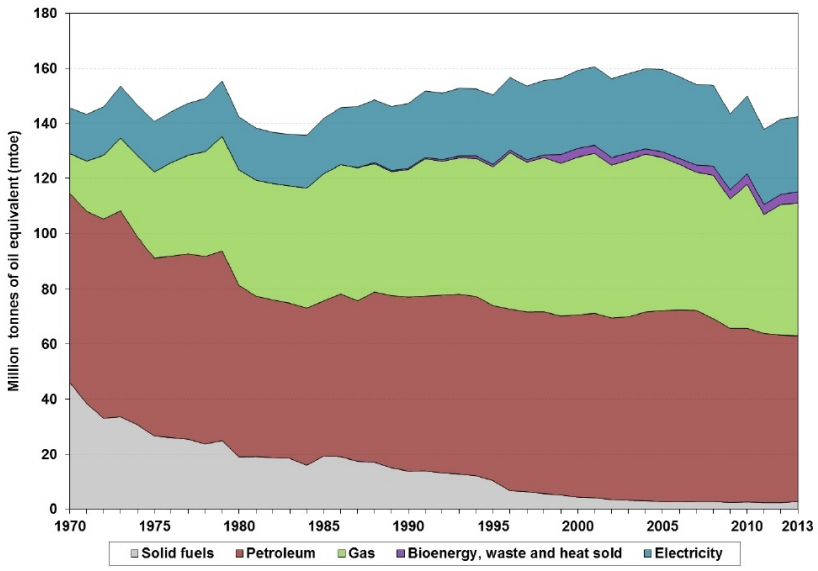

Figure 2.1.2: Energy Consumption by fuel in the UK from 1970 to 2013 ([49])

The Sankey diagram in Figure 2.1.3 shows the UK Energy system in 2013. From the diagram it can be seen that the domestic energy consumption is responsible for approximately 30% of the total UK energy consumption.

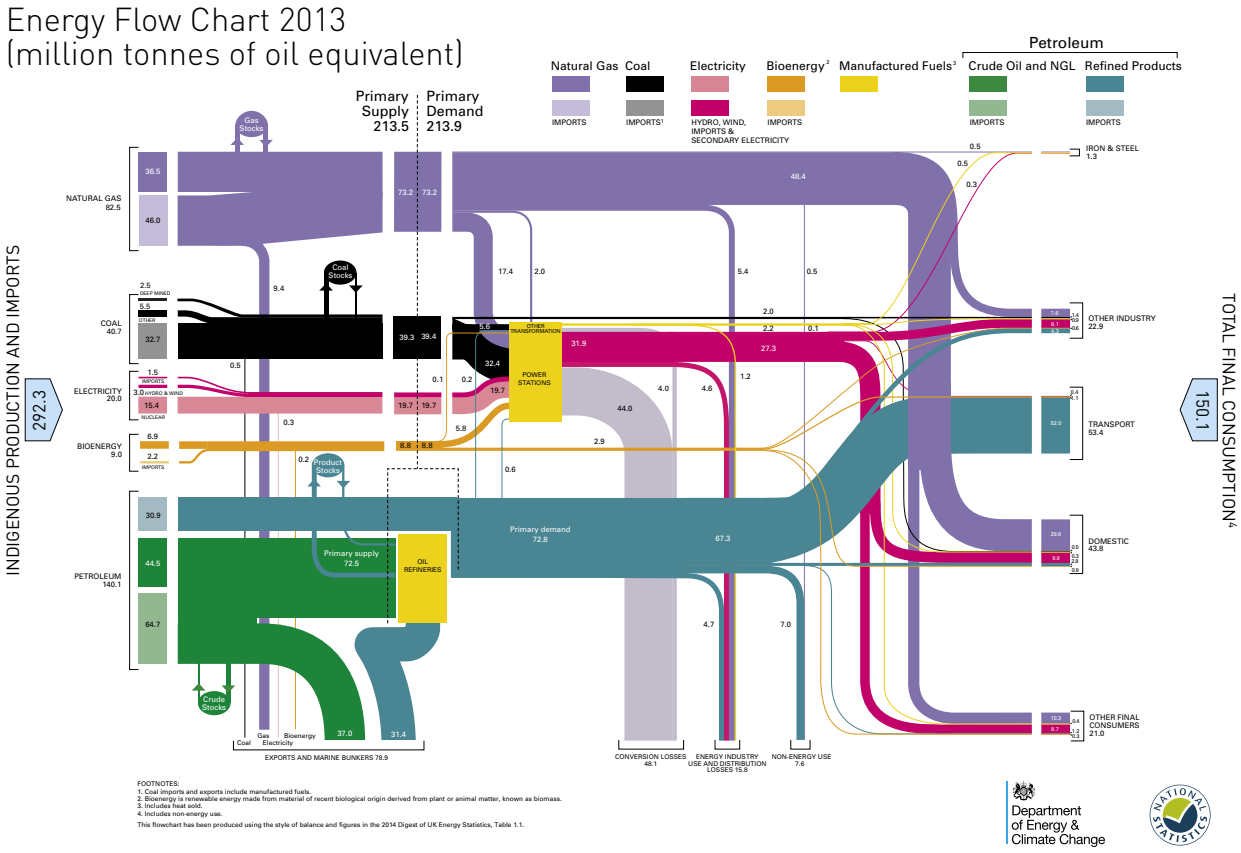

Figure 2.1.3: Sankey Diagram of UK Energy System in 2013 ([43])

UK energy policy concentrates on energy security as the country is now importing the majority of its energy. The priorities of the energy policy are to achieve the EU target of 20% reduction of the UK's energy consumption by 2020. This EU target is described in the European Commission's Emissions Trading System (EU ETS) and was first introduced by Directive 2003/87/EC [61]. The UK has also introduced a more optimistic target which has been implemented into the legislation as the Climate Change Act 2008 and is an 80% reduction in CO_2 emissions from 1990 levels by 2050 [82] . This will be achieved by implementing the measures defined within the EU Energy Efficiency Action Plan in the following sectors: transport, improved efficiency of equipment, changing citizens' energy behaviour, technology and energy savings in buildings [59].

2.2 Household Energy Demand

Household energy consumption was around a third of the final energy consumption in the UK in 2010. This is an increase of approximately 30% and 20% compared to the 1970 and 1990 levels respectively. Some of this increase has been caused by the additional UK households constructed in this period and the increase in the population since 1990. The main fuel in dwellings has also drastically changed since the 70s when the primary fuel was coal, followed by natural gas; In 2010 coal represented only 1% of the total household energy consumption whereas natural gas covered the majority (69%) [49]. The fuel mix of residential buildings since 1970 is represented in Figure 2.2.1.

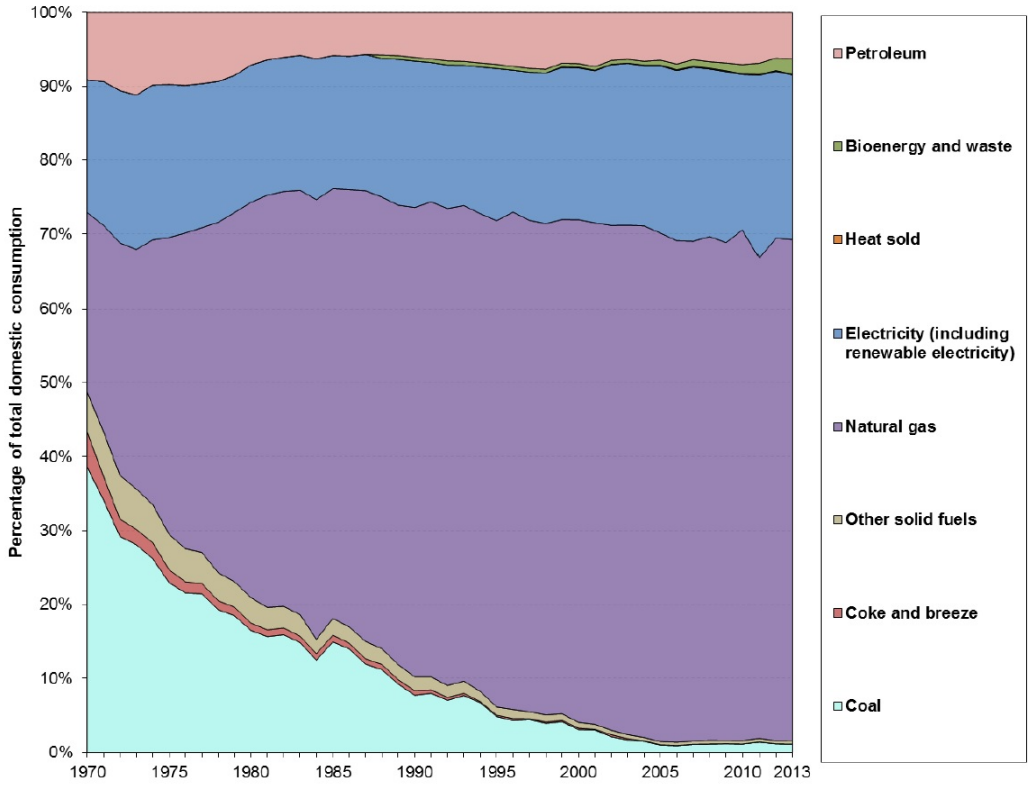

Figure 2.2.1: UK Domestic sector fuel mixture ([46])

Energy in domestic buildings is used primarily for space heating, domestic hot water (DHW), lighting, appliances and cooking. From 2007 the amount of energy consumed for lighting and appliances has increased significantly as it can be seen in Figure 2.2.2. The reduction of the total space heating energy that occurs since, can be justified by the introduction of energy efficiency measures in buildings and the increase in energy prices which led to a reduction in heating hours.

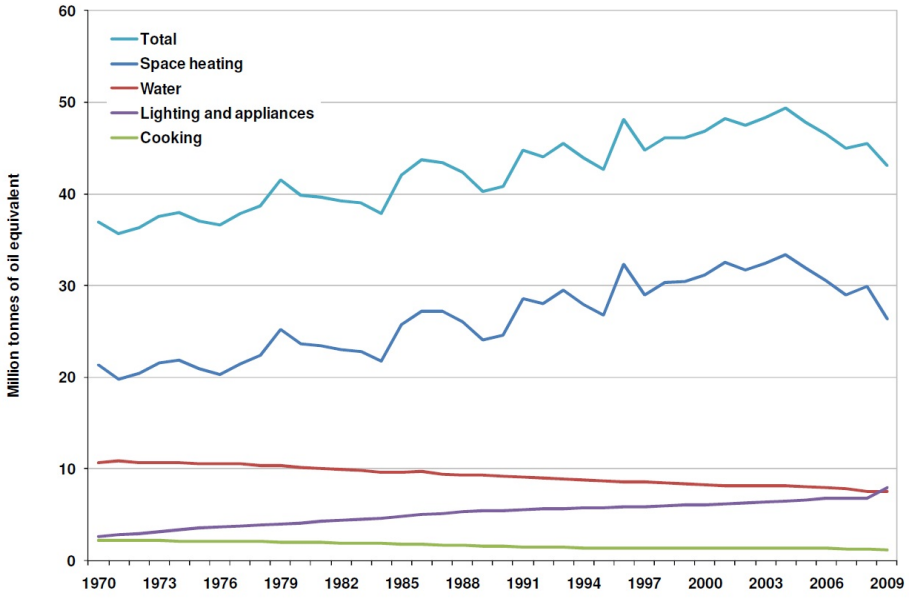

Figure 2.2.2: UK domestic final energy consumption by end user since 1970 ([46])

2.2.1 Energy Assessment of Buildings

The building energy policy is based on the European Energy Performance of Buildings Directive (EPBD) which has now been integrated into the UK legislation [60]. Building Regulations define the required energy efficiency standards for space heating and domestic hot water systems. All new buildings and buildings under refurbishment should comply with Building Regulations Part L in terms of their overall CO_2 emissions [81]. The document sets limiting targets for U values of all structural elements and air permeability values for the whole building. At the same time information is given on equipment efficiencies. The method of calculating total energy and CO_2 emissions proposed in Part L is the National Calculation Method (NCM). It suggests that for complying with the Building Regulations the annual energy consumption of a building should be compared with the energy consumption of a reference building.

The Standard Assessment Procedure (SAP) is a methodology that identifies compliance with building regulations and its latest version was published in 2012 [26, 27]. SAP is a methodology for the evaluation of the energy performance of buildings and works on estimates of energy consumption for all services of a dwelling such as space heating, domestic hot water, lighting and ventilation.

Another relevant document that should be read in conjunction with Building Reg-

ulations Part L is the Domestic Heating Compliance Guide (DHCG). The DHCG provides information on the various equipment that can be used in household heating and DHW, together with information on limiting seasonal efficiencies [83].

2.3 Domestic Micro-CHP

Micro-generation refers to systems suitable to generate energy at a small scale for use in domestic or small commercial properties. EU's Co-generation directive defines micro-generation as any system that generates electricity below 50 kWe [62]. In the UK however micro-generation is limited to 3 kW electrical and 20 kW thermal output [72]. Micro-generation can be broadly categorised in the following:

1. Micro-CHP technologies
2. Photovoltaics, solar thermal and wind turbines
3. Heating using biomass boilers or heat pumps.

A CHP system comprises of a prime mover, a power generator and a heat exchanger that recovers heat from the exhaust gases. A simplified diagram of the process is shown in Figure 2.3.1. CHP systems can capture the heat that in conventional plants is wasted and therefore they can achieve efficiency of up to 85% compared with 40-45% of conventional plants. In these systems, efficiency is defined as the sum of useful heat and power generated to the chemical energy of the input fuel.

CHP systems can use several technologies for driving the electrical power generator. In micro-CHP systems these technologies could be internal combustion engines, fuel cells, Stirling engines and others.

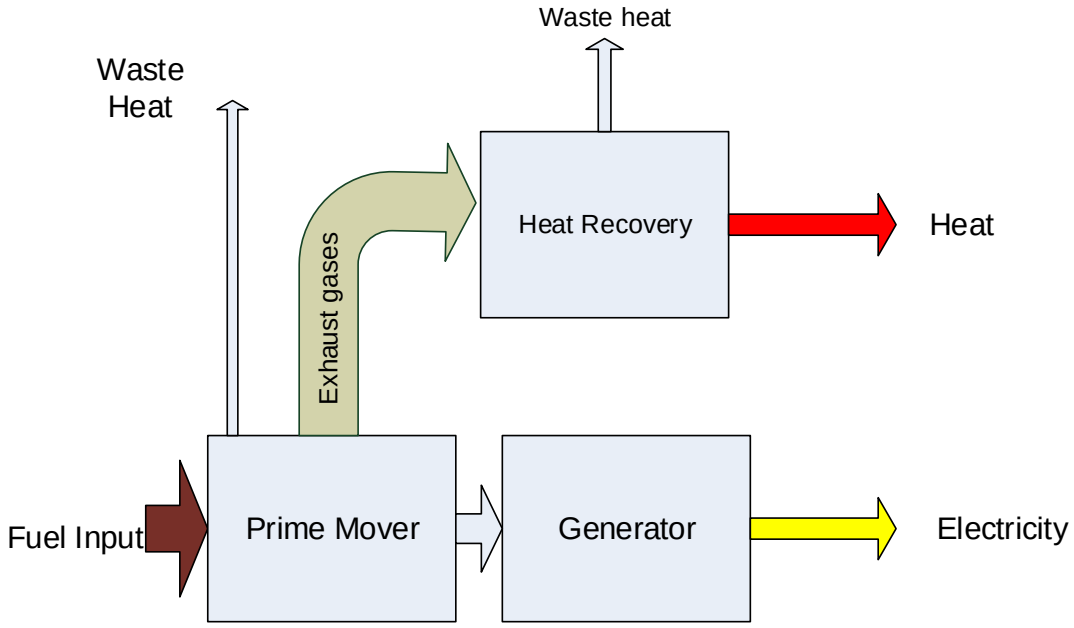

Figure 2.3.1: Simplified diagram of a CHP system showing energy flows

2.4 Fuel Cell Technology

2.4.1 Overview of Fuel Cell Technologies

The fuel cell generates electrical power using hydrogen supplied on the anode and oxygen on the cathode, which react within an electrolyte layer. Hydrogen on the anode splits into a proton and an electron. The proton travels via the electrolyte to bond with the electrons (which travel on an external circuit) and oxygen to form water.

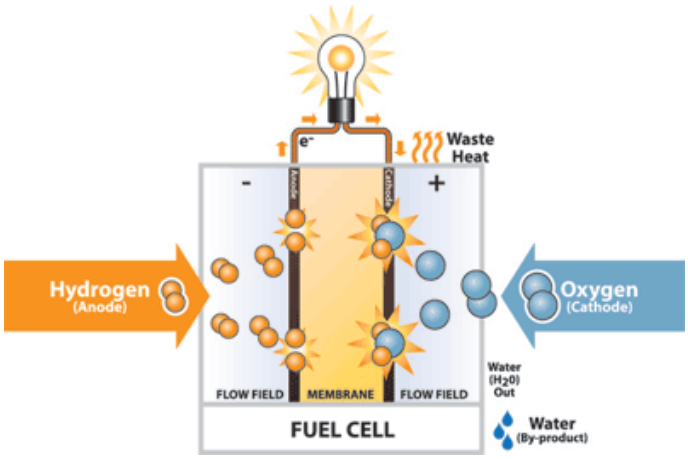

Figure 2.4.1: Fuel Cell Basic Operation ([65])

The overall fuel cell reaction is:

$$2H_2 + O_2 \rightarrow 2H_2O \tag{2.4.1}$$

There are different types of fuel cells categorised by their electrolyte. The most important are:

- Phosphoric Acid Fuels Cells (PAFC)
- Molten Carbonate Fuel Cells (MCFC)
- Proton Exchange Membrane Fuel Cell (PEMFC)
- Solid Oxide Fuel Cells (SOFC)
- Alkaline Fuel Cells (AFC) .

A comparison between the different types of fuel cells can be seen in the next table:

Table 2.1: Comparison of Fuel Cell Technologies ([122])

	PEMFC	**PAFC**	**MCFC**	**SOFC**
Charge Carrier	H^+ions	H^+ions	$CO_3^=$ions	$O^=$ions
Electrolyte	Polymeric membrane	Phosphoric acid solutions	Phosphoric acid (immobilised liquid)	Solid ceramic, Yttria stabilised zirconia
Construction	Plastic, metal or Carbon	Carbon, porous ceramics	High temperature metals, porous ceramic	Ceramic, high temperature metals
Oxidant	Air or O_2	Air or or O_2enriched air	Air	Air
Fuel	Hydrocarbons or methanol	Hydrocarbons or alcohols	Hydrogen, natural gas, propane	Natural gas or propane
Temperature	65-85 ^{o}C	150-200 ^{o}C	600-700 ^{o}C	700-1000 ^{o}C
Electrical Efficiency	25-35 %	35-45 %	40-50 %	45-55 %
Contaminants	CO, sulfur	CO, sulfur	sulfur	sulfur

SOFC and PEMFC have received more attention than the other types and there are many commercially available products for various stationary or mobile applications [10, 51, 122] .

2.4.2 Fuel Cell Operation

The open circuit voltage (OCV) of a fuel cell is given by the following equation:

$$E_{ocv} = \frac{-\Delta g}{2F} \tag{2.4.2}$$

where Δg is the Gibbs free energy and F the Faraday constant. This represents a "no losses" voltage and in practise is never achieved due to three main losses:

Activation Losses

Activation losses are related to the speed of the reactions on the surface of the electrodes that move the electrons to or from the anode. These losses can be

calculated using the Tafel equation:

$$\Delta V_{\text{act}} = \frac{RT}{2aF} \ln\left(\frac{i}{i_o}\right) \tag{2.4.3}$$

where a is a constant called the charge transfer coefficient. Its value depends on the reaction and the material of the electrode. For the hydrogen electrode, its value is about 0.5. For the oxygen electrode the charge transfer coefficient is between 0.1 and 0.5. i_o is called the exchange current density and is responsible for the control of the performance of the electrode. T is the temperature, R is the gas constant and i is the current density [89].

Ohmic Losses

This voltage drop is caused by the resistance to the flow of electrons through the material of the electrodes and is proportional to current density. The ohmic losses are given by equation (2.4.4)

$$\Delta V_{\text{ohm}} = ir \tag{2.4.4}$$

where r is the area-specific resistance.

Mass Transport or Concentration Losses

These result from the change in concentration of the reactants at the surface of the electrodes as the fuel is used. The voltage drop due to concentration losses is given by equation 2.4.5.

$$\Delta V_{\text{con}} = -\frac{RT}{2F} \ln\left(1 - \frac{i}{i_1}\right) \tag{2.4.5}$$

Overall the voltage is given by subtracting all the losses from the OCV:

$$V = E_{ocv} - \Delta V_{act} - \Delta V_{ohm} - \Delta V_{con} \tag{2.4.6}$$

All the above equations provide an understanding of the processes that take place in the fuel cell and their effect on voltage. Figure 2.4.2 shows the relation of voltage against the current density while figure 2.4.3 shows the power against current density for a PEMFC fuel cell using average values for the parameters for each section of the losses. In Figure 2.4.2 the area below the polarisation curve represents the useful electrical work that the fuel cell can deliver and the area between the curve and the

open circuit voltage represents the thermal losses, part of which can be utilised from a CHP unit.

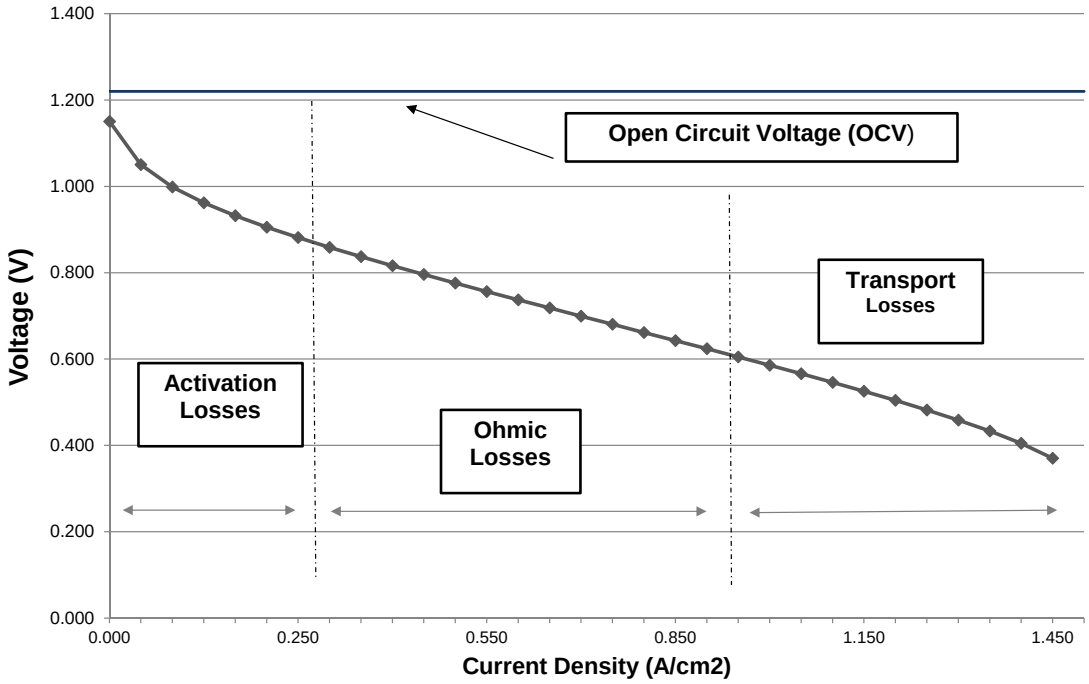

Figure 2.4.2: Graph showing the voltage of an average PEMFC fuel cell against the current density, illustrating the energy losses that occur

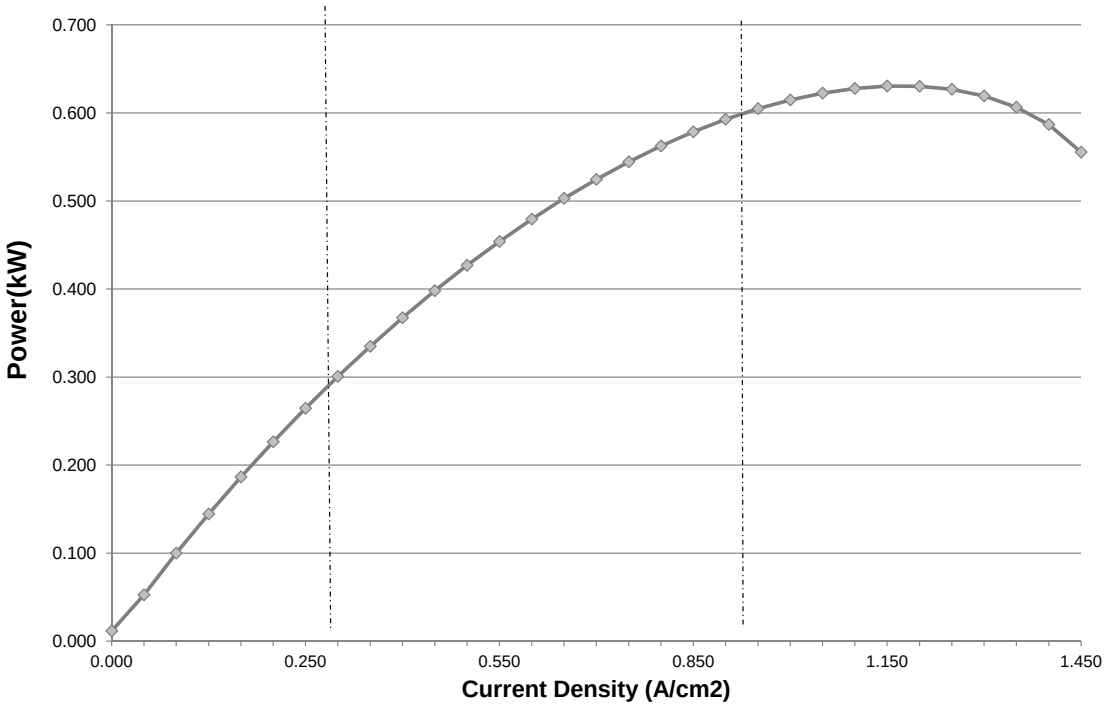

Figure 2.4.3: Graph showing the power output of an average PEMFC fuel cell against the current density

2.4.3 Fuel Cell Efficiency

Figure 2.4.4 illustrates the electrical, thermal and total efficiency of a fuel cell in relation to the the load factor, which is defined as the ratio of the electricity output to the maximum rated capacity [73]. The electrical efficiency represents the ratio of the DC power output of the fuel cell over the chemical energy contained in the fuel. The heat than can be recovered by the cooling medium over the energy in the fuel represents the thermal efficiency, while the sum of the two provides the total fuel cell efficiency. These graphs were generated from fitted data from various efficiencies at different load factors using the SOFC-CHP model developed by Hawkes et al. [73].

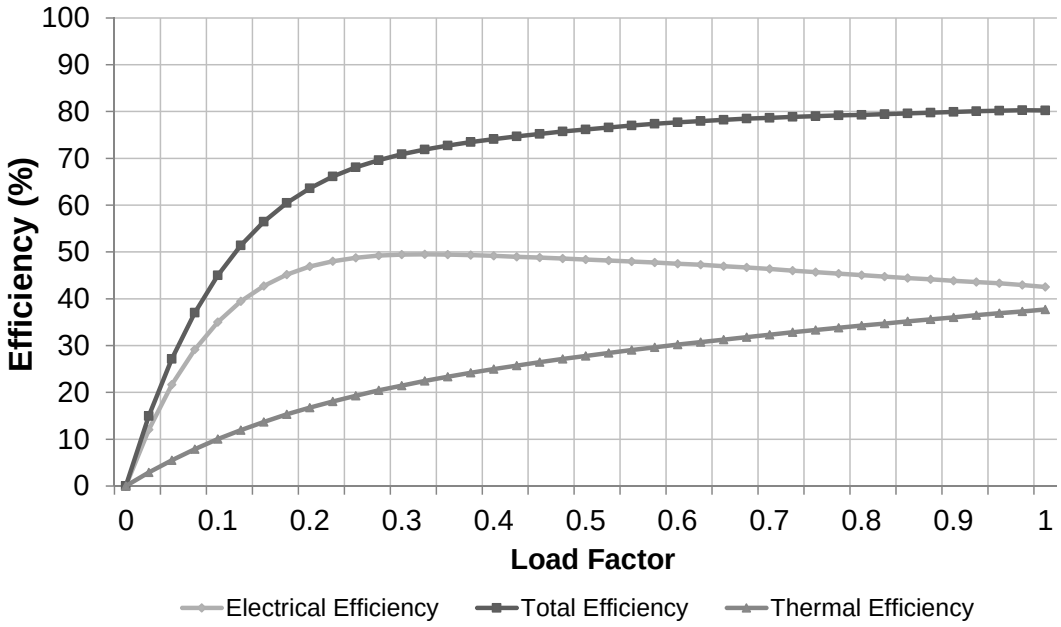

Figure 2.4.4: Graph showing the electrical, thermal and total efficiency of an SOFC in relation to the load factor [73]

2.5 Fuel cell micro-CHP system design

A fuel cell micro-CHP comprises of many process systems that work in conjunction with the fuel cell in order to effectively utilise the energy in the fuel input, convert it to heat and power and deliver it to the load. The typical components of a fuel cell micro-CHP are:

- a reformer to convert natural gas into hydrogen rich fuel mix.
- a desulfuriser to remove the various impurities of the fuel mix such as sulphur compounds which can be harmful to fuel cells.
- power conditioning such as transformers and inverters, to convert current from DC to AC and to transform the voltage to the required levels.
- a heat management system to remove heat from the stack and distribute it to the other process units of the system.
- a water management system to control the flow of water from the system.

- a control system to regulate fuel input, power output and operation.

An example of a fuel cell micro-CHP with all the components and interconnections is shown in Figure 2.5.1.

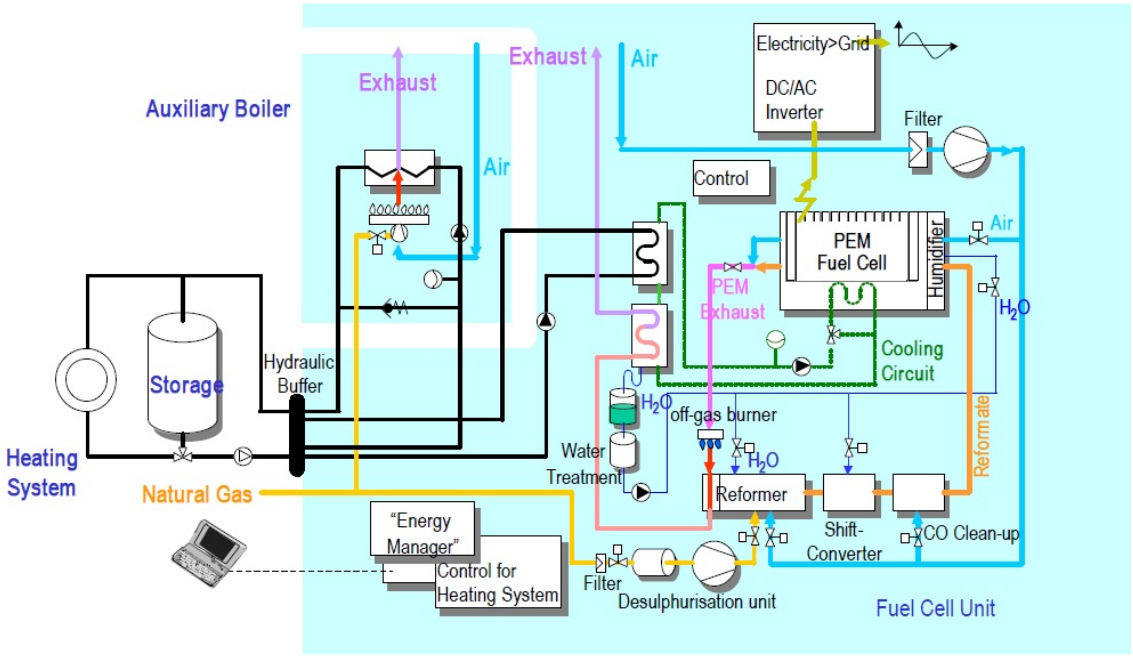

Figure 2.5.1: Schematic Diagram of fuel cell micro-CHP components ([125])

2.5.1 Fuel Processing

Hydrogen does not exist in nature as a fuel, therefore the use of carbon-based fuels such as natural gas is necessary. This requires the use of a reformer which provides a supply of hydrogen rich gas from the fuel source. The operating temperature of the fuel cell determines whether the reformer is internal or external. For the reformer to be internal, the operating temperature of the stack must be high. SOFCs operate at a high temperature and therefore reform internally avoiding the need of additional subsystems external to the fuel cell stack. However, a pre-reformer is sometimes used in medium temperature SOFCs.

The two main methods of reforming are endothermic steam reforming (SR) and exothermic partial oxidation reaction (POX). In the case of steam reforming, the fuel is combined with steam to produce CO and H_2 by vaporisation at high temperature. The methane steam reforming reaction is shown below:

$$CH_4 + H_2O \rightarrow CO + 3H_2 \tag{2.5.1}$$

$$[\Delta \text{H} = 206 \text{ kJ mol}^{-1}]$$

In the exothermic partial oxidation reaction, hydrocarbons and oxygen combine to form CO and H_2.The methane partial oxidation reaction is shown below:

$$CH_4 + \frac{1}{2}O_2 \rightarrow CO + 2H_2 \tag{2.5.2}$$

$$[\Delta \text{H} = -247 \text{ kJ mol}^{-1}]$$

The subsequent CO generated by either process is converted into CO2 with the addition of water in a water-gas shift reaction. The gas shift reaction is shown below:

$$CO + H_2O \rightarrow CO_2 + H_2 \tag{2.5.3}$$

$$[\Delta \text{H} = \text{-41 kJ mol}^{-1}]$$

Natural gas reforming is endothermic, so heat needs to be supplied to the reformer at high temperature for a reasonable conversion rate to be achieved.

2.5.2 Electricity Conditioning

The fuel cell produces DC electricity which must be converted to AC. The use of inverters is therefore necessary. Transformers are also used to obtain the required voltage. In domestic systems, the electricity is converted to a single phase AC voltage. In addition, current, voltage and frequency are controlled to ensure the quality of electricity is maintained [89, 103, 128].

2.5.3 Heat Management

In order to use heat within the fuel cell micro-CHP, a management system is required that can capture and exchange heat through heat exchangers. Heat utilisation and management in fuel cell micro-CHP is discussed in detail in Chapter 4.

2.5.4 Controls

Fuel cells micro-CHPs are complex systems, so in order to perform well, a control system must be in place. The fact that so many process units operate together as one system makes the control of a micro-CHP a complicated task. A control system includes valves, actuators and control units. SOFC fuel cells have long start up times mainly due to their high operating temperature. Degradation of fuel cell's performance over time can affect the projected lifetime of a micro-CHP system and affect the investment in the technology. An appropriate control strategy can minimise the effects of stack degradation [88, 92, 118, 129, 131].

2.6 Fuel cell micro-CHP Products

In terms of product availability, there are many manufacturers that produce fuel cell units for various applications and sizes, and a number of them produce packaged fuel cell micro-CHP units that can be installed in domestic properties. Companies such as Ceramic Fuel Cells, BG MicroGen, EcoPower, WhispeGen, Sulzer Hexis and Baxi are producing micro-CHP systems of various technologies and capacities. Japan and generally Asia is a developed fuel cell market with strong government support. The global sales market share for the Asian region exceeds 60% and reaches $1.5 billion [66, 120]. Japan is active on production of fuel cell products with Kyocera, TOTO and Nippon Oil developing micro-CHP systems around the 1 kWe capacity group [51].

Ceramic Fuel Cells has developed a fuel cell micro-CHP product named BlueGen. It is based on a solid oxide fuel cell system with a heat to power ratio of 0.5 kWth to 1 kWe, aiming to achieve a high electrical efficiency. An image of the BlueGen unit is shown in Figure 2.6.1a [34].

Sulzer Hexis produces the Galileo 1000N system which is based on a SOFC and generates 1 kW of electrical power and 2 kW of heat [113]. The unit includes an integrated 20 kW gas fired condensing boiler which can be used to cover heating and DHW when the fuel cell thermal output is not sufficient. An image of the unit is shown in Figure 2.6.1b.

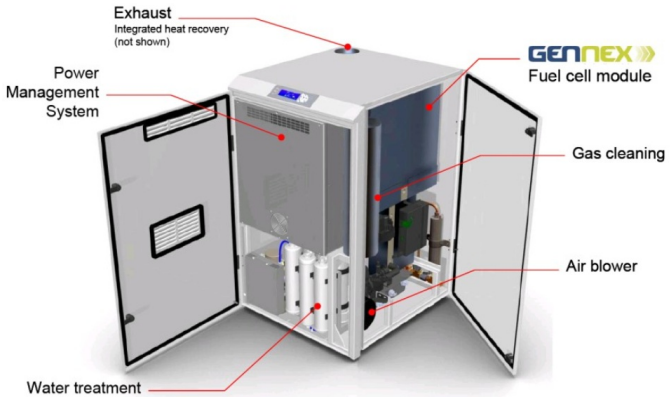

(a) Ceramic Fuel Cells Blue Gen micro-CHP unit [34]

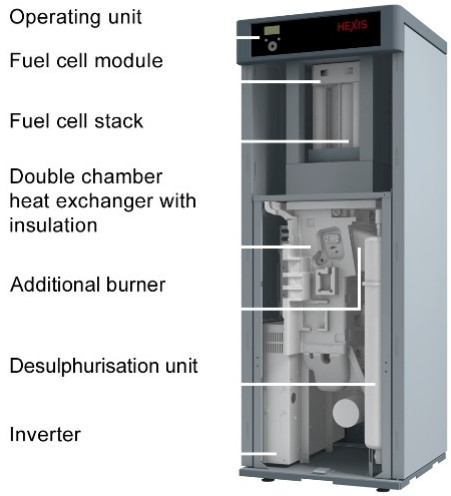

(b) Sulzer Hexis Galileo 1000N micro-CHP unit [113]

Figure 2.6.1: Images of fuel cell micro-CHP products [34, 113]

2.7 Fuel cell micro-CHP Cost

Despite the environmental benefits of fuel cell micro-CHPs, their future in the micro-generation market depends on costs and payback periods. Although more and more fuel cell based micro-CHP products become available and the capital cost is slowly reducing, generally the capital cost compared to engine based micro-CHPs is still higher. From discussions with Ceramic Fuel Cells in 2013 it was obtained that the price for their 1.5 kW BlueGen unit is £20,000. In 2010, the company sold 30 BlueGen units to the Australian Government for £30,000 per unit, a cost which can be decreased further with increased production [35]. The capital cost estimates

by the Environmental Protection Agency (EPA) for CHPs with larger capacities are shown in Table 2.2 [78]. These values are only for fuel cell stacks and are not representative of the total micro-CHP where the cost per kWe is higher but give an indication.

Table 2.2: Fuel Cell CHP 2014 cost estimates (source [78])

Installed System Costs	**System 1-PEMFC**	**System 2-SOFC**	**System 3-MCFC**
Nominal Capacity (kW)	0.7	1.5	300
Total Plant Cost ($/kW)	22,000	23,000	10,000

A report released from Imperial College in 2012 gives information on sale prices of current micro-CHP systems [110]. Indicative prices reproduced from that report are shown in Table 2.3. The average price as of 2012 varies between $25,000-30,000 per kWe.

Table 2.3: CHP 2012 cost estimates (source [110])

System	**Technology**	**Electrical Capacity (kW)**	**Year Price was Set**	**Price (USD)**
Eneos	PEMFC	0.7	2011	$21,800
Panasonic	PEMFC	1.0	2009	$28,800
Kyocera	SOFC	0.7	2012	$22,200

As there is no clear indication of the actual capital cost of fuel cell micro-CHPs many researchers have researched the problem, calculating a realistic capital cost for these systems in order to present a good investment for homeowners. Staffel et al. estimated the cost target for a 1 kWe fuel cell at £280-500 per kW in order to compare with boiler technologies [111]. This is far from the current range of costs and until high production rates can be reached, such low prices are difficult to be achieved. A study that investigated the requirements for high market penetration of various micro-CHP technologies concluded that low capital and fuel cost prices would allow micro-CHPs with low heat-to-power ratio, such as fuel cell based units, to increase their market share [115]. A possible way for this is by government incentives and change in policy [51].

2.8 Policy and Field Trials

The policy with regard to micro-generation is outlined in the "Micro-generation Strategy" of the Department of Energy and Climate Change (DECC) in 2011 [47]. The purpose of the document is to attract investments in micro-generation by introducing support schemes such as the Feed-in-Tariff (FIT) and the Renewable Heat Incentive (RHI) which reward financially every kWh of energy generated from renewables or micro-CHPs. Technologies such as fuel cells are also featured in the document. The document concludes that the most suitable buildings for such technology have to be determined. At the same time micro-CHP systems have to be established as flexible enough systems to satisfy the variable heat loads of buildings. Heat storage is also mentioned in the document and is considered a method that combined with CHP units can reduce CO_2 emissions.

Carbon Trust's report titled "Micro CHP Accelerator" demonstrates the benefits of micro-CHP field trials [32]. The programme included the installation of 87 micro-CHP units based on internal combustion and Stirling engines in domestic and commercial applications in the UK. The report presents the energy and cost savings in the field trials and concludes that the economics of micro-CHP systems can be improved further by increasing the electrical efficiency of the systems. According to the report the micro-CHP - household system would perform better if the electrical efficiency of the prime mover was higher and the electricity production similar to heat production. In addition, the report claims that with optimised controls, the carbon savings by domestic micro-CHP systems could potentially be higher. The trials did not include any fuel cell micro-CHPs as the commercially available products at the period the project started were limited. However, based on the heat-to-power characteristics and higher electrical efficiency, fuel cell based micro-CHPs may be more effective over other micro-CHP technologies which are based on thermal engines in terms of the potential to reduce energy consumption in buildings. Despite the beneficial technical characteristics of fuel cells, there has been small interest by manufacturers in developing fuel cell micro-CHPs compared to engine based technologies. The Energy Saving Trust places the fuel cell micro-CHP as an emerging technology in the energy market and suggests that this is due to the reason that the cost per kW of fuel cell is still much greater compared to established technologies such as the Stirling or internal combustion engines [56].

Ene.field [54] is a fuel cell micro-CHP trial programme that runs in 11 countries in Europe and aims to install up to 1,000 systems. The programme is supported by several European micro-CHP manufacturers and the data will be used to influence

policy support by demonstrating the cost and environmental benefits of the technology. However the reports [55] available on the programme's website do not present any results from the field trials suggesting that performance data of installed fuel cell micro-CHPs are not yet available.

Ceramic Fuel Cells together with Crest Nicholson, a UK contractor, has installed a BlueGen 1.5 kWe unit in a four-bedroom family home in Epsom, Surrey. The building that the fuel cell micro-CHP unit is installed in, is a high insulation home with very low space heating demand. The BlueGen can then provide all the heat demand of the house without a need for an auxiliary boiler [40]. Following the installation there are no subsequent reports from the contractor or the manufacturer on the environmental or cost benefits of this installation. This is to add to the overall lack of data from the field with regard to fuel cell micro-CHP installations.

2.9 Thermal Comfort and Heating Systems

Buildings require heating to maintain comfortable conditions for the occupants. Thermal comfort varies between different people depending on their health, age, metabolic rate, clothing and other environmental factors such as temperature and humidity. Engineers that design heating systems work on a common reference when conducting their design calculations: the internal design temperature. Table 2.4 shows the recommended by CIBSE internal design temperature for UK houses [37].

Table 2.4: Recommended internal design temperatures for dwellings in the UK as recommended by CIBSE ([37])

Room	**Temperature (°C)**
bathrooms	20–22
bedroom	17–19
hall/stairs/landing	19-24
kitchen	17-19
living rooms	20-23
toilets	19-21

Different building types and locations will have different requirements and constraints for heating systems. The main elements of any heating system design are [30, 36, 80, 102]:

- a heat source. This is usually a conventional gas or oil boiler. However

other sources of heat could be heat pumps [109], micro-CHP systems and solar thermal panels.

- a heat distribution system. Heat could be delivered using water or air. A pipe or a duct network is commonly used. In the case of a pipe network, this is called a Low Temperature Hot Water (LTHW) pipe network and uses water at temperatures in the range of 30-90 °C.

- a heat emitter. The radiator is the most popular heat emitter in UK houses. A temperature difference (ΔT) of around 10 °C which sometimes can be extended to 20 °C is maintained between the water temperature in the supply and return pipework. Underfloor heating despite being a more costly system is more efficient than radiators because of the lower operating temperature (30-50 °C). Figure 2.9.1 shows a radiator and an underfloor heating system. Figure 2.9.3 shows a common system design used in dwellings with a separate hot water tank.

- a control system that ensures that the heat source is operated at the correct output level. This usually requires a central controller with space temperature reading via a thermostat and in some cases secondary control on the heat emitters such as thermostatic radiator valves (TRV).

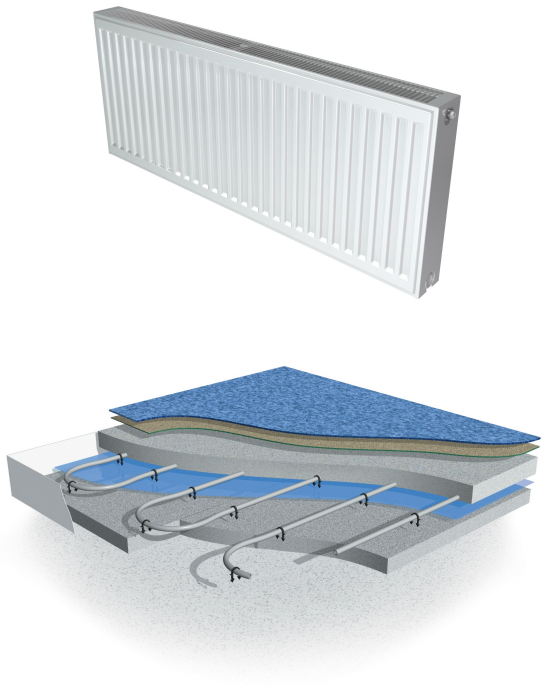

Figure 2.9.1: Images of Radiator and Underfloor Heating System ([112],[124])

There are many design configurations: one option is the use of a gas fired combination boiler (combi) which can generate heating and DHW directly. Water is heated directly from the mains water supply eliminating the need for a water storage cylinder. An alternative option for DHW is the use of an indirect system with a hot water cylinder where hot water is generated indirectly from a heating coil which is connected to the boiler's heating pipework. For domestic applications the capacity of the hot water cylinder varies between 75-250 L, with a minimum recommended of 115 L per dwelling [30], depending on the number of occupants and number of hot water outlets. Other configurations include two individual gas fired units, one for generating space heating and one gas fired heater to generate hot water. Details on applications of these different designs is given in Table 2.5. Cogeneration for domestic applications is analysed in detail in the following chapters so it is not mentioned here.

Simplified schematics of the first two configurations are shown in Figures 2.9.2 and 2.9.3 [39, 79].

Table 2.5: Comparison of common heating services design configurations. ([36, 38, 96])

System	Details	Applications
Gas Fired Combi Boiler	Single combi boiler that generates hot water for space heating and DHW	Individual Flats, Small Houses
Gas Fired Boiler with DHW tank	Single or multiple boilers which serve heating and one indirectly heated hot water cylinder for DHW	Individual Flats, Central Heating
Gas Fired Boiler and Electric DHW	Single boiler which serves space heating and electric water heaters installed locally on DHW outlets	Individual Flats
Electric Space Heating and Electric DHW	Electric heat emitters and electric water heaters installed locally on DHW outlets	Remote Applications where gas or oil supply is not available
Individual Gas Fired Boiler and and Gas Fired Water Heater	Single Gas boiler serves only space heating and separate gas fired water heater serves DHW	Central Heating, Large Applications

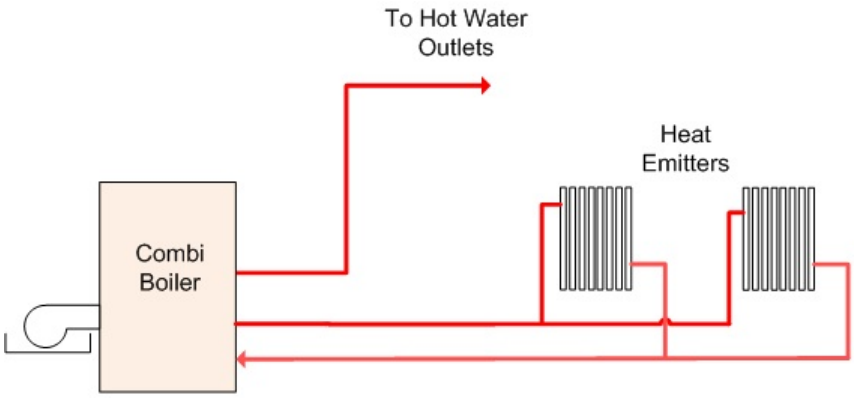

Figure 2.9.2: Simplified Schematic of Combi Boiler

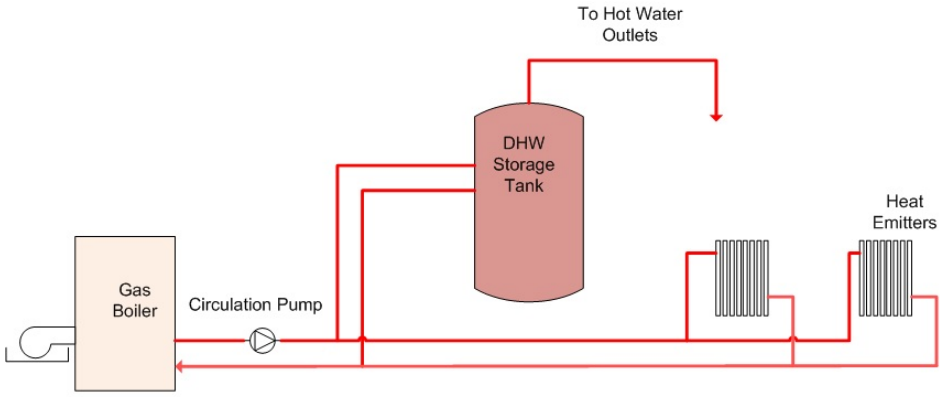

Figure 2.9.3: Simplified Schematic of Gas Fired Boiler and DHW Storage Tank

In some designs, a low loss header is included. A header allows for circuits of different temperatures and flow rates to be connected to central plant via the header, ensuring that correct flow to central plant is maintained. A manufacturer's low loss header installation manual suggests that "...the low-loss header acts as hydraulic break, decoupling boiler and system circuits from each other." [123].

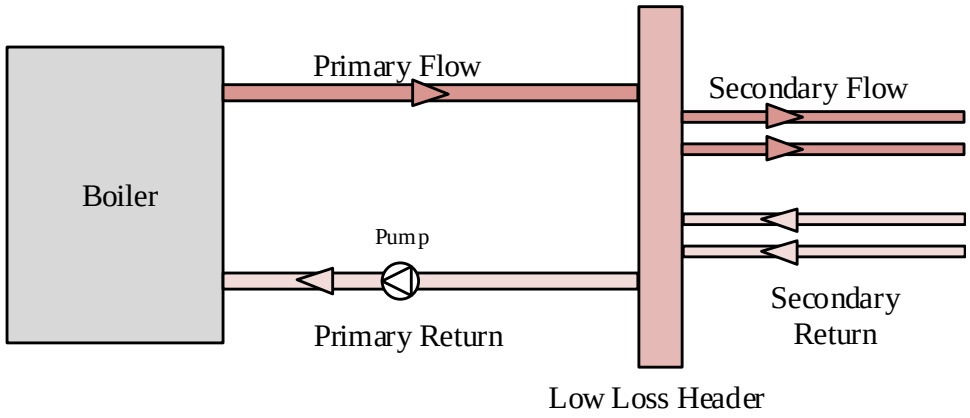

Figure 2.9.4: Schematic showing the operation of a low loss header illustrating primary and secondary circuits [2].

Chapter 3

Previous Work

3.1 Modelling Fuel Cell micro-CHPs for domestic applications

As field data have been limited, many researchers have developed models to predict the performance of fuel cell micro-CHPs in dwellings [13, 15, 16, 21, 52, 70]. The use of models to examine various scenarios is natural as fuel cell micro-CHPs are an emerging and not an established technology. However, the potential benefits of fuel cells and the increasing number of available products increase interest in modelling fuel cells for micro-generation [9]. Usually researchers estimate energy savings or cost reduction from the use of fuel cell systems. Some researchers use simulation methods to evaluate different scenarios: simulation can identify values for a specific characteristic of the system under examination over a period of time. Researchers also develop optimisation models of systems and use them to identify optimal values for their chosen design variables in relation to an objective function [7, 8, 10]. Optimisation can provide useful results as the fuel cell micro-CHPs and their design is currently under development, so optimisation techniques can identify ways of improving it. Many studies based on single objective optimisation have chosen total cost as the design objective. Techno-economic studies can identify trade-offs between different characteristics such as cost and efficiency or electrical power [74]. Hawkes et al., in a two-part report, calculated the additional capital cost for a fuel cell micro-CHP system compared to a conventional heating system and the impact of degradation of the fuel cell stack on the performance of the system [75, 76].

3.1.1 Modelling Processes and Methods

In the review of current fuel cell micro-CHP models in literature there were found two approaches:

Firstly, detailed fuel cell and sub-component models which may include thermodynamics and electrochemical kinetics or other characteristics but neglect the building that the fuel cell micro-CHP will be installed into and its energy demand. The main goal is usually the calculation or maximisation of the electrical efficiency or the power delivered by the fuel cell. Studies that have selected this approach are included in references [13, 20, 97].

Arsalis et al. have developed a model for a residential micro-CHP system based on a PEMFC. The system covers electricity, DHW and space heating for a home in Denmark. A detailed fuel cell micro-CHP system is modelled . However the "house" side of the system with its varying electrical and heating demand profiles is not equally considered but has been simplified into three time periods: winter, summer, and spring (autumn) [13]. Palazzi et al. have implemented a techno-economic model of a SOFC micro-CHP. They formulated the model as an MINLP problem assigning different fuel processing options to binary variables. Their model can identify the optimum solutions for system efficiency and specific investment cost [97].

Secondly, there are fuel cell micro-CHP models which consider the interaction of the energy plant with the building and its energy characteristics. Usually each researcher would define a "typical house" that will be determine the energy demand; a definition which varies from study to study. They often use real data taken from field studies or use Building Modelling Software to generate their own. The most popular software for building modelling is TRNSYS, ESP-R, IES and TAS [58, 87, 116, 119]. In some cases researchers obtain data of energy demand from actual or simulated dwellings and use them to determine the capacities and operating patterns of fuel cell systems. These models describe the system more accurately without only focusing on the fuel cell system. Studies that have followed this approach are included in [21, 73, 95].

Hawkes et al. in order to investigate the impact of the house demand profile, examined patterns of heat demand that favour SOFC based micro-CHP. They looked at different heat demand profiles for a UK dwelling with their model and performed a techno-economic analysis. A similar study was performed by Barelli et al. who developed a residential micro-CHP model consisting of the fuel cell, the required balance of plant and an auxiliary hot water boiler. The purpose of the study was the evaluation of the performance of fuel cell based CHP systems under variable electrical and thermal loads. Oh et al. performed an economic analysis of a sys-

tem which has its capital cost covered by government funding. They performed an optimisation study for a 1 kW PEMFC micro-CHP system achieving up to 20% savings in the operational cost of the PEMFC-based CHP system, when the installation is covered by the government [95]. Other researchers have applied their models to systems located in other climates where heat demand is different and cooling might also be required. Ashari et al. presented a techno-economic study of a PEMFC fuel cell power CHP system designed for a residential building located in Tehran. They looked at the variation of the operating conditions of the system in relation to the electricity cost [16].

Studies that use dwelling data together with fuel cell micro-CHPs sometimes also investigate policy requirements that would allow the fuel cell micro-CHP market to grow. Pellegrino et al. investigated the technical and policy aspects of the fuel cell micro-CHP residential market, evaluating combinations of plant and operating modes together with various support schemes. They concluded that dwellings with high energy consumption would benefit more from support schemes such as the feed-in tariff [99].

Another trend among researchers seems to be the comparative analysis of various micro-CHP technologies suitable for domestic applications. They usually examine the feasibility of technologies which are already available in the market for micro-generation in dwellings. Publications on this topic are included in references [19, 77, 117].

The coupling of thermal storage tanks (TST) with micro-CHP plants is a common approach, so many researchers have modelled such systems. Most studies identify the optimum size of the storage tank for diffrent cases and constraints. The constraints vary and could be space or cost limitations. Publications that focus on the effect of thermal storage are included in references [17], [24], [106].

Other researchers have also looked at the effects of plant capacity and control methods on system performance [64, 69]. A study that moves one step forward in terms of the involvement of the dwelling side of the fuel cell micro-CHP system was conducted by Gandiglio et al. [68]. They have modelled a 1 kWe PEMFC based micro-CHP system together with the balance of plant, coupled with an underfloor heating system. However, even though the heating system is considered, no system sizing is attempted as the study is based on a 1 kWe fuel cell unit.

Some studies are based around the attempt of integration of different plant and equipment that can be used with a micro-CHP system. Such studies can be found in references [98, 100, 101, 114].

A review paper that provides useful information on fuel cell and optimisation has been prepared by Ang et al. [10]. It reviews the modelling advances in fuel cell systems and is not limited to stationary micro-CHP applications. It also looks at the models that have been developed for portable, stationary and transportation applications using fuel cells.

3.1.2 Modelling Results

The main conclusions arising from performing a literature review in the field of fuel cell micro-CHP modelling are the following:

- A building with a lower heating than electricity demand would be better suited to a fuel cell micro-CHP system because of its low heat-to-power ratio. Additionally, houses with large energy demands favour such systems as they allow the fuel cell micro-CHP to operate for longer periods without its energy output being limited by low demand. Hawkes et al. in [73] found that SOFC micro-CHP is more suitable to heat emiters that are slower in response and therefore have to be constantly on during the winter period. Thermal energy storage becomes more useful when the heating demand follows very high peaks compared to the base load.

- Fuel Cell micro-CHPs are still costly, so support schemes implemented through government policy are essential for them to be an attractive option for micro-generation [95].

- Thermal storage increases the operating hours of fuel cell micro-CHP systems as it enables the excess heat to be stored when thermal demand is low [73]. This reduces the operating cost and increases the environmental benefits of the investment.

- A different "typical dwelling" exists in many studies which leads to different modelling results. This is expected as there is no clear definition of a "typical" house.

- Optimisation studies focus primarily on identifying design parameters within the fuel cell CHP boundary itself that minimise cost or energy but there is limited information on heat integration between the fuel cell and the house services design. The main challenge in process design lies in identifying how the various processes are interlinked to affect the heat quality and amount of energy production. There is a link between the type of fuel cell chosen in the

design, its heat output and how it can be efficiently applied into a dwelling's heat distribution system.

As so little available data exist of installed fuel cell micro-CHP systems -except from data from the field trials-, it is possible that the modelling results gathered from current literature carry some assumptions that could be unrealistic. When the fuel cell market evolves and more fuel cell micro-CHPs are installed, the collective experience and knowledge from installations and monitoring of such systems, would make these models more robust.

3.1.3 Concluding remarks

As seen in the literature review, fuel cell micro-CHP modelling has been and remains a focus for many researchers around the world. Different methods and techniques were proposed to model fuel cell systems. However in most studies the design of the heating system that the fuel cell micro-CHP would be pluged into is not considered in the models. The water mass flow rates and temperatures in the heating and DHW pipework determine this design. This design involves understanding of LTHW systems and imposes limitations on sizing, control and operation of the selected plant. The influence of components ranging from the balance of plant to the pipe network could be considered in designing and optimising a fuel cell micro-CHP system for residential applications. Adding information of heating system design with water flow rates and temperatures into a fuel micro-CHP model is something that has not been done before and could broaden the understanding of the process of integrating fuel cell micro-CHPs in dwellings.

Chapter 4

Options for Residential Building Services Design Using Fuel Cell Based Micro-CHP

Fuel cell micro-CHP design in dwellings requires that heat demand is satisfied by harvesting heat from various sources within the fuel cell micro-CHP while at same time satisfying the temperature constraints of the heat emitters. Therefore a balance has to be established between the energy source and the demand, which can be identified using modelling tools.

Part of the work presented in this chapter has been published in [2].

4.1 The potential for integration with building services

Fuel cells would displace more energy and avoid operational problems when they limit their start up circles and operate at their maximum output. Heat emitters choice (i.e. radiators or underfloor heating) would influence the decision on the maximum capacity of the fuel cell and the auxiliary boiler. In the case of underfloor heating systems which are suited better in buildings with smoother load patterns, the need for high plant capacity is reduced. Fuel cells are not flexible enough to follow the variability of the energy demand of a dwelling. Therefore in many cases a thermal storage tank is included in the design to act as buffer between heat plant and demand. Finding the ideal size of the thermal storage tank can be proved challenging, as space, cost and heat constraints affect the decision. A rule of thumb for the volume of the store is 10 litre of storage volume per kW of boiler capacity. Thermal stores

sized on a higher ratio of volume against plant capacity can be effective when changes in loads occur many times across a day [96].

Figure 4.1.1: Storage Tank for use in a micro-CHP system ([31])

In some cases the fuel cell even when combined with the thermal tank cannot satisfy the whole heat load of the house due to possible rapid increases in the DHW load or by very cold winter days, therefore an auxiliary natural gas boiler is required. This could be integrated in the fuel cell micro-CHP or could be a separate unit. The Baxi Innotech Gamma 1.0 includes a 1 kWe/1.7 kWth PEMFC fuel cell and an integrated 20 kWth natural gas boiler [22].

Some simplified design alternatives are shown in Figures 4.1.2, 4.1.3 and 4.1.4 [2].

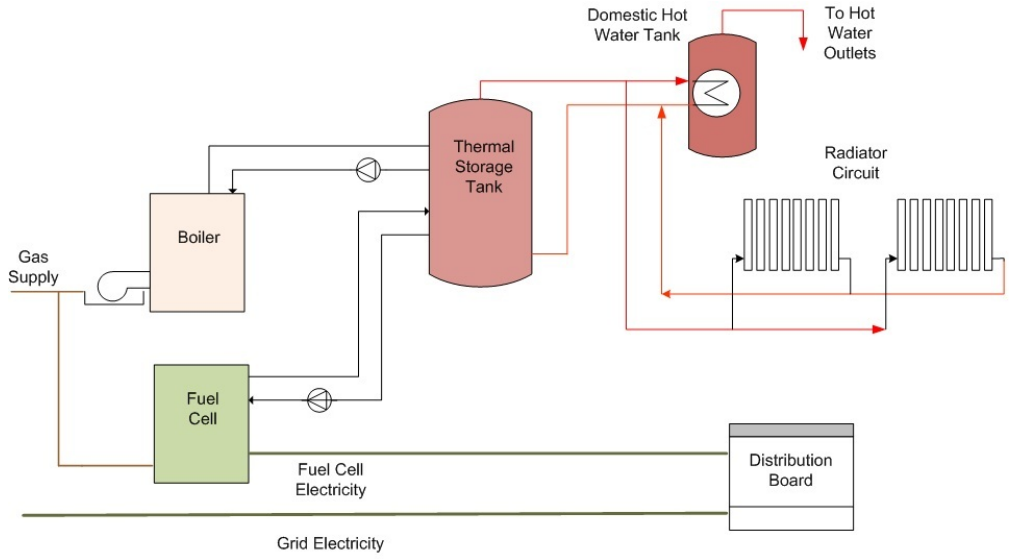

Figure 4.1.2: Simplified Schematic Diagram of Fuel Cell micro-CHP system - Configuration 1 - Thermal Storage Tank Present

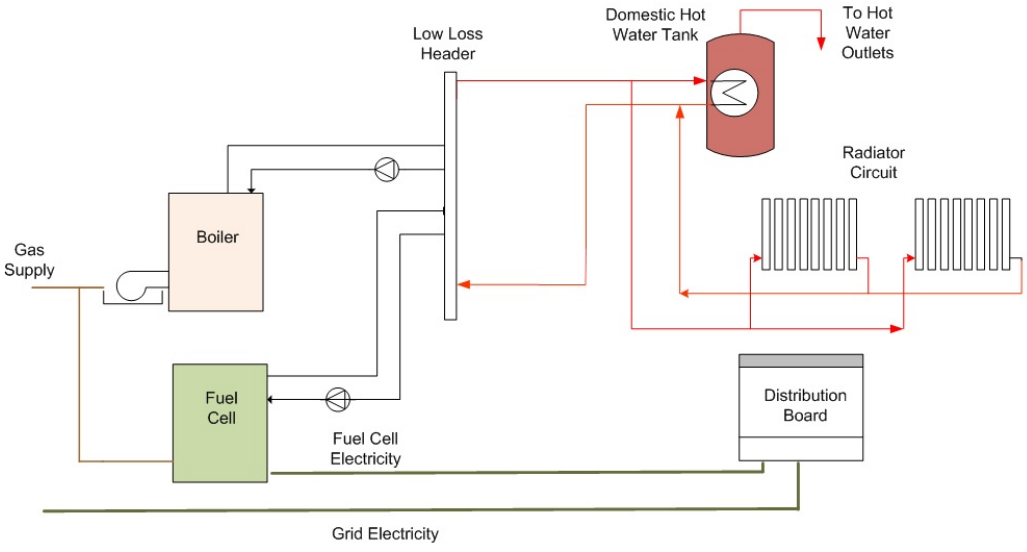

Figure 4.1.3: Simplified Schematic Diagram of Fuel Cell micro-CHP system - Configuration 2 - Without Thermal Storage Tank

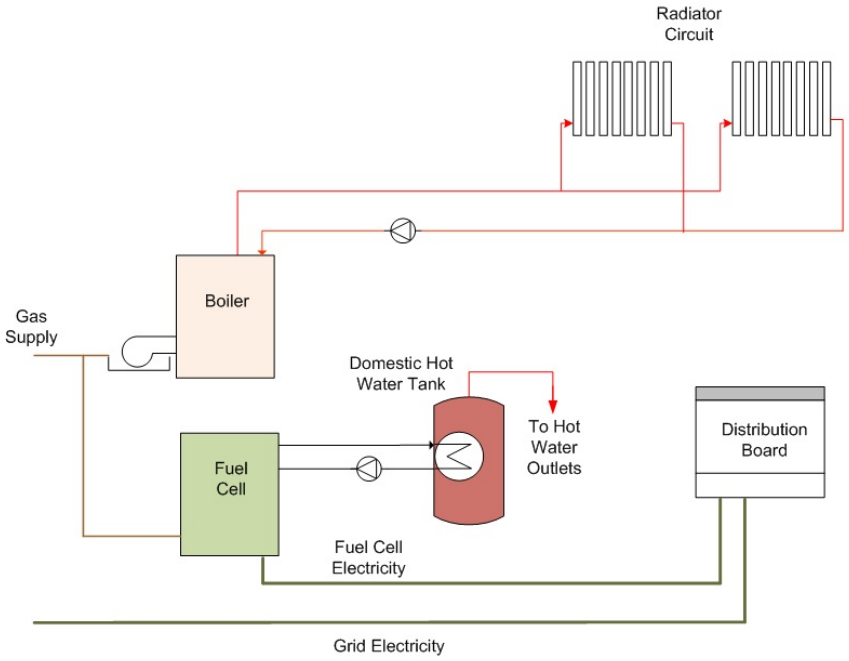

Figure 4.1.4: Simplified Schematic Diagram of Fuel Cell micro-CHP system - Configuration 3 - Fuel cell serves DHW

4.2 Heat recovery in fuel cell micro-CHPs systems

The fuel cell stack is the central element of the micro-CHP unit. The required balance of plant includes several components supportive to the stack that are needed for the fuel cell micro-CHP to run smoothly and function as a system. Figure 4.2.1 presents a schematic diagram of a PEMFC micro-CHP. The heat demand of the dwelling can be fulfilled using different heat sources within the fuel cell micro-CHP and also by an auxiliary boiler. The micro-CHP requires management of heat, fuel, air, and water to function. At the same time the produced DC power requires power conditioning to be used in the dwelling.

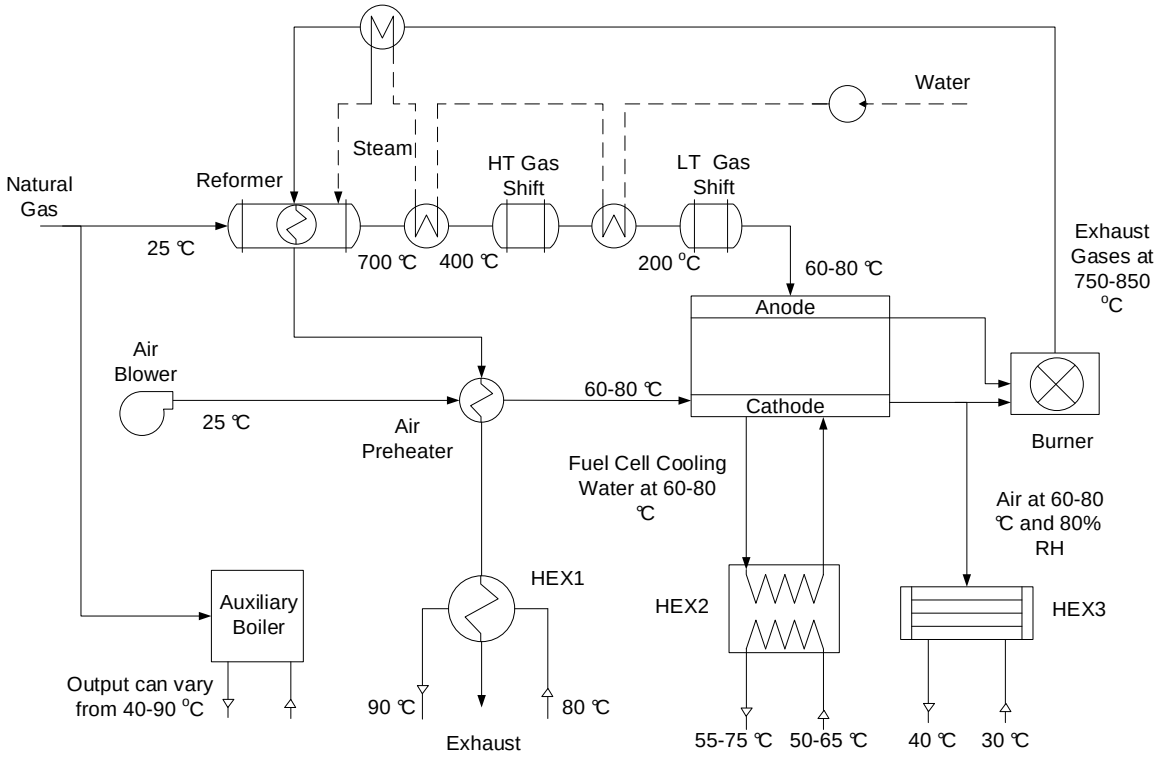

Figure 4.2.1: Schematic illustration of a PEMFC micro-CHP system showing options for heat recovery. [2]

The heat generated by the operation of the fuel cell has to be removed as it could dry out the electrolyte membranes should the temperature exceed 100 °C [130]. Heat recovery from a fuel cell can be performed in different ways, using water or air as a medium. It depends on the type of fuel cell and on the amount of heat needed in each process within the unit. The existance of temperatures at different levels, such as as the high temperature at the exit of the burner (700-900 °C) and the low temperature (60-80 °C) at the cooling circuit of a PEMFC allows for different grades of heat to be recovered and used in loads of different temperature constraints within the fuel cell and the dwelling. Various processes within the fuel cell micro-CHP system demand or emit heat, such as the processes occuring at the fuel cell stack, the afterburner and the fuel processor. Therefore, there is potential for an optimisation process to identify the optimal heat paths from the source to the demand.

4.2.1 Heat recovery options in PEMFC systems

In practice, the amount of heat that can be recovered from a fuel cell micro-CHP will be related to fuel cell technology and the system design and control. Despite this, some textbook calculations can provide an approximate indication of the available resource.

4.2.1.1 Fuel Cell Stack

Conventional PEMFCs work in the temperature range of 60 °C to 80 °C. A temperature lower than 60 °C would impact the reaction kinetics and could cause problems on water management [130]. The cooling circuit of the fuel cell prevents stack overheating and protects the membrane from drying. For a 1 kWe fuel cell and using average values for voltage, fuel cell area, cell number in the fuel cell stack and fuel utilisation factor, the rate of heat generation is calculated at around 1.1 kW. Part of this heat can be recovered from the cooling water and the gas exiting the cathode of the fuel cell. In terms of cooling medium, fuel cells rated at capacities smaller than 2 kW_{th} are usually air cooled. In the case of a micro-CHP system though, a water cooling system is more suitable as it could be used as the heating medium in a building. The cooling water exits the fuel cell stack at a temperature between 60-80 °C. The return temperature of the cooling water to the fuel cell stack has a 5-20 °C temperature difference to the water exit temperature from the fuel cell stack [70]. The cathode off-gas stream consists of humid air at 80%-100% relative humidity at around 60-80 °C [89]. Heat from this stream would be suitable to be recovered and used in a low temperature heat emitter like underfloor heating [2].

4.2.1.2 Afterburner and Exhaust gases

It is common practise that an afterburner is used for any unreacted hydrogen exiting the fuel cell stack, to be combusted. The rich in H_2 gas mix from the anode (contains also CH_4 from the reformate) and the cathode off-gas which contains O_2, N_2 and H_2O can be fed directly to a burner. Alternatively instead of the cathode-off gas, a fresh air supply can be fed to the burner using a separate fan [89, 93]. An option for the burner is to be of thecombined type that can combust natural gas additionally to the anode off-gas. This would ensure that the temperature of the afterburner off-gas would be high enough to increase conversion of H_2 in the fuel processor. PEMFCs that require external reforming can use a combined burner effectively. If stoichiometric amounts of the reactants were fed into the combustion chamber, the

exhaust stream temperature would be calculated in the range of 2000-2200 °C using the heat of reaction method [63]. The afterburners will overheat at these high temperatures, so for practical reasons the reactions occur in excess of air. The typical exhaust stream temperature is between 700-900 °C.

4.2.1.3 Fuel Processor

A fuel processor is used to convert a hydrocarbon-based fuel supply to hydrogen, so it can be used a fuel cell. Partial oxidation and steam reforming are the most popular methods for producing hydrogen from hydrocarbons. Steam methane reforming (SMR) produces a higher electrical efficiency than partial oxidation and is generally the preferred method of the two [90]. The heat supplied by the afterburner can be used to preheat the input streams of fuel and air, generate steam and drive the fuel processor. For the reforming reaction to occur, the minimum temperature is 600 °C, but is recommended to be higher to increase the conversion rate of CH_4 to H_2. The reformate exists the reformer at at 650-750 °C and is cooled down to 400-450 °C before it enters the high-temperature gas shift reactor, and to 200-250 °C as it enters the low temperature gas shift reactor. An open water stream is used for these temperature changes between the various reactors which is also used for the production of steam for the reformer, as shown in figure 4.2.1.

4.2.2 Heat recovery options in SOFC systems

SOFCs do not need an internal reformer because their high operating temperature allows for direct feed of hydrocarbon fuels. Removal of carbon monoxide is not required as well, so SOFC have simple fuel processors. Recently micro-CHPs based on SOFCs have shifted from the traditional high-temperature operation (850-1000 ^oC) into the intermediate temperature (IT) of 500-750 ^oC [28]. This provides flexibility in the types of materials to be used, reduces life cycle cost and increases lifetime. This lower operating temperature allows for quicker startup and shutdown [5]. Figure 4.2.2 shows a process diagram for a SOFC-based micro-CHP system. Cooling of the fuel cell stack is provided by air using a blower. As it is the case with PEMFCs, there is an afterburner that the anode and cathode off-gas streams are fed to, for combustion. Heat from the afterburner is used in a similar manner as in the PEMFC for preheat of fuel and air and steam generation while any remaining heat can be used in a house heating system for DHW and space heating.

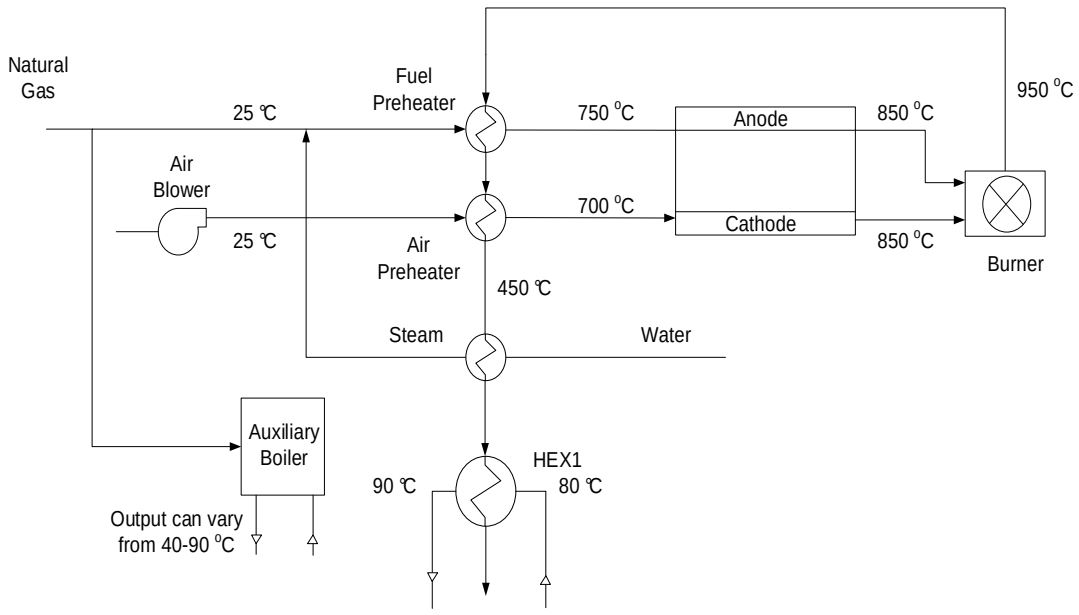

Figure 4.2.2: Schematic illustration of a SOFC micro-CHP system showing options for heat recovery.

4.2.3 PEMFC and SOFC differences in terms of heat recovery

SOFCs have simpler fuel processing systems, can use directly hydrocarbon fuels and therefore do not require a pure hydrogen supply as PEMFCs (typically less than 10 ppm CO for PEMFC) [89]. The design of SOFCs is therefore simpler as there are less process units involved in their operation. However, PEMFCs benefit from higher power densities and shorter start-up periods compared to SOFCs [4]. In PEMFCs heat can be recovered from least two heat sources: the cooling water from the fuel cell stack at low temperature and the exhaust gas from the afterburner at higher temperature. In SOFCs there is only the option of the exhaust gases for heat recovery.

4.3 Design options for integration for fuel cell based micro-CHP

Figure 4.3.1 shows a representative schematic for the integration of a fuel cell micro-CHP unit and an auxiliary gas boiler to a dwelling showing the heat distribution

side. As there are numerous possibilities for connections between all components, the optimal design to achieve an energy efficient and robust operation is not immediately obvious. This becomes a more difficult task as there is limited information in literature on bringing together such systems. Existing models lack the temperature information of heat sources and loads and the constraints of the heat distribution system in the dwelling.

In order to capture achieve this, a new modelling framework has been developed that attempts to provide a link between the energy source and the demand. This modelling approach that considers energy plant and demand can provide manufacturers and designers with valuable information about sizing and operation of the system, thermal management strategy and heat exchanger design while minimizing CO_2 emissions.

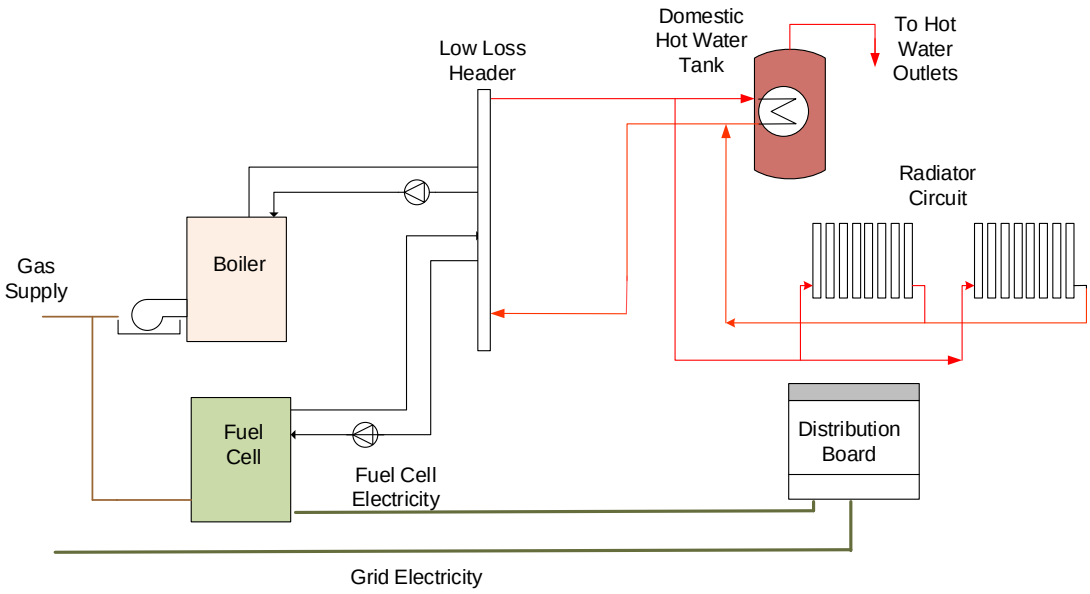

Figure 4.3.1: Schematic diagram of fuel cell micro-CHP design for a dwelling

The first step towards developing this framework is the development of a building model that will be the basis for comparison for all the proposed designs. The process of modelling the reference building is presented in the next chapter.

Chapter 5

Reference Building and Dwelling Energy Data

5.1 Reference Building

Energy demand data for dwellings that include heating, domestic hot water and electricity information can either be obtained by using Building Information Modelling (BIM) or can be obtained from real houses from various sources. A source for such data is the English Housing Survey, which is a survey of English houses and provides information of the condition and energy efficiency [42].

All the case studies that are presented in this thesis are compared against a reference building. The reference dwelling has been developed according to the existing literature and own interpretation. The reference building is modelled with building modelling software and is a house served by a conventional heating and electricity system. It is considered that using modelling data for the house energy demand instead of existing consumption data would provide "clean" data that can easily be used in the next steps. Real data require attention as they can be influenced by unknown factors such as the accuracy of sensors, occupants etc. For the purposes of the model a robust data set was needed to develop the methodology. It was decided that such dataset can be obtained using building information modelling.

Overall there are two reference buildings defined here. They share the same shape, size and area but differ on the energy characteristics. The building is located in London and is a four bedroom house with two storeys; a total floor area of about 190 m^2. A large house with higher energy requirements is be able to identify more clearly the characteristics of the proposed solutions. House A is a building which

is compliant with Building Regulations Part L2B with regard to the U values and air permeability while House B is a typical 1970's UK house in terms of energy characteristics. Table 5.1 shows the U values and air permeability that have been used in this study for the two reference buildings. Architectural drawings of the building were also developed in AutoCad and are included in Appendix A.

Table 5.1: U Values of Houses A and B used as input in the building information modelling software

	House A	**House B**
	U Value (W/m^2K)	**U Value** (W/m^2K)
Roof	0.20	0.40
Wall	0.30	0.60
Floor	0.25	0.50
Windows, Rooflights	2.00	4.80
Doors	2.00	3.00

- Heating is provided by a gas fired condensing boiler. Boiler system efficiency is compliant with Domestic Heating Compliance Guide [83]. Boiler efficiency was set at 90% and 85% for House A and B respectively.
- Electricity is supplied from the grid.

A building model requires information about the physical and thermal characteristics of the dwelling, but also an approximation of how the house is used. Operational profiles are assigned for all uses and actions that affect energy consumption and describe the operation of lights, use of rooms, hot water consumption etc. Examples of these profiles are shown in Figures 5.1.1 and 5.1.2. Some profiles are displayed as ratios such as the occupancy ratio in each room (which is the ratio of the current number of occupants to the maximum number predefined by the modeller) and other have absolute values (e.g. temperature). These profiles are taken from the National Calculation Method (NCM) and are used in many commercial BIM software packages [26].

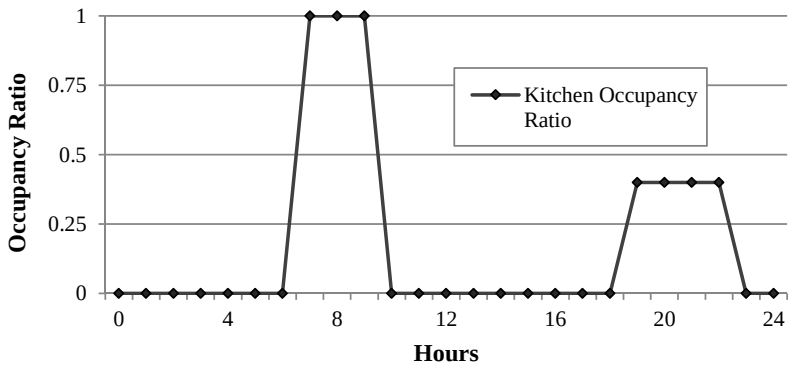

Figure 5.1.1: Daily profile of the occupancy ratio (reproduced from IES VE [87])

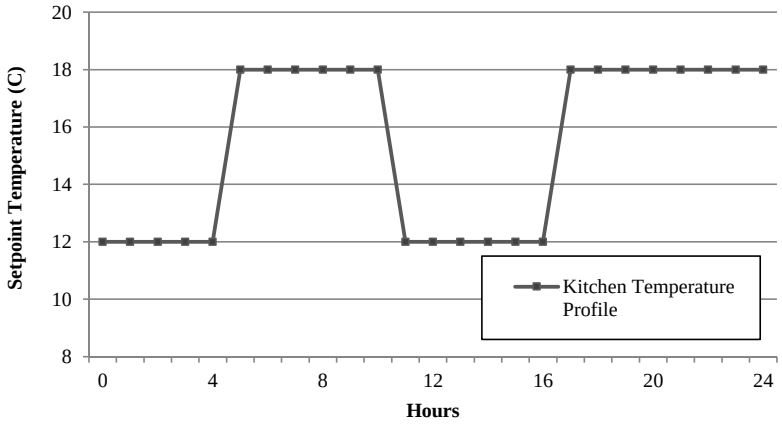

Figure 5.1.2: Daily profile showing the internal set-point temperature (reproduced from IES VE [87])

Also internal design set points have to be defined as per Table 5.2 within the guidelines of CIBSE Guide A [37].

As the characteristics of the reference building were defined, the choice of the most suitable software package was the next step. IES VE [87] is an Approved Software by the Department of Energy and Climate Change for performing energy simulations and producing energy performance certificates (EPC). It was chosen among other similar programmes for its simplicity and because it has been extensively used

Table 5.2: Internal temperatures for selected dwelling

Room	**Temperature (°C)**
bathrooms	21
bedroom	19
hall/stairs/landing	21
kitchen	18
living rooms	21
toilets	21

and tested in the building modelling industry. This software allows designers to evaluate different design options, calculate energy use ,CO_2 emissions, EPC ratings and provide predictions on occupant comfort. This is achieved by constructing a three-dimensional model of the house and then applying all its attributes in different sub-programmes of the software. Part of the modelling process is to set the weather files relatively to the location of the building using the IES sub-programme APlocate. In this case, weather data for the London Heathrow area were used. The weather file contains values for temperature, solar radiation, wind velocity, cloud coverage and atmospheric pressure [86]. Images of the produced 3d model are shown in Figures 5.1.3 and 5.1.4.

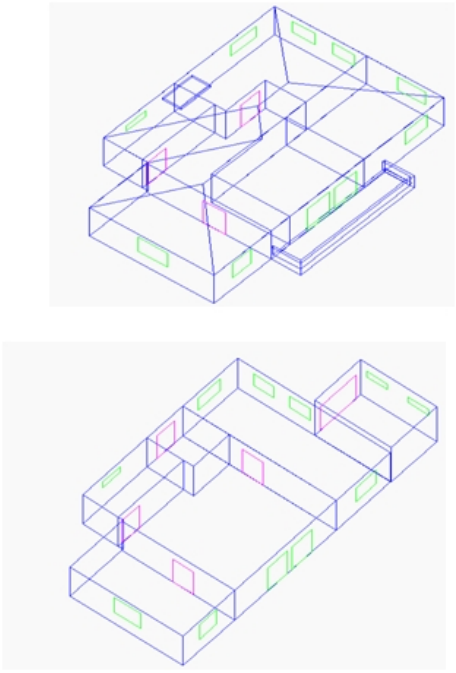

Figure 5.1.3: Image showing the structure of the 3D model. This image is used to illustrate the process of creating the structure of the model which is using series of rectangular blocks to develop the final shape of the building.

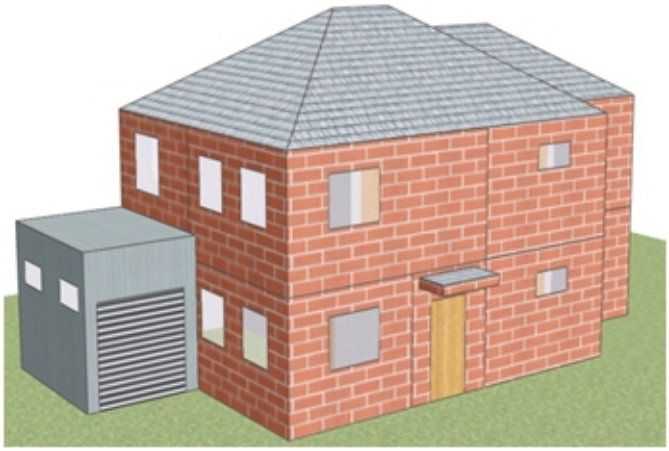

Figure 5.1.4: Image showing the exterior of the 3D model

The purpose of modelling the building in IES is to obtain energy data for a whole calendar year for a reference building designed with a conventional heating system.

The heat demand is a function of the outside temperature, the U Values, the internal set-point temperatures and their use profiles. The data presented in section 5.2 will be used as the basis for comparison of fuel cell micro-CHP designs and conventional systems for residential applications.

The choice of a new Part L compliant dwelling and an older typical UK dwelling ensures that the studies presented can capture a wide range of the UK building stock. It will then be feasible to extract conclusions about the feasibility of the studies on a larger scale without being limited by the scope of a single case study.

5.2 Dwelling Energy Data

This chapter presents the energy demand data for heating, DHW and electricity for Houses A and B. The loads differ according to the different heat emitters for both houses. The base case for all examples presented represents a dwelling that is designed with a natural gas boiler to satisfy heating and hot water requirements and is connected to the electricity grid. The dataset obtained contains yearly data with 5 minute timesteps. However, as this results in a large number of data, a 1 hour timestep has been used throughout.

The complete yearly dataset of 8760 hours is presented here. It is then used to extract segments and to create subsets to examine various case studies presented in Chapters 6 and 7. Subsets could be single winter or summer days comprised of 24 hours or larger.

Figure 5.2.1 shows the 24-hour heat demand of the DHW tank. This is to maintain water in the storage tank at 60 °C at all times. It takes into account the hot water consumption profile of the occupants and storage losses at a rate of 0.0075 kWh/lday. Modelling the DHW system has been carried out using IES's sub-programme ApacheView [85] . It remains unchanged for both houses regardless of the choice of heating system and follows a 24-hour pattern that repeats throughout the year. The DHW demand peaks in the morning when typically people have showers and also in the evening hours when people typically return from work and occupancy increases.

Figure 5.2.2 shows the electricity demand which follows a weekly repetitive pattern with higher demand on weekends. This weekly pattern is the repeated throughout the year. The increased demand in weekends can be explained by the additional electricity load for lights and electronic devices during weekends because of the increased occupancy. At the same time, on a daily basis the electricity demand follows

the occupancy pattern with morning and late afternoon peaks.

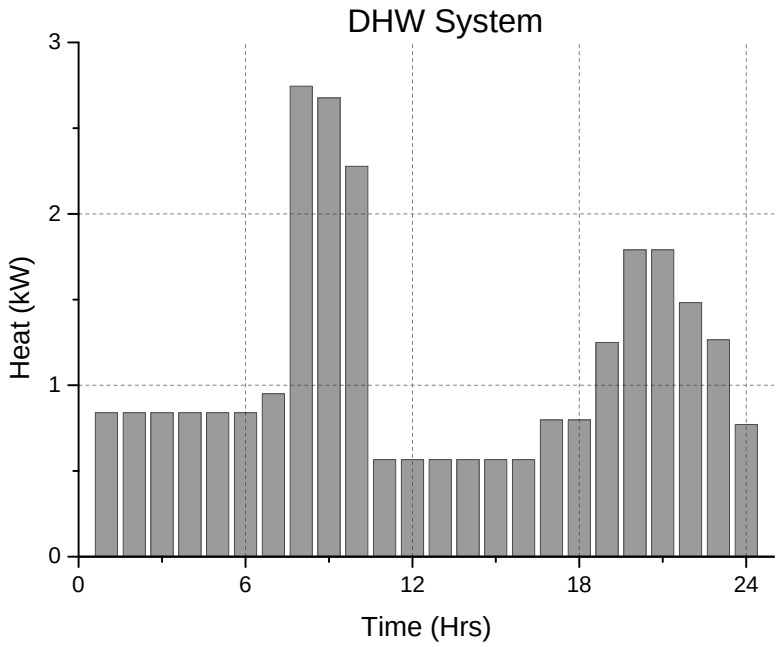

Figure 5.2.1: Graph representing the 24-hour heat demand for DHW pattern for the reference dwelling. The graph shows the relation between the occupancy, which is high in the morning and in the evening hours, and the DHW demand.

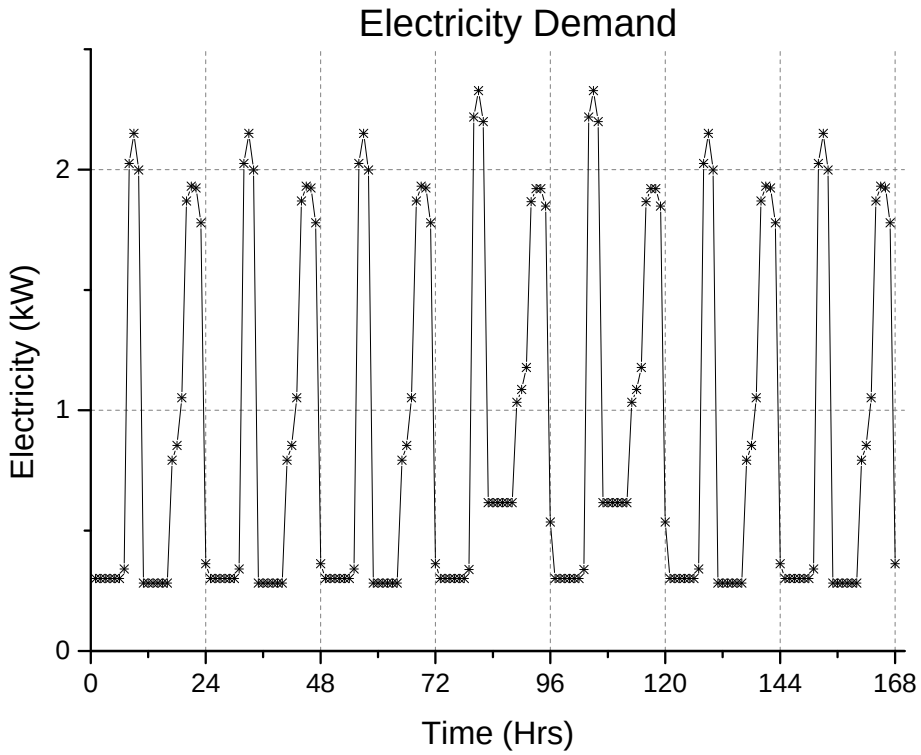

Figure 5.2.2: Graph representing the weekly electricity demand for House A. This weekly electricity pattern repeats throughout the year and peaks in the weekends.

5.2.1 House A - Part L Building

5.2.1.1 UFH System

The maximum space heating load for the UFH system is 7.9 kW which is a low value considering the area of the house. However, the low U-Values and air permeability that are in line with Part L regulations results an efficient system with lower heat demand.

The UFH is generally a slow response system that requires longer heating hours and less peaks compared to a radiator system. The space heating demand for House A served by underfloor heating can be seen in Figure 5.2.3.

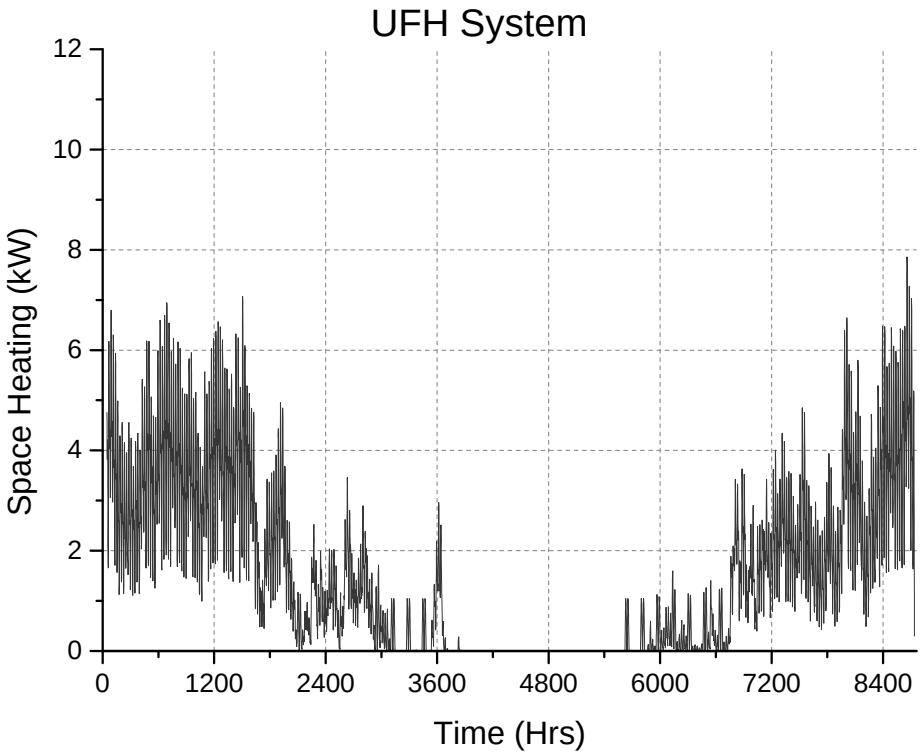

Figure 5.2.3: Graph representing the demand of the base case for House A served by an underfloor heating system

A segment of the dataset presented in Figure 5.2.3 can be extracted to show the daily or weekly variation of space heating demand such as the one shown in Figure 5.2.4. The graph shows the daily variation of space heating demand and demonstrates how smooth the heating pattern is, allowing for long heating periods and not many peaks.

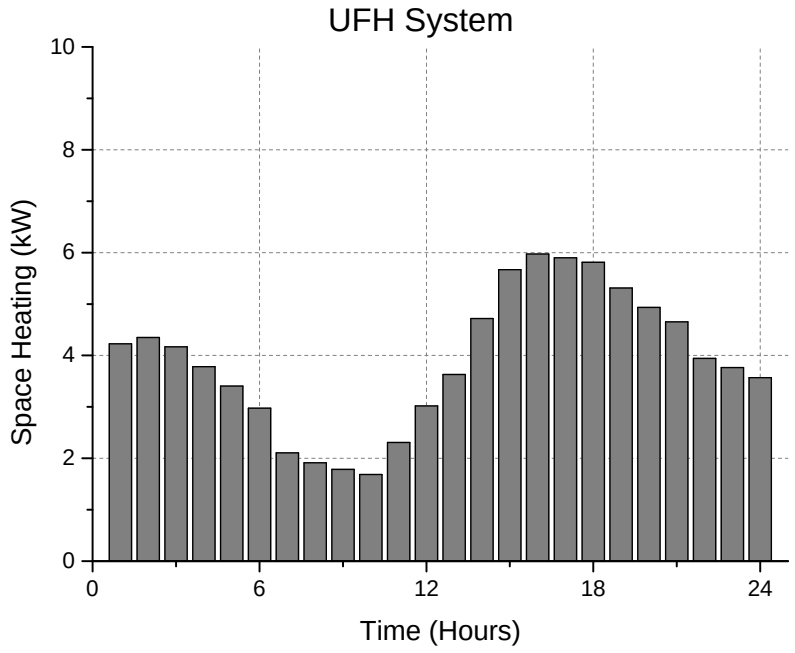

Figure 5.2.4: Graph representing the winter space heating demand of the base case for House A served by a underfloor heating system on a 24-hour segment of the complete annual dataset

5.2.1.2 Radiator System

The heating demand for space heating on annual basis can be seen in Figure 5.2.5. The variation of heat demand for the radiator system follows a more rapid pattern with higher peaks compared to the smoother pattern of the UFH system depicted in 5.2.3. Space heating demand peaks at 11 kW for House A for the case of the radiator system.

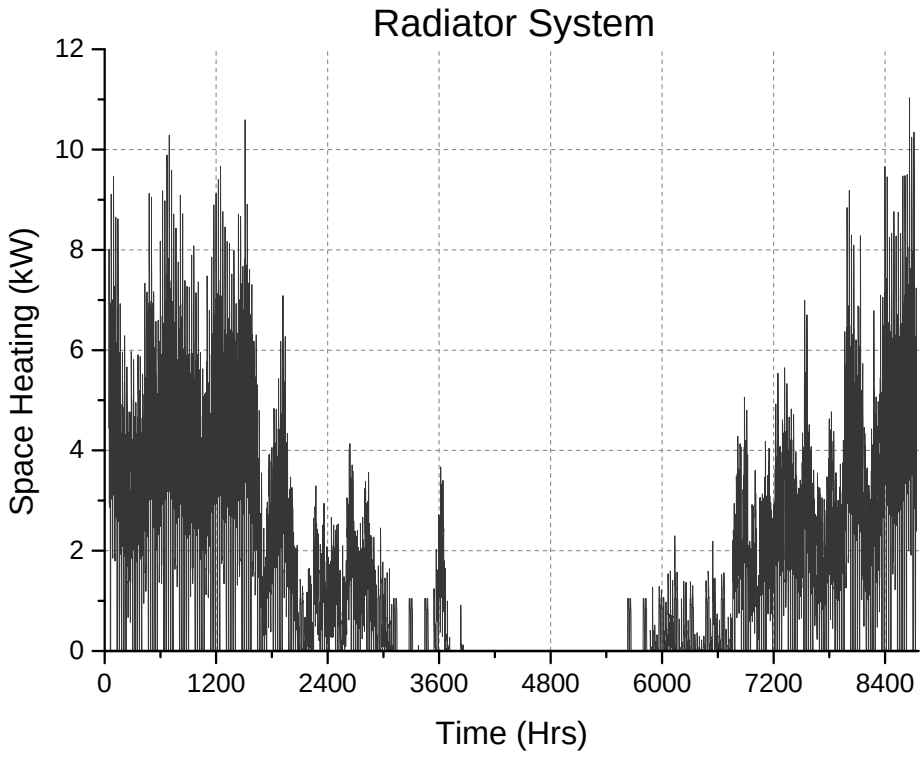

Figure 5.2.5: Graph representing the demand of the base case for House A served by a radiator system

The 24 hour segment of the dataset presented in Figure 5.2.6 shows the rapid pattern of the space heating demand.

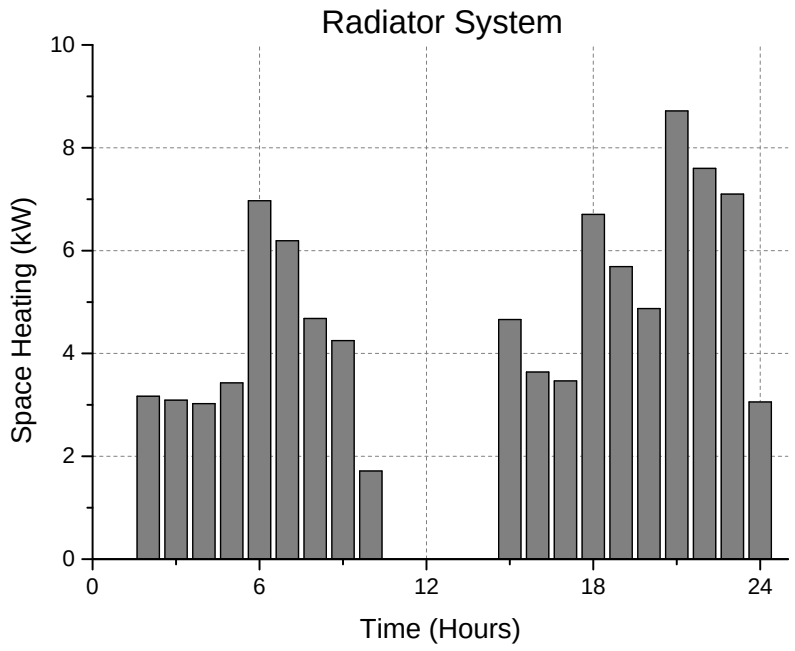

Figure 5.2.6: Graph representing the winter heating demand of the base case for House A served by a radiator system on a 24-hour segment of the complete 8760 hour dataset

5.2.2 House B - Typical UK Dwelling

Heat for DHW and electricity demand remain as per House A, however there is difference in terms of the space heating demand for House B. The shape of the space heating demand graph is similar to the respective graphs for both cases (UFH or radiators) however the peaks are higher for House B, being a poorly insulated building compared to House A.

5.2.2.1 UFH System

The space heating demand for House B when served by underfloor heating system peaks at 31.4 kW and it is shown in Figure 5.2.7.

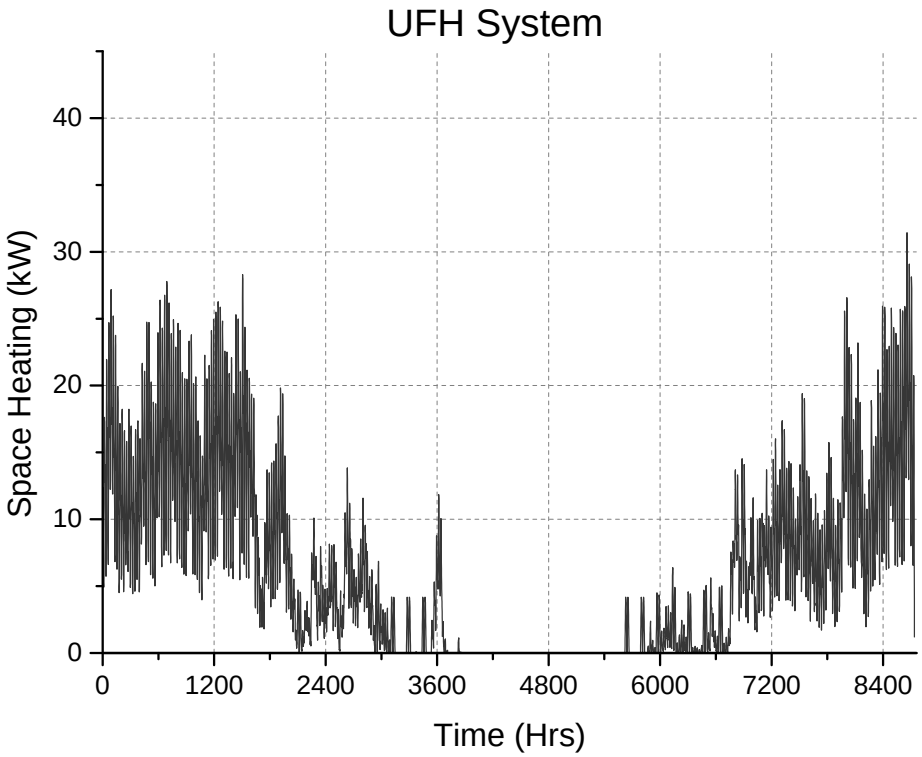

Figure 5.2.7: Graph representing the demand of the base case for House B served by an underfloor heating system

5.2.2.2 Radiator System

The variation of the heating and electricity load for House B is shown in Figure 5.2.8. The heating demand for the poorly insulated building peaks at 44.1 kW.

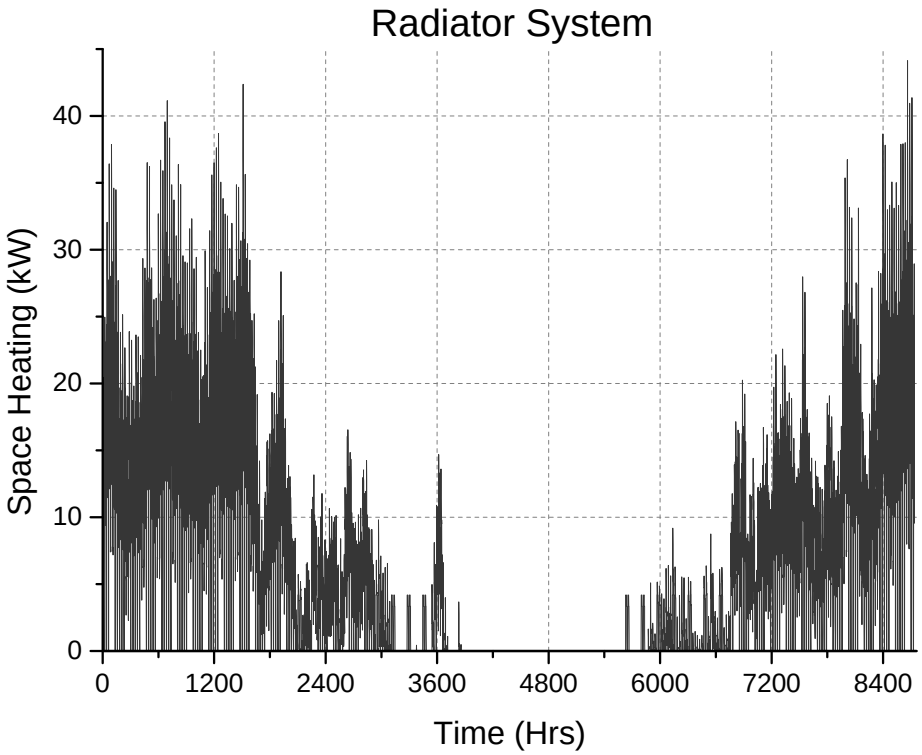

Figure 5.2.8: Annual variation of heating load for House B

5.3 Datasets for Modelling

As discussed earlier the complete annual dataset is used as the basis to create various datasets that are used in Models 1 and 2 presented in the following chapters. The datasets used in Model 1 are single days comprised of 24 1-hour timesteps and a combined winter-summer 48-hour dataset. The datasets used in Model 2 comprise of 12 days of 24 hourly timesteps. For both models the days are selected using the middle day of the month. The reason behind this is to ensure that each day in the dataset is the same number of days away from the next sample day. A dataset that includes the first, second, or any day of each month could have equally been used. The dataset that includes the first day of each month would be expected to have higher space heating demands than the dataset that uses the last day of each month. However regardless of the exact choice of day, the trend in energy demands of the datasets would be similar.

As each day in the dataset represents one month, the developed datasets might not contain data for the coldest day of the year. At first this might suggest that the proposed designs might not be able to meet the heating load of the dwelling at the particular day. However in reality the results that can be obtained from a a modelling study would require interpretation and assessment before proceeding to plant selection. Extra plant capacity is added to the calculated to shorten the preheat period of the heating space in cases of the heating being turned off for a big period of time [96]. At the same time there is uncertainty already involved on the accuracy of the heating load calculation caused by assumptions while estimating the U-values. According to Biddulph et al. "Unfortunately the actual U-value may be different from those values obtained using assumptions about the materials, their properties and the structure of the wall after a cursory visual inspection." [25]. The heat demand is related to the users of the building, their perception of thermal comfort and their behaviour in terms of the way they operate the room thermostat which could be completely unpredictable. Therefore developing a smaller dataset that can describe the heat demand of a whole year cannot be done without a compromise. The developed datasets are used in the models to identify trends and patterns for decision variables. The concept of identifying trends in the resulting designs is behind the consideration of different scenarios and buildings in the models presented.

Another issue with regard to the developed datasets is the effect of the temporal precision. The idea of having a 1-hour timestep allows for smaller datasets that can capture a whole year cycle without having to use too many data. However, there is information lost as the variations of energy demand during this hourly period are averaged on the 1-hour timestep. That could lead to lower maximum values for heating or electricity loads that are to be met and therefore variations in the conclusions about overall primary energy reductions offered by a system. This view is supported by Hawkes et al. "...coarse temporal precision leads to averaging effects that result in misleading environmental and economic outcomes for cost-optimal micro-CHP systems" [71]. Napoli et al. suggests that when modelling micro-CHP systems, the electrical profiles may need higher temporal precision than the heating ones as as the presence of a thermal storage tank will smoothen the heating load [93]. An implication of using averaged 1-hour timesteps is that the ramping and capacity constraints that define the performance of the fuel cell micro-CHP would have less significance in a model compared to a more detailed dataset that uses 5-minute timesteps. As a result the choice of 1-hour timesteps in the input energy data of the models might lead to results that favour electricity generation from the fuel cell micro-CHP while also underestimating the total CO_2 emissions of the systems.

5.4 Summary of Results

The resulting CO_2 emissions of the reference building as used in the different models are shown in Tables 5.3 and 5.4.

Table 5.3: Reference Building emissions for House A as used in Model 1

Dataset	CO_2 Emissions (kg)
Winter Day	45.1
Summer Day	16.5
48-hours	61.5

Table 5.4: Reference Building emissions for Houses A and B as used in Model 2 for the 288-hour datasets

		CO_2 Emissions (kg)
House A	UFH	289
	Radiators	292
House B	UFH	567
	Radiators	572

5.5 Concluding Remarks

This chapter presented the reference buildings that will be used for comparison with the various designs presented in the next chapters. An effort has been made to capture the old and the new: houses of the existing building stock and houses that are designed according to the latest requirements of building regulations. This diversity in the dataset provides a generality in the attempted analysis and the opportunity for a critical study.

Chapter 6

Model 1 - An MINLP model for high level evaluation of a SOFC micro-CHP design in dwellings

This model attempts to identify optimal designs in terms of CO_2 emissions for SOFC based fuel cell micro-CHP in dwellings without using any electrochemistry equations. The methodology is treating all plant as "black boxes" with efficiencies assigned to them and considers DHW and space heating as one demand. The purpose of the model is to provide a simple tool for a high level evaluation of a fuel cell micro-CHP design that can be used in the early stages.

Part of the work presented in this chapter has been published in [3].

6.1 Optimisation methods in energy systems

As part of this PhD project optimisation techniques have been used. The exact methodology will be explained in detail later, however the purpose of this chapter is to summarise the key features of optimisation that are relevant to the study.

In an optimisation problem a mathematical model of the system has to be formulated. The model consists of the following elements:

1. Variables,
2. Parameters,
3. Constraints, and

4. Mathematical Relationships

A definition of any optimisation problem is the following:

$$maximise/minimize\ f(x) \tag{6.1.1}$$

with

$$x = (x_1, x_2, ..., x_n) \tag{6.1.2}$$

subject to the equality and inequality constraints

$$h_i(x) = 0 \qquad \text{i=(1,2,...,k)}$$

$$g_j(x) \leq 0 \qquad \text{j=(1,2,...,l)}$$

In the case of optimisation in the built environment involving micro-CHP plant the objective function could be the total cost (capital or operational), the total energy consumption (or CO_2 emissions) of the system, the efficiency etc. The variables involved could represent the energy output of each source and the capacity of each plant. The parameters could be energy requirement data, cost information (i.e £ per kWh of imported electricity) etc. Constraints are usually energy balances or technical constraints of the plant involved.

An optimal solution of a problem contains values for the variables that satisfy the constraints while optimising the objective function.

The models that will be presented here are primarily MINLP as non-linear terms are used in efficiency or energy balance equations that describe the systems. The most common method implemented to solve MINLP models is the Branch and Bound method (BB) [53].

Software package for modelling and solving optimisation problems has been developed over the last 15-20 years and is available either free or as commercial product. The more widely used include GAMS (General Algebraic Modelling System), AIMMS, Matlab and others [6, 29, 91].

6.2 Problem Statement

The overall problem for the high level design of a SOFC micro-CHP in a dwelling can be stated as follows.

Given:

- Known availability of heat an electricity generating plant (j : fc,gb) ;
- The total heat (space heating and DHW combined) and electricity demand for a dwelling (k: heat,ele);
- Process limitations and constraints in terms of energy generation

Determine:

- The sizing and operational characteristics of this design.

So as to minimise the resulting CO_2 emissions from the dwelling energy system.

6.3 Basis for the Model

The model overview can be seen in Figure 6.3.1. Natural gas and grid electricity are the energy inputs of the system, while CO_2 emissions the output. The fuel cell is supplying heat to the TST and from the TST heat can be supplied to the dwelling for space heating and DHW. An auxiliary gas boiler is supplementing the fuel cell and TST with heat. Electricity is served by the fuel cell and grid electricity. The total heat and electricity demand need to be satisfied at all times. There is a single demand of heat in the model and this is the combined space heating and DHW.

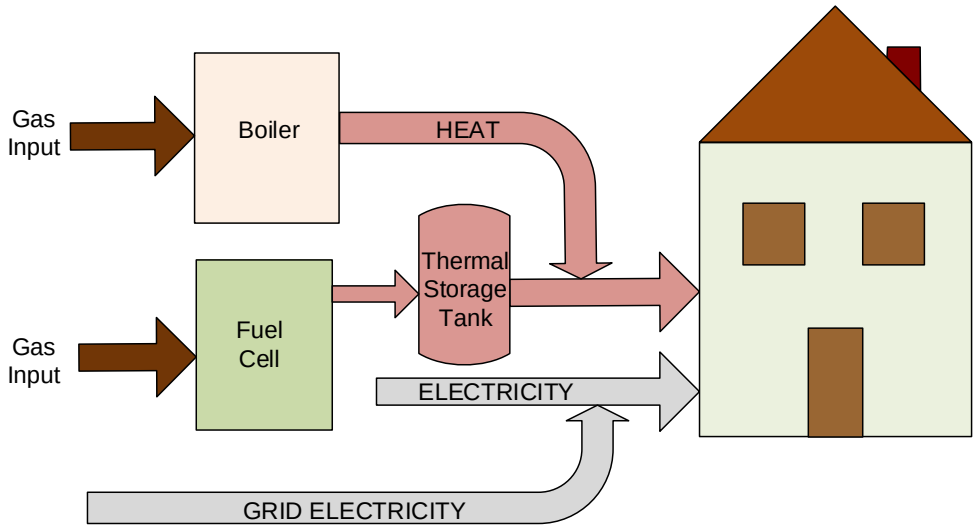

Figure 6.3.1: Basic structure of the model

The operation of all heat generating plant is subject to losses that are represented with an efficiency term. At the same time fuel cell and grid electricity are also subject to losses. Therefore for a given demand, the size and energy contribution of each plant determines the performance of the whole system. This performance can be measured in terms of a characteristic of interest such as CO_2 emissions or cost. There is uncertainty on cost data for fuel cells as explained in section 2.7. A study focusing on cost would have to examine other micro-CHP technologies to compare the fuel cell costs against. Therefore as the study focuses on system efficiency and design it was considered appropriate that the performance of the system is evaluated in terms of total system CO_2 emissions.

6.4 Modelling Methodology

Details of all indeces, parameters and variables can be found in the Symbols chapter.

6.4.1 Submodels

6.4.1.1 Fuel Cell

The fuel cell's electricity and heat generation rate are given by equations 6.4.1 and 6.4.2 :

$$Q_{fc,ele}(t) = y_{fc}(t) \cdot P_{fc} \cdot r_{fc}(t) \tag{6.4.1}$$

$$Q_{fc,heat}(t) = \frac{Q_{fc,ele}(t)}{\eta_{fc,ele}(t)} \eta_{fc,heat}(t) \tag{6.4.2}$$

The variable $y_j(t)$ is a binary variable that takes the value 1 when plant j is operational and 0 when it is off. P_j represents the maximum capacity in kW and $\eta_{j,k}(t)$ the efficiency of plant j . Variable $Q_{j,k}(t)$ represents the energy output of plant j (kW).

The operation of the fuel cell is affected by various limitations such as a minimum turn down ratio. In this study it was set at 20% [77] and the ramp up rate (ra) at 15 W_e/min or (0.9 kW_e/hr) [75].

$$0.2P_{fc} \leq Q_{fc,ele}(t) \leq P_{fc} \tag{6.4.3}$$

$$\frac{d}{dt} Q_{fc,ele}(t) \leq ra \tag{6.4.4}$$

The SOFC micro-CHP converts the chemical energy of the fuel to electricity and heat according as per its efficiency. The fuel cell micro-CHP thermal and electrical efficiency equations in relation to the load factor $r_{fc}(t)$ are taken from Hawkes et al. and given by Equations 6.4.5 and 6.4.6 [73].

$$\begin{aligned} \eta_{fc,heat}(t) = &-23.548 r^6_{,fc}(t) + 131.17 r^5_{fc}(t) - 295.99 r^4_{fc}(t) \\ &+355.63 r^3_{fc}(t) - 251.5 r^2_{fc}(t) + 121.96 r_{fc}(t) \end{aligned} \tag{6.4.5}$$

$$\begin{aligned} \eta_{fc,ele}(t) = &-1065 r^6_{fc}(t) + 4114.7 r^5_{fc}(t) - 6437.1 r^4_{,fc}(t) \\ &+5224.5 r^3_{,fc}(t) - 2330.7 r^2_{fc}(t) + 536.81 r_{fc}(t) \end{aligned} \tag{6.4.6}$$

6.4.1.2 Gas Boiler

The boiler's heat production rate is given by equation 6.4.7.

$$Q_{gb,heat}(t) = y_{gb}(t) P_{gb} r_{gb}(t) \tag{6.4.7}$$

The gas boiler's efficiency $\eta_{gb}(t)$ is set to 90% which is in line with the Domestic Heating Compliance Guide [83]. In the case of the gas boiler $Q_{gb,ele}(t) = 0$.

The heat production rate of the boiler is limited by a minimum turn down ratio of 30% and it cannot exceed its maximum capacity:

$$0.3P_{gb} \leq Q_{gb,heat}(t) \leq P_{gb} \tag{6.4.8}$$

6.4.1.3 Thermal Storage Tank

The model for the thermal storage tank includes all energy flows to/from the TST and energy balances. The only source of heat for the TST is the fuel cell micro-CHP.

The energy content of the storage tank E^{st} (kJ) is given by equation 6.4.9

$$E^{st}(t) = V^{st} \cdot \rho \cdot cp \cdot (T^{st}(t) - T^{emv}(t)) \tag{6.4.9}$$

, where V^{st} (m^3) is the storage volume, ρ the water density and $T^{env}(t)$ (^{o}C) a reference environmental temperature.

Energy balance in the storage tank is given by equation6.4.10 .

$$\frac{d}{dt}E^{st}(t) = Q_{fc,heat}(t) - Q^{stout}(t) \tag{6.4.10}$$

, $Q^{stout}(t)$ (kW) is the heat delivered from the TST to the system and $E_{st}(t)$ energy content of the storage tank.

Figure 6.4.1 shows the energy flows of the thermal storage tank.

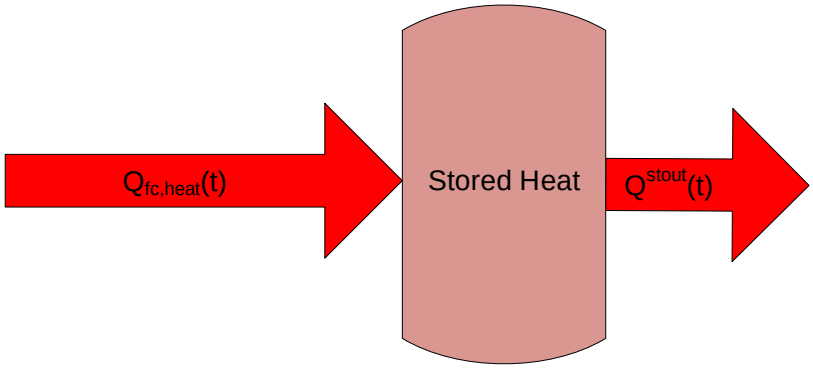

Figure 6.4.1: Thermal Storage Tank energy flows in model 1

$Q^{stout}(t)$ is constrained to be less than the maximum energy content of the TST.

The following constraint must be added:

$$Q^{stout}(t) \leq \frac{d}{dt}E^{st}(t) \tag{6.4.11}$$

6.4.1.4 Thermal balance

The thermal energy balance is given by equation 6.4.12 and can be visualised in Figure (6.3.1).

$$Q_{gb,heat}(t) + Q^{stout}(t) = Q^{req}_{heat}(t) \tag{6.4.12}$$

$Q_{gb,heat}(t)$ represents the total heat output of the gas boiler and $Q^{stout}(t)$ is the output of the TST which includes the current fuel cell heat and the fuel cell heat that has been stored in the tank.

6.4.1.5 Electricity balance

National grid electricity E^g(t) (kW) can be imported at any timestep should the fuel cell electricity generation $Q_{fc,ele}(t)$ be insufficient to satisfy the dwelling's electricity demand $Q^{req}_{ele}(t)$. This is shown on equation 6.4.13

$$E^g(t) + Q_{fc,ele}(t) = Q^{req}_{ele}(t) \tag{6.4.13}$$

No electricity export to the grid is considered in this study.

6.4.1.6 Total System CO_2 emissions

The function calculating the total CO_2 emissions resulting from the operation of the house is used as the objective function of this design problem which is minimised. The CO_2 emissions are caused by the fuel cell, the auxiliary gas boiler and the imported grid electricity. This is expressed in equation 6.4.14.

$$\min z = M^{fc} + M^{el} + M^{gb} \tag{6.4.14}$$

The fuel cell CO_2 emissions are given by equation 6.4.15.

$$M^{fc} = f_g(\sum_t \frac{Q_{fc,ele}(t)}{\eta_{fc,ele}(t)}100) \tag{6.4.15}$$

,where f_g is the natural gas emissions factor taken from [26].

The gas boiler CO_2 emissions are given by equation 6.4.16.

$$M^{gb} = f_g \sum_t (\frac{Q_{gb,heat}(t)}{\eta_{gb,heat}(t)}100) \tag{6.4.16}$$

Total CO_2 emissions resulting from importing grid electricity are calculated using the national average electricity emissions factor f_e [26].

$$M^{el} = f_e \sum_t E^g(t) \tag{6.4.17}$$

6.5 Formulation and Solution Approach

The overall problem is formulated as MINLP model. The resulting optimisation model is non-convex resulting from non-convex functions in the model. There are three "sets" in the model, the timestep "t" which is set as 1 hour steps, the type of plant "j" (fuel cell -fc- or gas boiler-gb) and the type of energy k (heat (heat) or electricity (ele)). "Heat" here represents both the space heating and the DHW load.

Parameters of the model are the total heat demand $Q_k^{req}(t)$, calculated from IES, gas and electricity emission factors, fuel cell ramp up rate and auxiliary boiler efficiency. Table 6.1 shows the values of the parameters used in the model.

Table 6.1: Details of model's parameters.

Parameter	**Description**	**Value**	**Units**
Q_k^{req}(t)	Energy Demand at Timestep t	Varies	kW
ra	Fuel Cell Ramp Up Rate	0.9	$\frac{kW}{h}$
ϱ	Water Density	1000	kg/m^3
T^{env}	Environment Temperature	10	^{o}C
f_g	Natural Gas Emission Factor [26]	0.194	$\frac{kg}{kWh}$
f_e	Grid Electricity Emission Factor [26]	0.517	$\frac{kg}{kWh}$
cp	Specific Heat Capacity of Water	4.2	$\frac{kJ}{KgK}$

Table 6.2 lists the low and upper bounds of the variables of Model 1.

Table 6.2: Variable low and upper bounds for Model 1.

Variable	**Description**	**Lower Value**	**Upper Value**	**Units**
P_j	Maximum capacity of plant fc	0	3	kW
	Maximum capacity of plant gb	0	20	kW
$r_j(t)$	Load factor of plant fc	0.2	**1**	-
	Load factor of plant gb	0.3	1	-
$Q_{j,k}(t)$	Energy Ouput k from plant j	0	∞	kW
Q^{stout}(t)	Heat from TST to demand	0	∞	kW
$\eta_{j,k}(t)$	Efficiency k of plant j	0	100	%-
$E^g(t)$	Grid electricity input	0	Q_{ele}^{req}(t)	kW
$E^{st}(t)$	Heat stored in TST	0	∞	kJ
V^{st}	TST Volume	0	2	m^3
$T^{st}(t)$	TST Temperature	10	80	^{o}C
M^{fc}	CO_2 emissions caused by fuel cell	0	∞	kg
M^{gb}	CO_2 emissions caused by gas boiler	0	∞	kg
M^{el}	CO_2 emissions caused by grid electricity	0	∞	kg
z	Total CO_2 emissions	0	∞	kg

The operational constraints introduced for the auxiliary gas boiler and in particular the 30% turn down ratio is based on the Greenstar 12 domestic boiler product by Bosch-Worcester which modulates between 4-12 kW [127].

It was decided that GAMS [29] will be used as the platform of the optimisation model. GAMS is a modelling tool for mathematical programming and optimisation. The solver SBB was used for the analysis of this chapter [67]. Other solvers such as BARON and AlphaECP were evaluated but SBB gave results within the predefined relative optimality gap in a shorter computational time. SBB can achieve better results than other solvers on smaller models that have difficult non-linearities which is the case here [12]. Taking that into account it was decided that SBB will be used. The SBB solver is built around the Branch and Bound method and a number of NLP solvers for solving the relaxed NLP submodels. The required time for all solvers to provide a solution was improved by linearising the efficiency function as described in section 6.5.1.

The optimality gap is defined as $|BP - BF|/BP$ where BP is the best possible solution and BF is the best integer solution found by the solver. The optimality gas was set to 1% for all cases presented in this chapter. For most models a 0% optimality gap was not feasible and not all case studies could be solved, so a 1% was the first possible gap that provided solutions for all case studies.

It was decided that this analysis will focus on 3 subsets of the complete 8760 hour yearly dataset presented in Chapter 5.

1. A winter day comprised of 24 timesteps.
2. A summer day comprised of 24 timesteps.
3. A combination of the two above data sets (48 timesteps).

The significance of the weather conditions and associated energy demands can be observed by carrying out the analysis on these three time periods. Analysing the winter and summer days separately the design is tested for two different demand patterns, a high heat-to electricity pattern and a low. The 48-hour analysis would provide a design proposal that trades off better than the smaller datasets the different requirements of the whole year while being a simple model that is easy to converge.

The initial value aspect of the problem and in particular the initial energy level of the TST can be proved important and influence the optimisation results on a 24-hour dataset as there is a thermal mass stored in the system at the first timestep. This also is valid for the last timestep where any heat stored in the tank will not be used in the building but has influenced the result. This can generally be avoided by using the complete 8760-hour dataset to reduce the significance of the initial and final values. Alternatively, a constraint can be added that forces the final energy

content of the TST at the end of each day to be equal to the initial value. This method ensures that there is no energy transfer from the TST to the dwelling that is not taken into account in the objective function.

6.5.1 Equations Transformation

Continuous functions and variables cannot be represented in a computer except as a sequence of discrete values. In order to implement equations 6.4.4 and 6.4.10 into the mathematical model they were discretised. They are converted into equations 6.5.1 and 6.5.2. When the timestep is 1 hour δt takes the value of 3600s.

$$Q_{fc,ele}(t+1) \leq \delta t(ra) + Q_{fc,ele}(t) \tag{6.5.1}$$

$$E^{st}(t+1) = \delta t \left(Q_{fc,heat}(t) - Q^{stout}(t)\right) + E^{st}(t) \tag{6.5.2}$$

The efficiency functions shown in equations 6.4.5 and 6.4.6 use non linear terms as these equations are based on fitting these functions from experimental data as described in [73, 74]. The low bound for variable $r_{fc}(t)$ is 0.2 which is the lowest output that the the fuel cell can operate on. So, it is only needed to approximate the functions linearly for all $r_{fc}(t) \geq 0.2$. This is done by choosing a number of breakpoint pairs between which the function can be approximated linearly.

The function $f : \mathbb{R} \to \mathbb{R}$ has domain the interval $[l, u]$, with l < u . For $n \geq 2$, a number of n breakpoints is chosen $l = \xi^1 < \xi^2 < \ldots < \xi^{n-1} < \xi^n = u$. Then, we approximate f linearly by a set of linear functions between adjacent pairs of points. So, f is approximated by $\hat{f}(x)$ as shown in 6.5.3.

$$\hat{f}(x) = \sum_{p=1}^{n} \lambda_p f(\xi^p) \tag{6.5.3}$$

, where we require that

$$\sum_{p=1}^{n} \lambda_p = 1 \quad for\, p = 1, \ldots, n$$

$$\lambda_p \geq 0 \,, for\, p = 1, \ldots, n$$

and also an adjacency condition that at most two of the λ's are strictly positive. This condition on λ's can be modelled by introducing one binary variable y_p for each section which is 1 if the interval $\left[\xi^p, \xi^{p+1}\right]$is activated for $p = 1, 2, \ldots, n-1$.

As only one of the intervals is active, another constraint has to be introduced so that the sum of the binary variables is 1:

$$\sum_{p=1}^{n-1} y_p = 1 \quad for\, p = 1, \ldots, n$$

The efficiency equations then take the form of equation 6.5.4.

$$\eta(t) = \sum_{p=1}^{3} \left[y_p(t)\left(A_p \cdot r_p(t) + B_p\right)\right] \quad for\, p = 1, \ldots, n \tag{6.5.4}$$

with A, B being vectors that include the linear function coefficients for each function.

The following 3 intervals have been selected $[0.2, 0.325]$, $[0.325, 0.625]$, $[0.625, 1.0]$. The vectors A, B below are the coefficients for each linear function transforming the electrical efficiency function.

$$A = \begin{bmatrix} 20.8 & -7.4 & -12.7 \end{bmatrix}$$

$$B = \begin{bmatrix} 42.7 & 51.9 & 55.2 \end{bmatrix}$$

Similarly the vectors for the linear functions of each interval for the thermal efficiency are given below:

$$A = \begin{bmatrix} 45.5 & 27.7 & 18.6 \end{bmatrix}$$

$$B = \begin{bmatrix} 7.7 & 13.4 & 19.12 \end{bmatrix}$$

Figure 6.5.1 and 6.5.2 show the two functions and their linear approximations together with the cutting points.

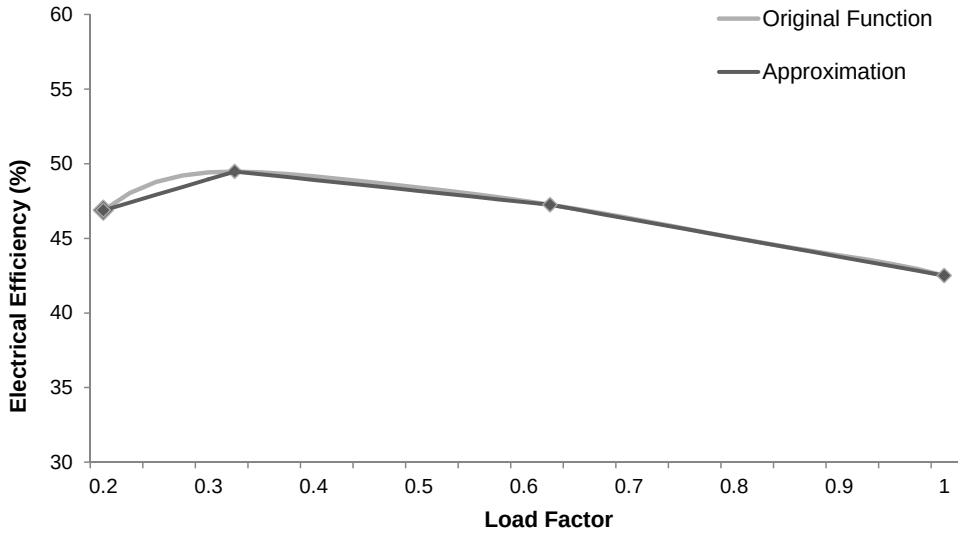

Figure 6.5.1: Linearisation of the electrical efficiency $\eta_{fc,ele}(t)$ of an SOFC showing cutting points

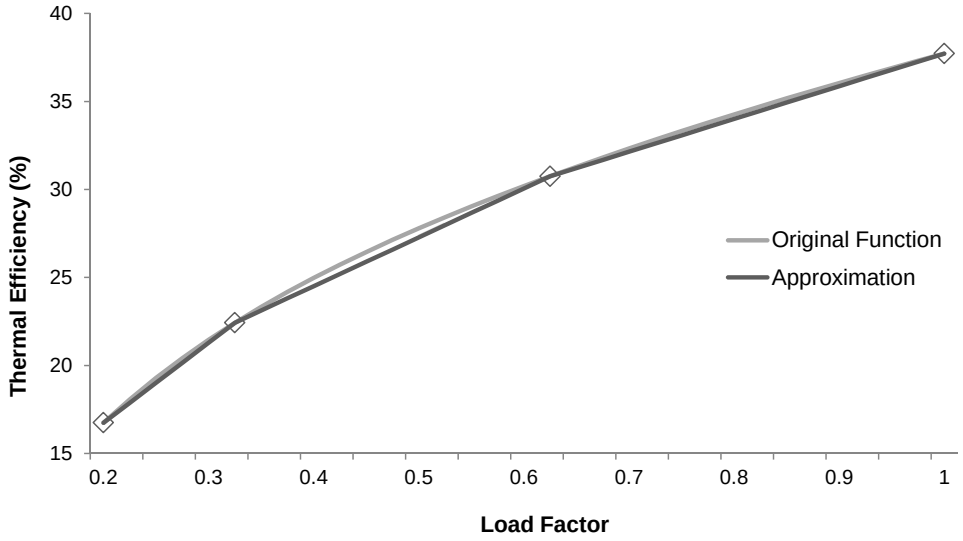

Figure 6.5.2: Linearisation of the thermal efficiency $\eta_{fc,heat}(t)$ of an SOFC showing cutting points

Apart from the efficiency equations, equation 6.4.1 is modified:

$$Q_{fc,ele}(t) = y_{fc}(t) \cdot P_{fc} \cdot \sum_{1}^{3} (y_p(t) \cdot r_p(t)) \tag{6.5.5}$$

and the following constraint has to be added:

$$\sum_{p=1}^{3} y_p(t) = 1 \tag{6.5.6}$$

The formulation of the model is still MINLP. Even though the efficiency equations have been linearised there are still equations in the model that non-linear. This step was essential to simplify the model and to allow it to run.

6.6 Modelling Results

The presentation of the results for each dataset is divided in two cases: first, a design without the option of a TST (Cases 1, 3, 5) and then a design with the storage tank included (Cases 2, 4, 6).

6.6.1 Winter Day Analysis

6.6.1.1 Case 1

The values for the objective function and optimisation variables for the winter day analysis are shown in Table 6.3. It can be seen from the table that the minimum CO_2 emissions occur for a fuel cell capacity of 1.9 kWe and a boiler of 11.1 kWth. This plant if operated as described below can result an approximate 7 % reduction in CO_2 emissions from the reference building on a winter day. This system will be referred to as "Case 1" in the analysis. The fuel cell capacity calculated is slightly higher compared to similar studies in literature. Hawkes et al. calculated systems ranging from 0.9 kWe to 1.3 kWe to provide a house with electricity and heat [73]. Many studies on fuel cell micro-CHPs are carried out around the 1 kW value for electrical capacity [14, 15, 18, 52]. However the value found here is still within the domestic range for fuel cell capacities: Ang et al. mention that fuel cell systems in the range of 1 to 10 kWe are suitable for dwellings [10]. Dodds et al. specify that domestic fuel cell micro-CHPs are most widely used around the 1-3 kW thermal output [51]. This higher value can be related to the temporal precision which ignores operational

limitations of the fuel cell in periods smaller than the averaged-out hourly timestep that is used here. Should 10-minute steps of dwelling energy demand were used, the fuel cell electrical capacity would be expected to have been found smaller.

Table 6.3: Optimisation variables for Case 1 and comparison with reference building

Variable	**Description**	**Units**	**Case 1**	**Reference Building**	**Reduction (%)**
P_{fc}	Fuel Cell Maximum Electrical Output	kW	1.9	-	
P_{gb}	Auxiliary Boiler Maximum Heat Output	kW	11.1	14.3	
z	Total CO_2 emissions	kgCO_2	41.8	45.1	7.3

The operating strategy is described by the load factor which shows how the units operate against their maximum output. The load factor variation for the fuel cell micro-CHP and the auxiliary gas boiler is shown in Figure 6.6.1.

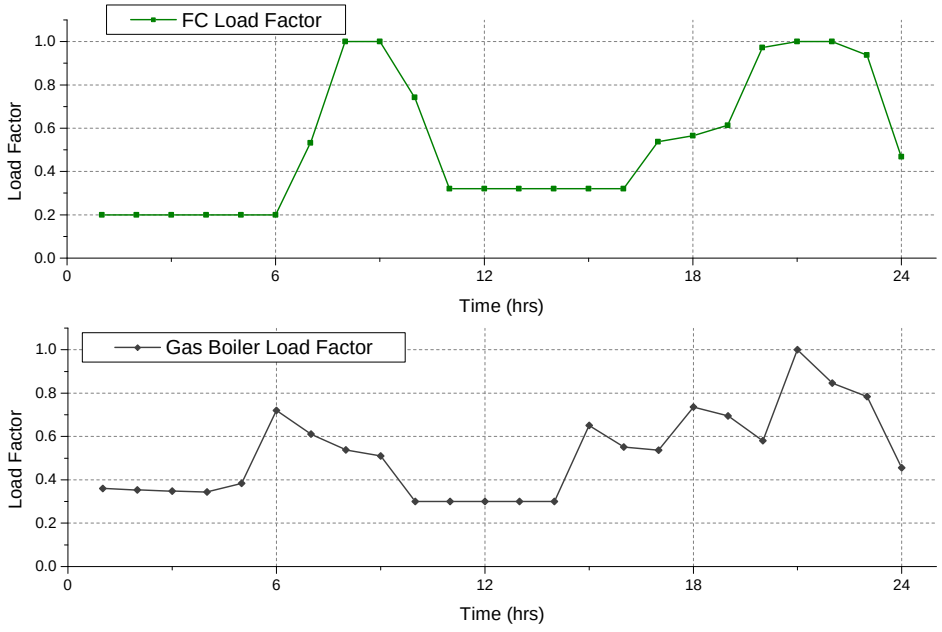

Figure 6.6.1: Graph representing the load factor of the fuel cell micro-CHP and auxiliary boiler for Case 1

Figure 6.6.2 shows the variation of electrical and thermal efficiencies of the fuel cell

micro-CHP for the 24 hour period.

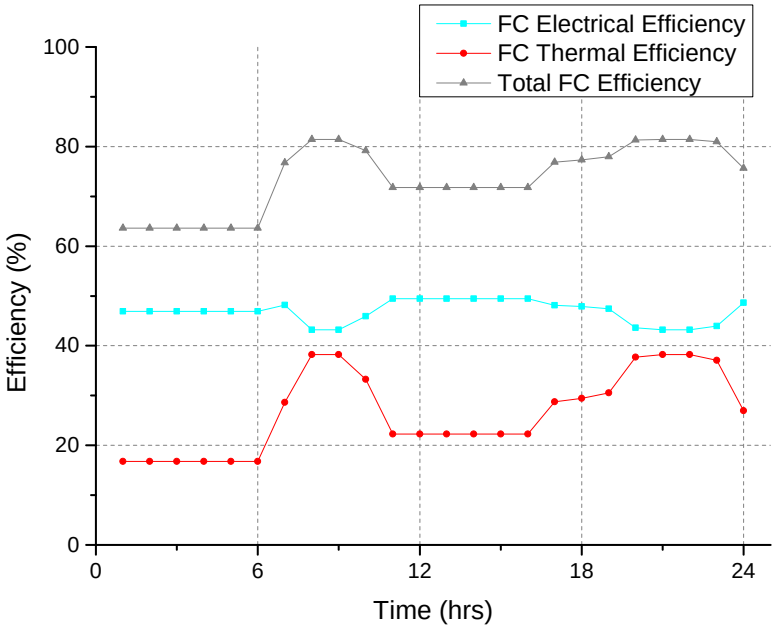

Figure 6.6.2: Graph representing the electrical and thermal efficiencies of the fuel cell micro-CHP for Case 1

Figures 6.6.3 and 6.6.4 represent the electricity and heat output of the fuel cell and auxiliary gas boiler together with the electricity input from the grid. The two graphs show that the fuel cell energy production peaks between 7-11 in the morning and 20-22 in the evening following the occupancy patterns. Also it can be observed from the two figures that the the fuel cell is sized to cover most of the electricity demand and a small proportion of the heating demand. The total electricity input from the grid is kept to a total of 2.25 kWh on the whole day as it is carbon intensive and increases the objective function. Electricity from the grid is only imported at times of high electricity demand in the morning.

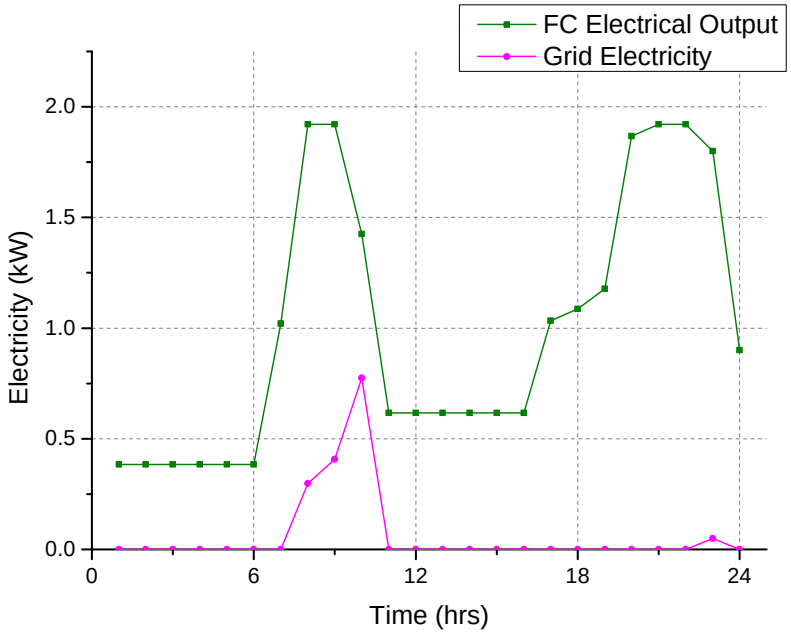

Figure 6.6.3: Graph representing the electricity output of the fuel cell micro-CHP and grid electricity for Case 1

The high heat demand of a winter day cannot be covered by the fuel cell micro-CHP itself but requires the input from an auxiliary gas boiler. The gas boiler operates constantly during the day matching the remaining heat demand. The fuel cell covers a heating load which varies between 0.1-1.9 kW.

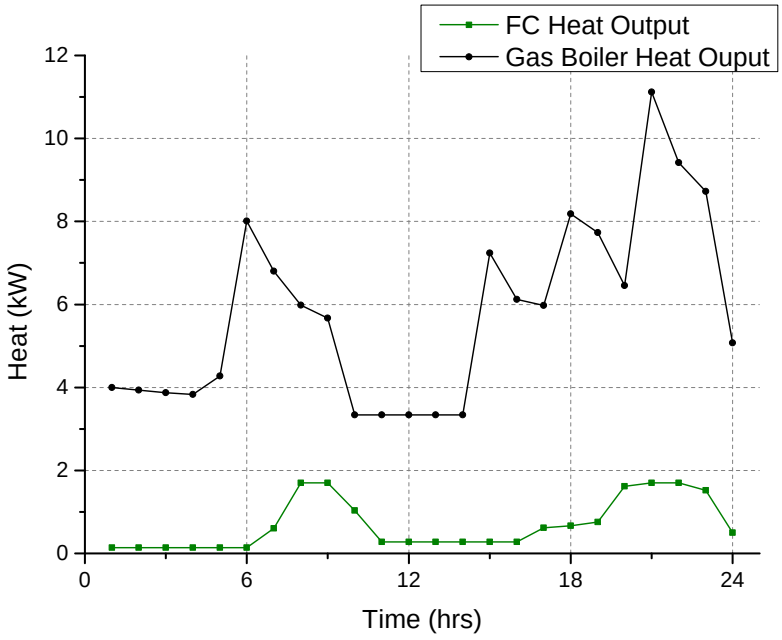

Figure 6.6.4: Graph representing the heat output of the fuel cell micro-CHP and auxiliary gas boiler for Case 1

6.6.1.2 Case 2

The addition of the thermal storage tank has a significant effect on the total emissions and also on the maximum capacity of plant required to meet the demand. A summary of the results is shown on Table 6.4. The fuel cell capacity is similar to Case 1 but the boiler capacity is lower. This happens because the boiler at times of high space heating load is not needed, as that peak load heat can be supplied by the TST. The size of the thermal storage tank is 490 L which despite being within the expected range it could cause space problems.

Table 6.4: Optimisation variables for Case 2 and comparison with reference building

Variable	Description	Units	Case 2	Reference Building	Reduction (%)
P_{fc}	Fuel Cell Maximum Electrical Capacity	kW	1.9		
P_{gb}	Boiler Maximum Output	kW	8.5	14.3	
V_{st}	Storage Volume	m^3	0.49		
z	Total CO_2 emissions	kgCO_2	40.9	45.1	9.3

Figure 6.6.5 shows the variation of the load factor of the fuel cell and boiler of Case 2.

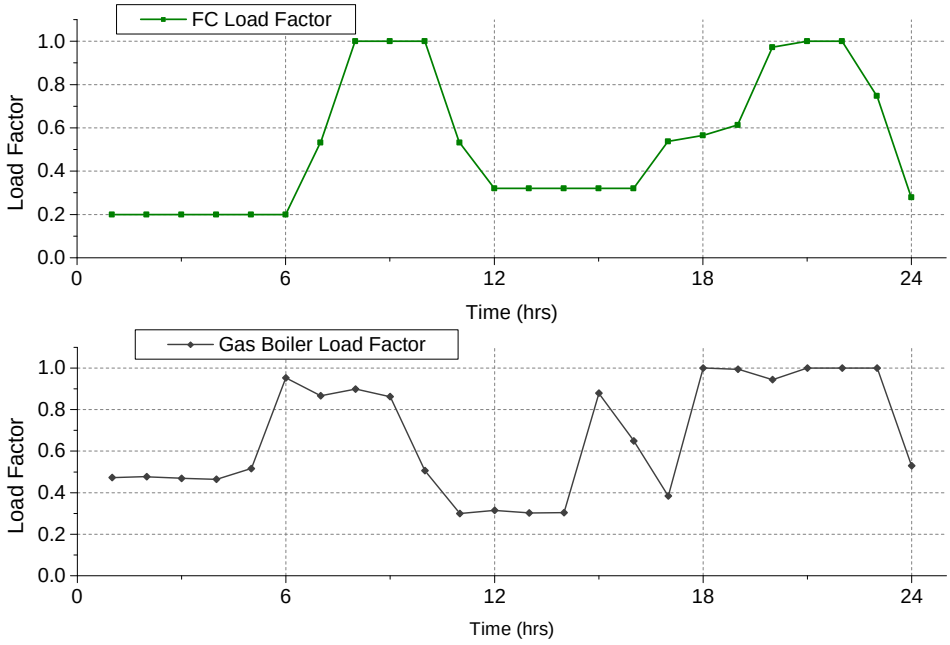

Figure 6.6.5: Graph representing the load factor of the fuel cell micro-CHP and auxiliary boiler for Case 2

This configuration with the storage tank allows the fuel cell to operate even at low heat demand as fuel cell heat can be stored in the TST. This shows that the constant operation of the fuel cell is favoured because of the fuel cell heat which can be stored.

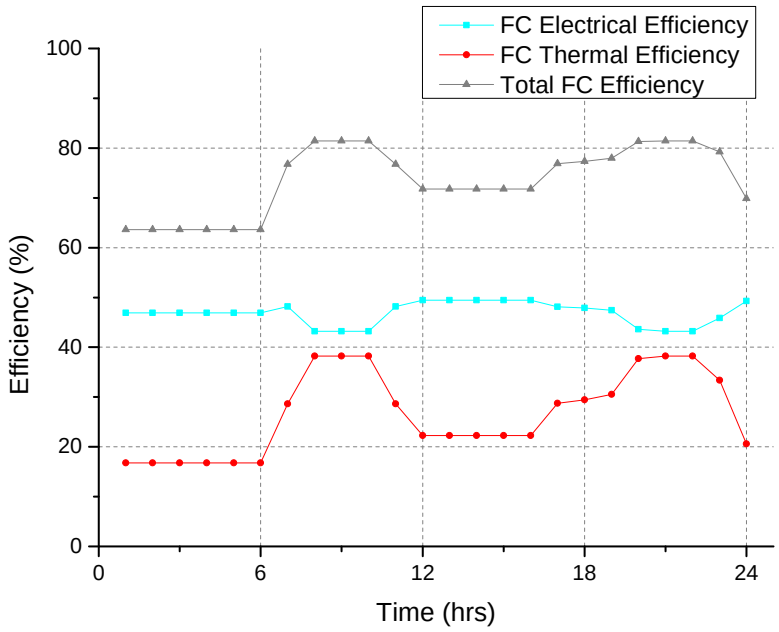

Figure 6.6.6: Graph representing the electrical and thermal efficiencies of the fuel cell micro-CHP and auxiliary boiler for Case 2

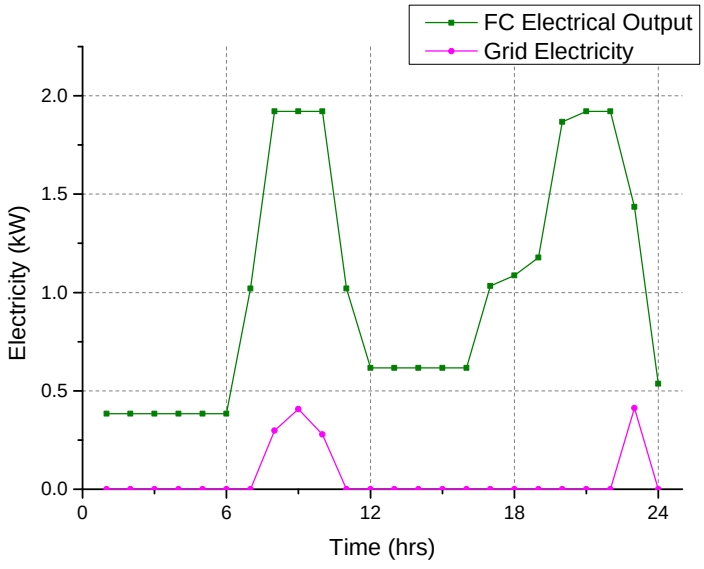

Figure 6.6.7: Graph representing the electricity output of the fuel cell micro-CHP and grid electricity for Case 2

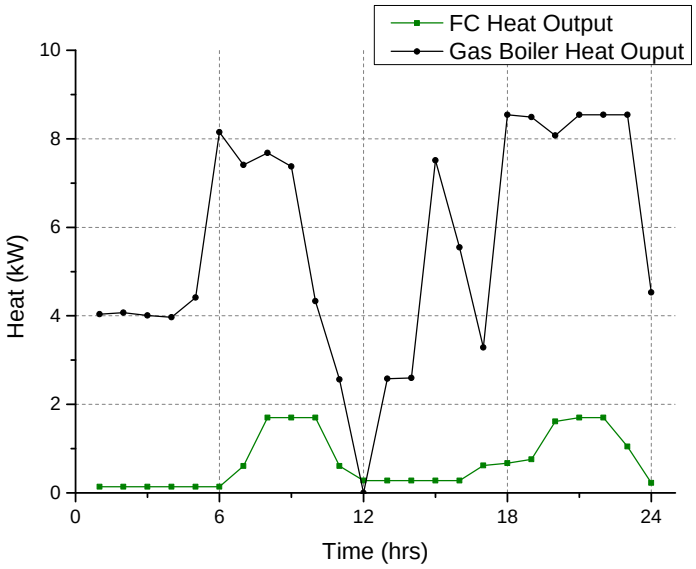

Figure 6.6.8: Graph representing the heat output of the fuel cell micro-CHP and auxiliary boiler for Case 2

The effect of the storage tank is more obvious in figures 6.6.8a, 6.6.9 and 6.6.10 where it can be seen that in the evening hours when heat demand is high, the heat output of the auxiliary boiler is supplemented by heat from the tank. At the end of the 24 hours there is still heat left in the tank which can be used in the next hours if necessary.

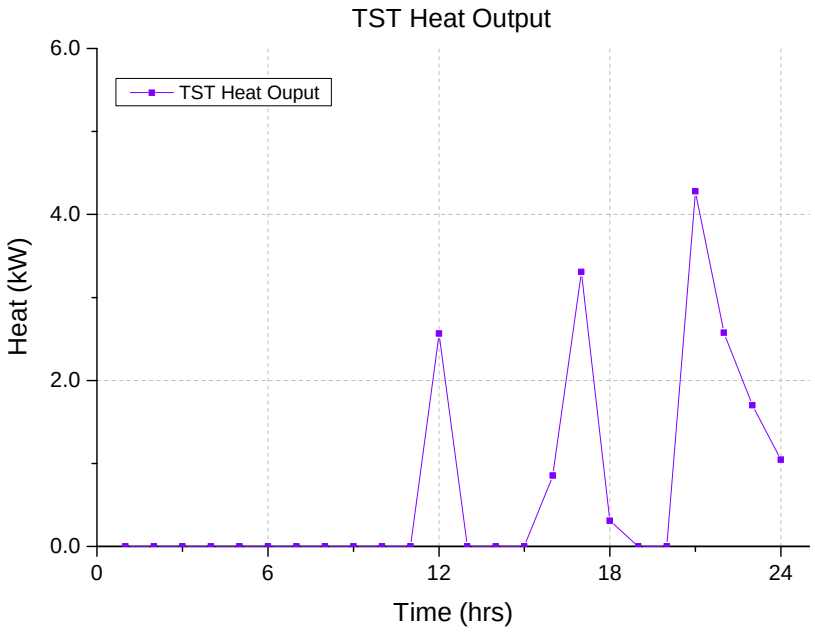

Figure 6.6.9: Graph representing the heat output from the thermal storage tank to the house for Case 2

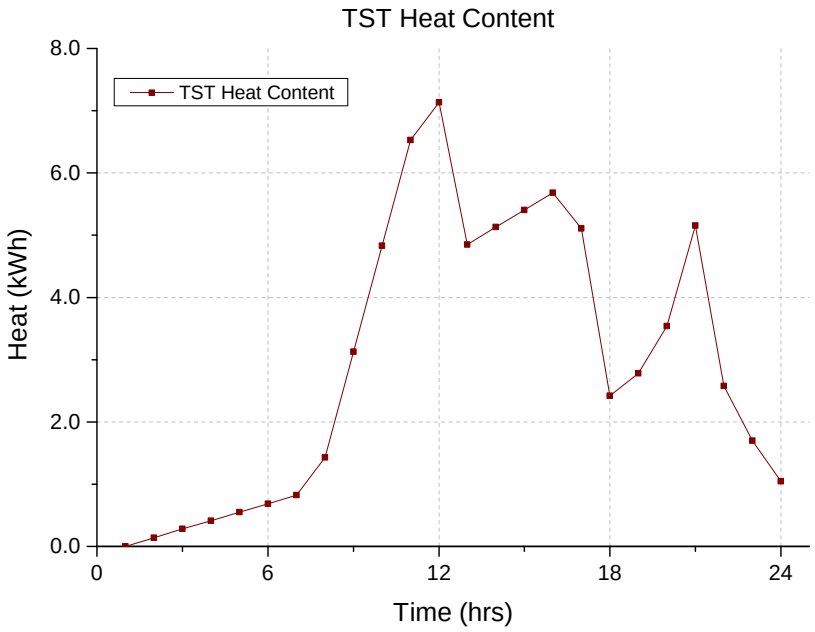

Figure 6.6.10: Graph representing the heat content of the thermal storage tank for Case 2

6.6.2 Summer day analysis

6.6.2.1 Case 3

Optimisation for the summer day has different results from the winter day. The results are summarised in Table 6.5. The total percentage reduction in emissions from the reference building is higher than in Case 1 and 2 and reaches approximately 22%. The optimisation variables also have different values from the winter peak day: the fuel cell is sized at a similar capacity as before and covers the electricity load which has not changed from the winter operation. The gas boiler maximum output has fallen down to 1 kW and serves the DHW load which cannot be covered entirely by the fuel cell's heat output.

Table 6.5: Optimisation variables for Case 3 and comparison with reference building

Variable	Description	Units	Case 3	Reference Building	Reduction (%)
P_{fc}	Fuel Cell Maximum Electrical Capacity	kW	2.0	-	
P_{aux}	Boiler Maximum Output	kW	1.0	14.3	
z	Total CO2 emissions	kgCO_2	12.9	16.5	21.6

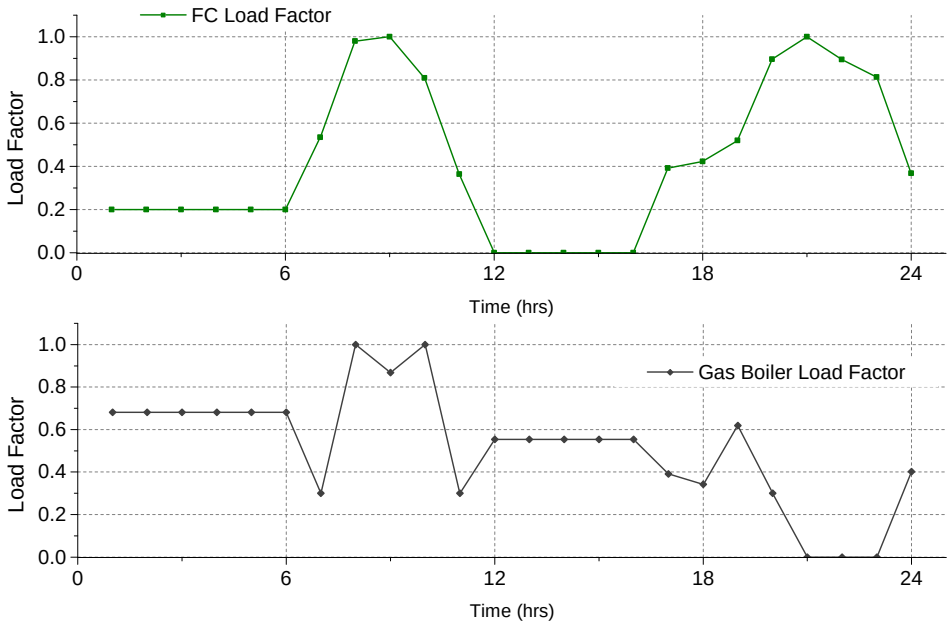

Figure 6.6.11: Graph representing the load factor of the fuel cell micro-CHP and auxiliary boiler for Case 3

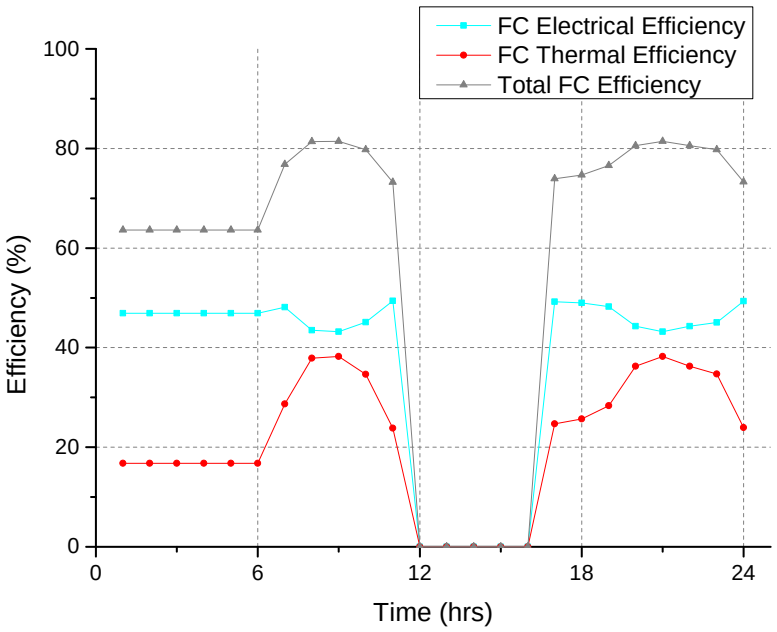

Figure 6.6.12: Graph representing the electrical and thermal efficiencies of the fuel cell micro-CHP for Case 3

Figure 6.6.13 shows that between 12.00 and 16.00, grid electricity is imported rather than generated from the fuel cell. Although at first this might seem unnatural it occurs because at those points the electricity and heat demands are low and the fuel cell would have to operate at low load factor which would result a low total efficiency. In addition to that the fuel cell and boiler operation is constrained to a minimum 20% and 30% turn down ratio respectively. This means that the fuel cell can generate 400 We (20% of 2 kWe) and less than 200 Nth while the house requirement then is 300 We and 600 Nth. It is therefore more efficient to generate the heat from the boiler and import electricity from the grid for that time period. This can be confirmed by looking at figure 6.6.14 which shows that the boiler operates between 12.00 and 16.00 to cover the heat load.

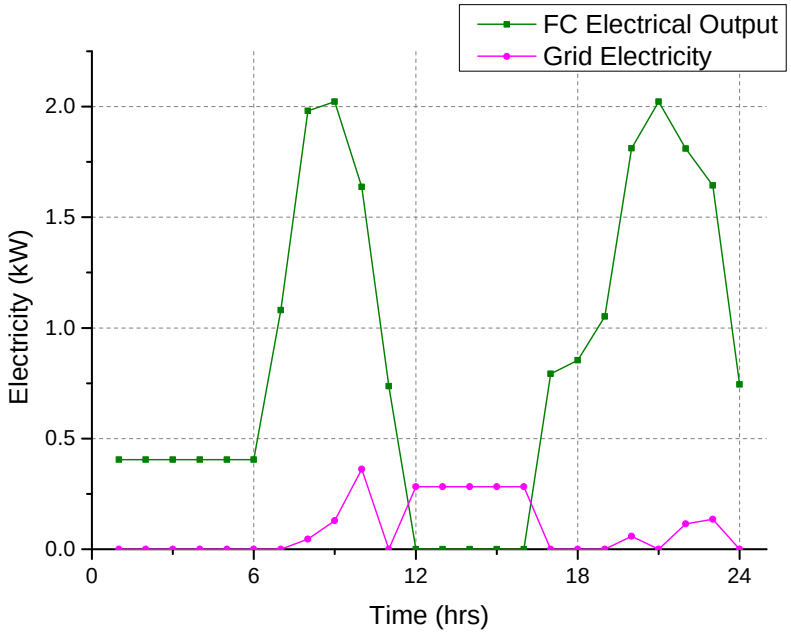

Figure 6.6.13: Graph representing the electricity output of the fuel cell micro-CHP and grid electricity for Case 3

The heat-to-electricity demand of the dwelling in the summer day analysis is low and varies between 1-2 for the majority of the time steps. Therefore the large reduction in CO_2 emissions (up to 20%) from the optimised system shows that the fuel cell micro-CHP operates better for types of dwellings with with low heat to power demand compared to the winter day where the heat-to-electricity ratio goes up to 10 for some time steps.

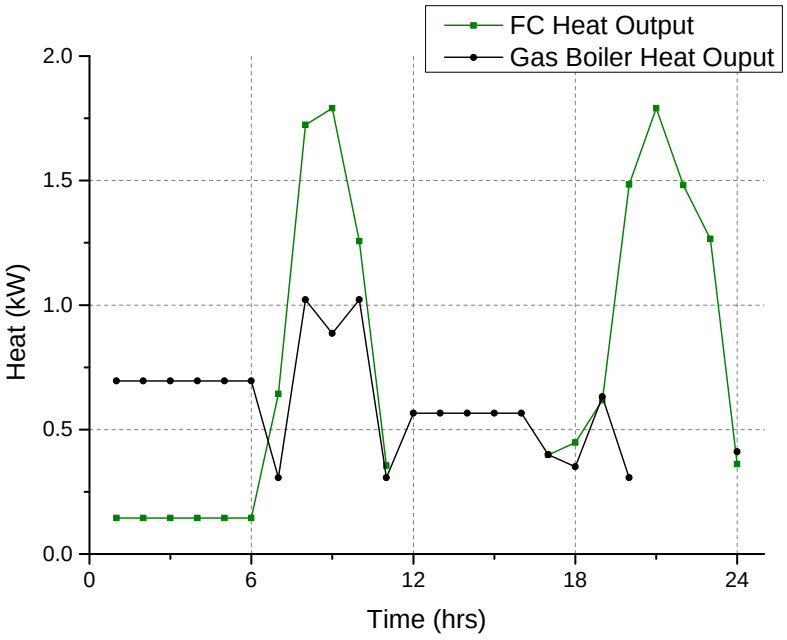

Figure 6.6.14: Graph representing the heat output of the fuel cell micro-CHP and auxiliary boiler for Case 3

6.6.2.2 Case 4

The inclusion of thermal storage in the system for the summer day represents an approximate 21% reduction from the reference building. This is similar to Case 3 where no storage is included. This suggests that systems with lower heat-to-power ratio (as in the summer day) seem to benefit less from the inclusion of thermal storage.

Table 6.6: Optimisation variables for Case 4 and comparison with reference building

Variable	**Description**	**Units**	**Case 4**	**Reference Building**	**Reduction (%)**
P_{fc}	Fuel Cell Maximum Electrical Capacity	kW	2.2	-	-
P_{aux}	Boiler Maximum Output	kW	2.3	14.3	-
V_{st}	Storage Volume	m^3	0.29	-	-
z	Total CO2 emissions	kgCO_2	13.1	16.5	20.6

The capacity of the auxiliary boiler is decreased from Case 2 from 8.5 to 2.3 kW but the capacity of the fuel cell is similar (from 1.9 kW to 2.2 kW). There is no gas boiler product rated at 2.3 kW and this number is only indicative of the capacities needed to satisfy demand.

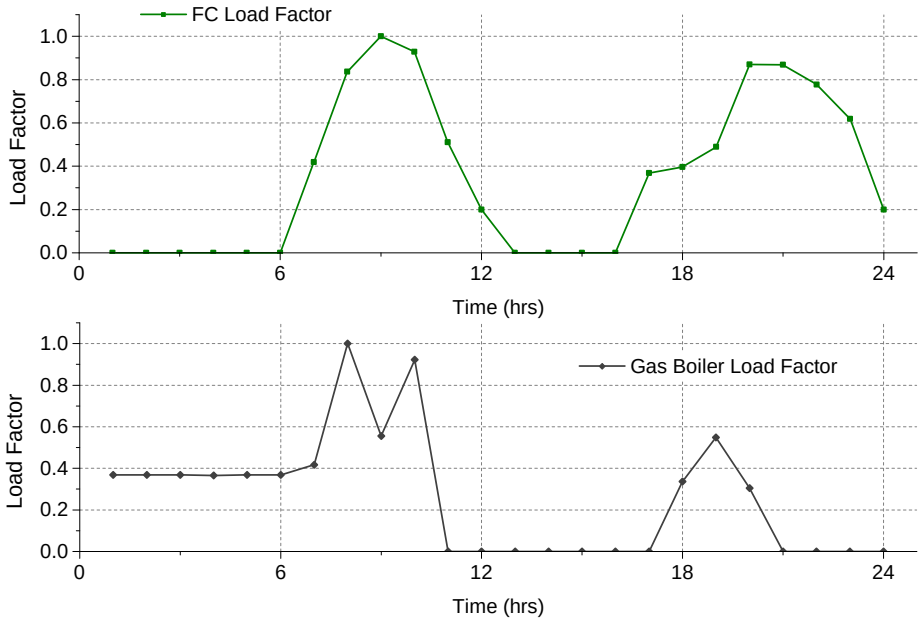

Figure 6.6.15: Graph representing the load factor of the fuel cell micro-CHP and auxiliary boiler for Case 4

The size of the storage tank in this scenario is 290 L which lies within the availability limits of products. The effect of the storage tank in the summer scenario does not seem to benefit the reduction of CO_2 emissions compared to Case 3.

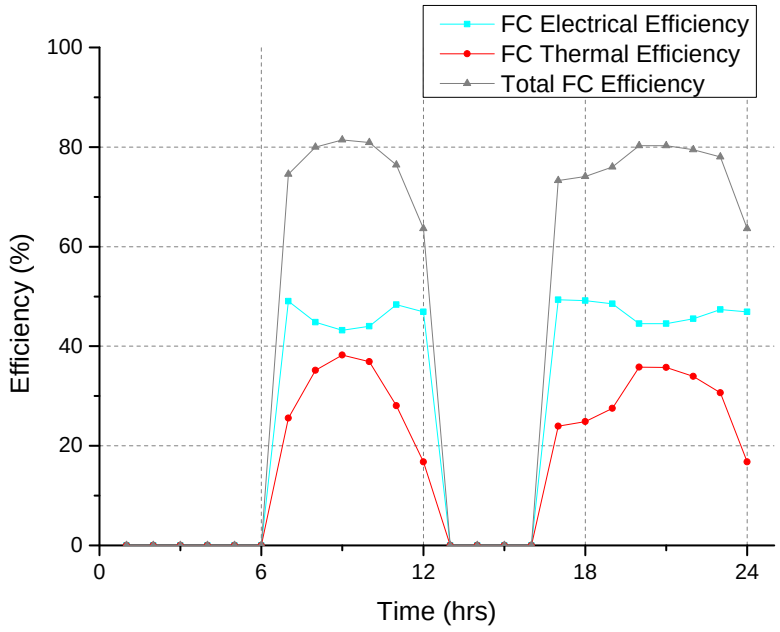

Figure 6.6.16: Graph representing the electrical and thermal efficiencies of the fuel cell micro-CHP and auxiliary boiler for Case 4

Figure 6.6.15 shows that the operation of the auxiliary boiler is reduced compared to Case 3 (figure 6.6.11). The boiler operates only in the morning hours between 7.00-10.00 and 18.00-20.00 when DHW is needed. The fuel cell also only operates at periods of high electricity demand, between 7.00-10.00 and 17.00-22.00. This can be seen in figure 6.6.16.

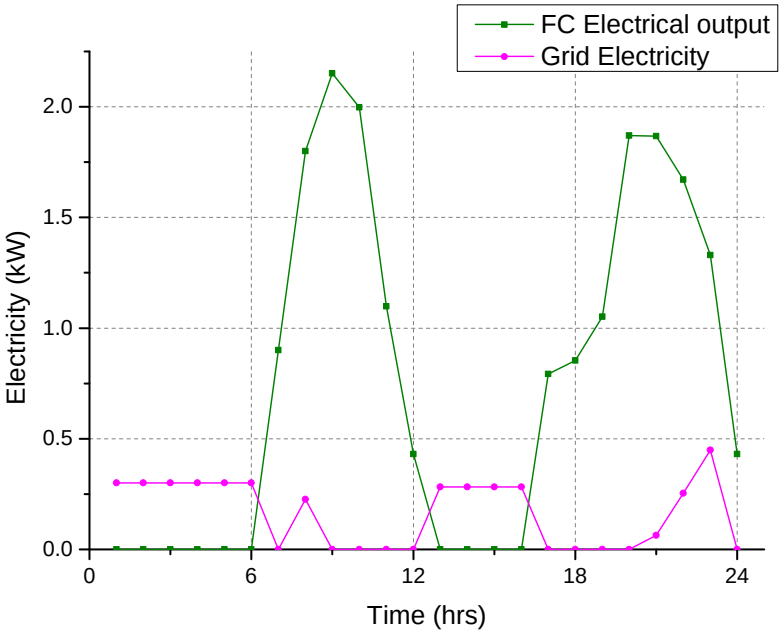

Figure 6.6.17: Graph representing the electricity output of the fuel cell micro-CHP and grid electricity for Case 4

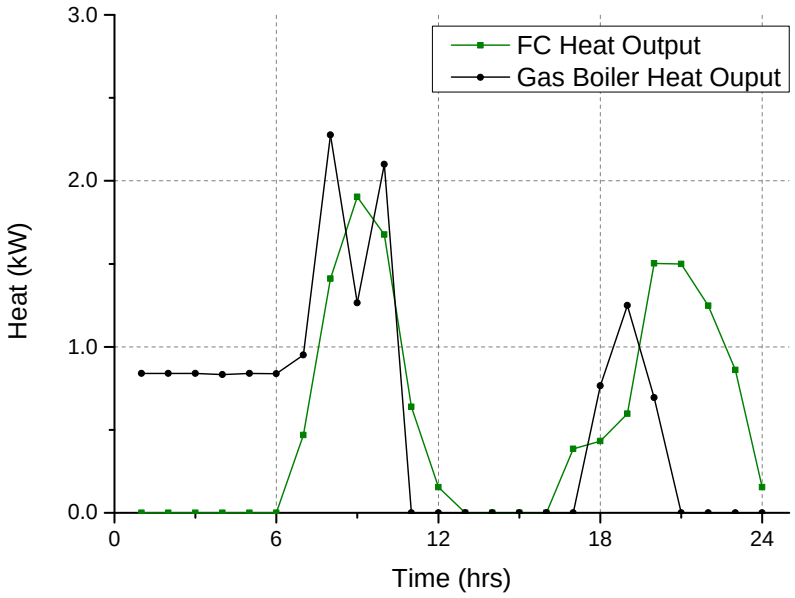

Figure 6.6.18: Graph representing the heat output of the fuel cell micro-CHP and auxiliary boiler for Case 4

Figures 6.6.17 and 6.6.18 demonstrate that at periods of low energy demand between 11.00-16.00 both the fuel cell and boiler are not operating and the small electricity load is covered by import from the grid and by utilising the heat stored in the storage tank. This is more efficient from operating the fuel cell to supply a small electricity load.

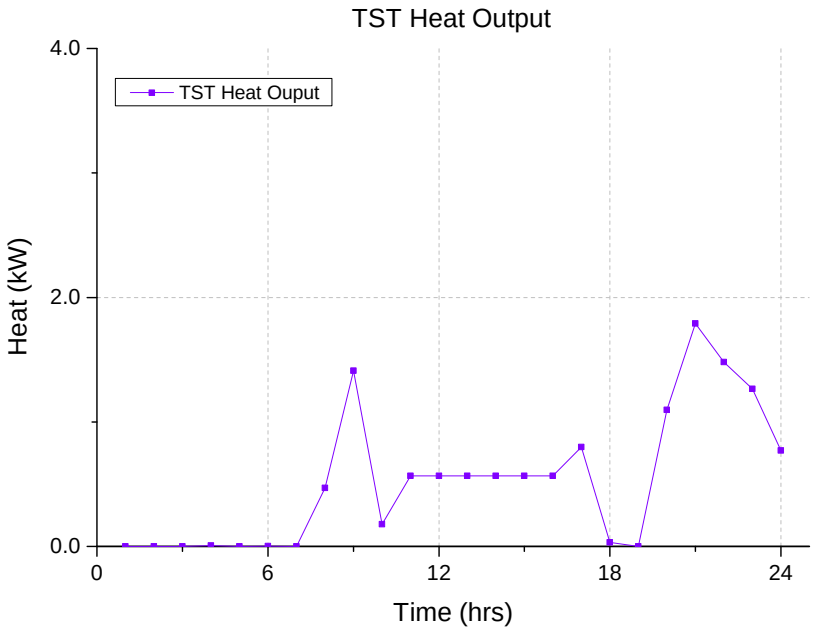

Figure 6.6.19: Graph representing the heat output from the thermal storage tank to the house for Case 4

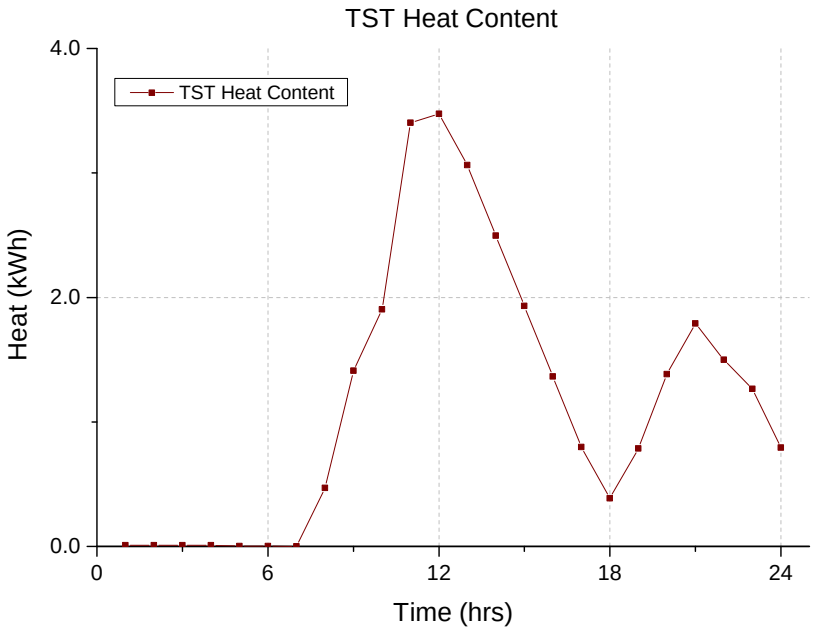

Figure 6.6.20: Graph representing the heat content of the thermal storage tank for Case 4

Figures 6.6.19 and 6.6.20 show that the storage tank is "charged" first before it releases heat to the house.

The analysis for 48 hours will identify the optimum sizing of these systems taking into account a more diverse dataset that resembles better a whole year period.

6.6.3 Combined 48-hour Dataset

6.6.3.1 Case 5

Table 6.7 shows the optimisation results for the 48-hour analysis. The larger data set increases the complexity of the problem causing converging difficulties to the solver.

Table 6.7: Optimisation variables for Case 5 and comparison with reference building

Variable	Description	Units	Case 5	Reference Building	Reduction (%)
P_{fc}	Fuel Cell Maximum Electrical Capacity	kW	2.0	-	-
P_{aux}	Boiler Maximum Output	kW	11.0	14.3	-
z	Total CO2 emissions	kgCO_2	61.2	61.5	0.05

The design proposed in Case 5 cannot offer any reduction in CO_2 emissions from the reference building. This is caused by the gas boiler which is sized to cover both the winter and summer load and its 30% minimum turn down ratio. Sizing the boiler for the winter load ensures that heat demand would be covered at all times but it creates an issue in the summer. The boiler's minimum heat output in some timesteps exceeds the low summer heat demand and this unused heat causes the additional CO_2 emissions. This is demonstrated for the summer period in figures 6.6.21 and 6.6.24. This suggests that this configuration might not be ideal for primary energy consumption reduction. The addition of a storage tank between the load and the fuel cell should enable the fuel cell to operate more hours and reduce the operation of the boiler. This case will be examined next.

A solution was also obtained for a lower 25% limit for the turn down of the boiler and the resulting CO_2 emissions were reduced to 60.6 kgCo2, confirming the point made above.

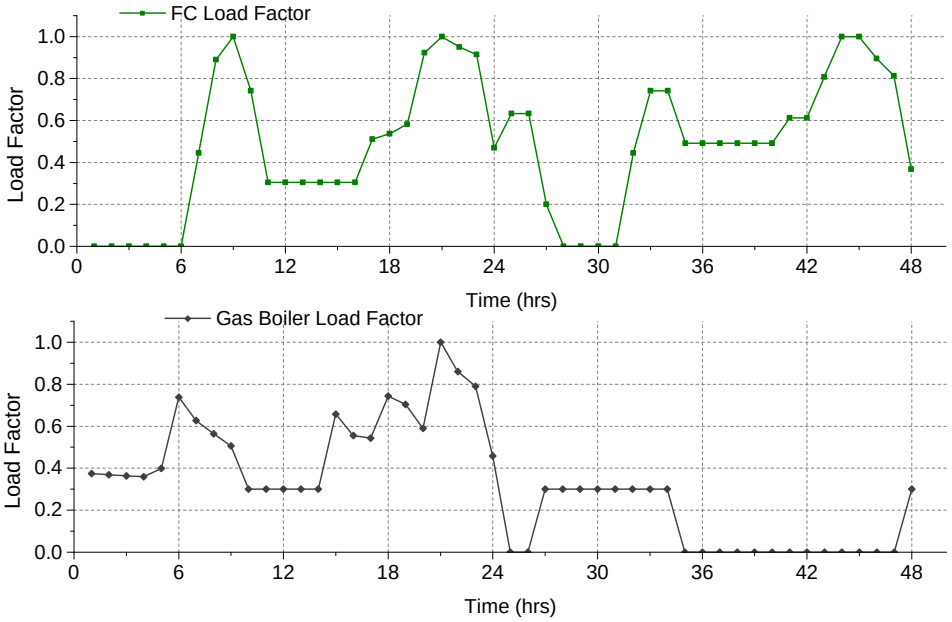

Figure 6.6.21: Graph representing the load factor of the fuel cell micro-CHP and auxiliary boiler for Case 5

The fuel cell operates most of the time unless it cannot cover the electricity load or it is more efficient to cover the house loads by a combination of electricity from the grid and heat from the boiler. This can be seen in figures 6.6.24 and 6.6.23.

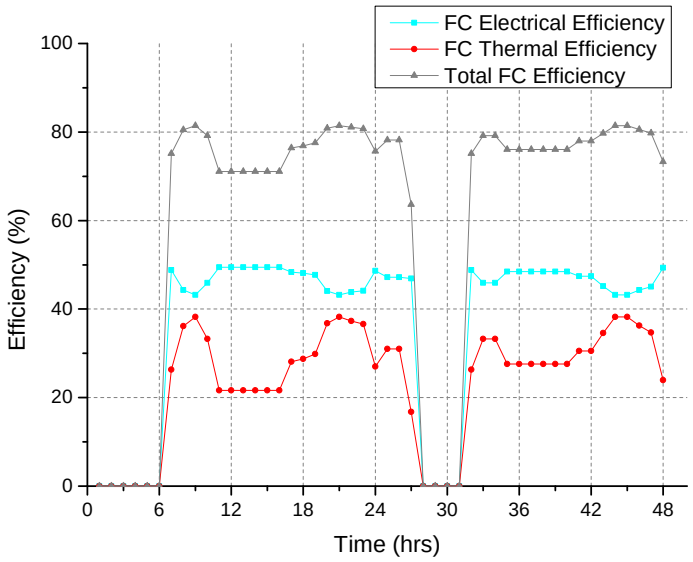

Figure 6.6.22: Graph representing the electrical and thermal efficiencies of the fuel cell micro-CHP for Case 5

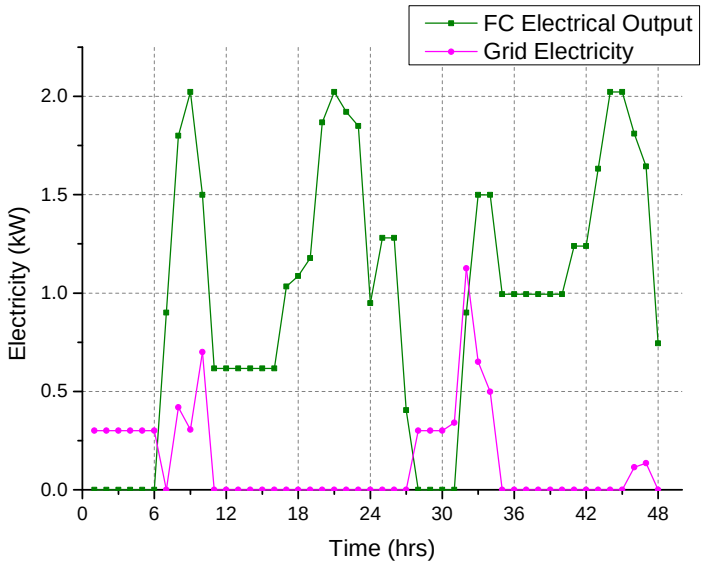

Figure 6.6.23: Graph representing the electricity output of the fuel cell micro-CHP and grid electricity for Case 5

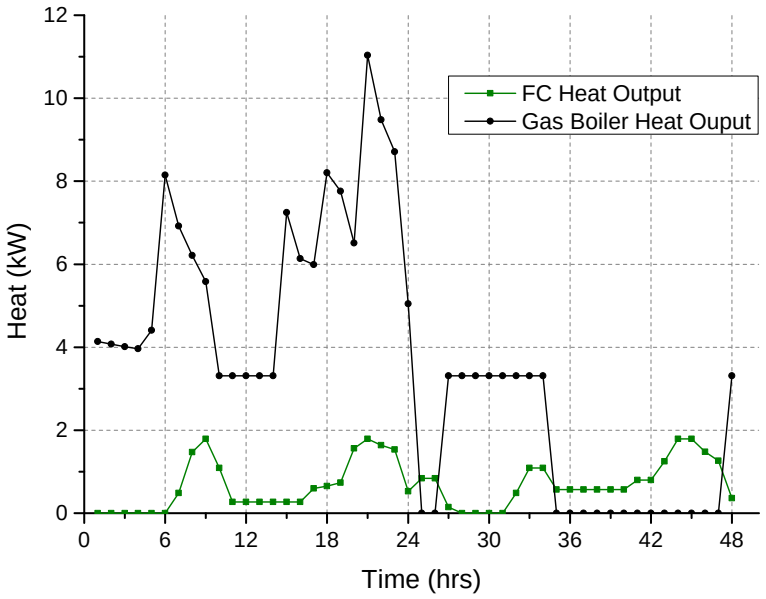

Figure 6.6.24: Graph representing the heat output of the fuel cell micro-CHP and auxiliary boiler for Case 5

6.6.3.2 Case 6

Table 6.8 shows the optimisation results for the 48 hour analysis for a system that includes thermal storage in the design.

Table 6.8: Optimisation variables for Case 6 and comparison with reference building

Variable	**Description**	**Units**	**Case 6**	**Reference Building**	**Reduction (%)**
P_{fc}	Fuel Cell Maximum Electrical Capacity	kW	2.5	-	-
P_{aux}	Boiler Maximum Output	kW	10.3	14.3	-
V_{st}	Storage Volume	m^3	0.76	-	-
z	Total CO2 emissions	$kgCO_2$	54.6	61.5	11.3

Case 6 represents an 11.30% reduction from the reference building. The optimisation process sized the fuel cell at 2.5 kW a larger capacity compared to all cases. This

capacity enables the fuel cell to operate at high load factors and provide heat to the storage tank.

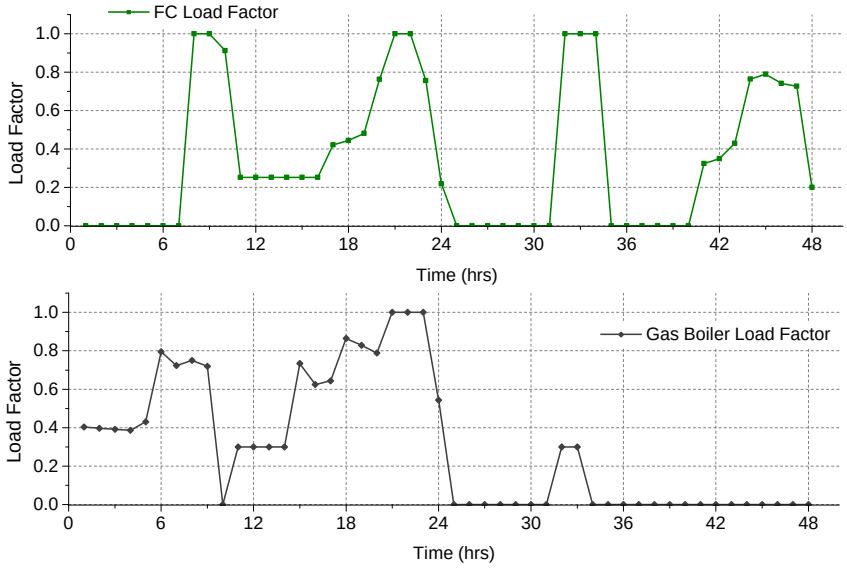

Figure 6.6.25: Graph representing the load factor of the fuel cell micro-CHP and auxiliary boiler for Case 6

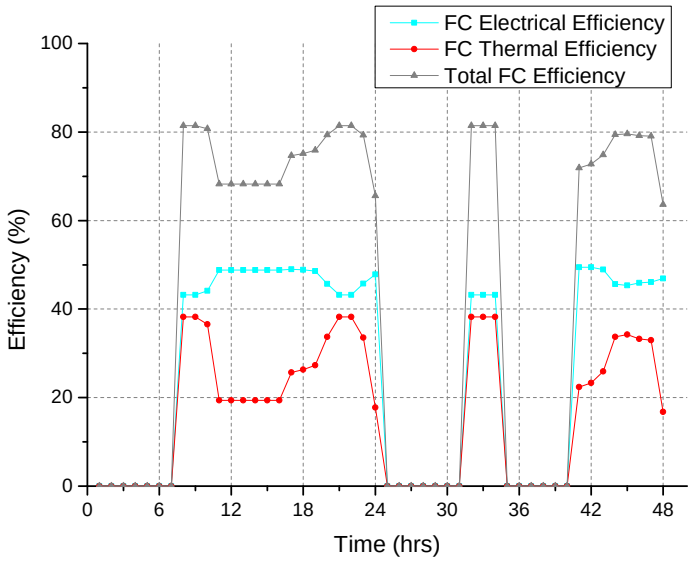

Figure 6.6.26: Graph representing the electrical and thermal efficiencies of the fuel cell micro-CHP for Case 6

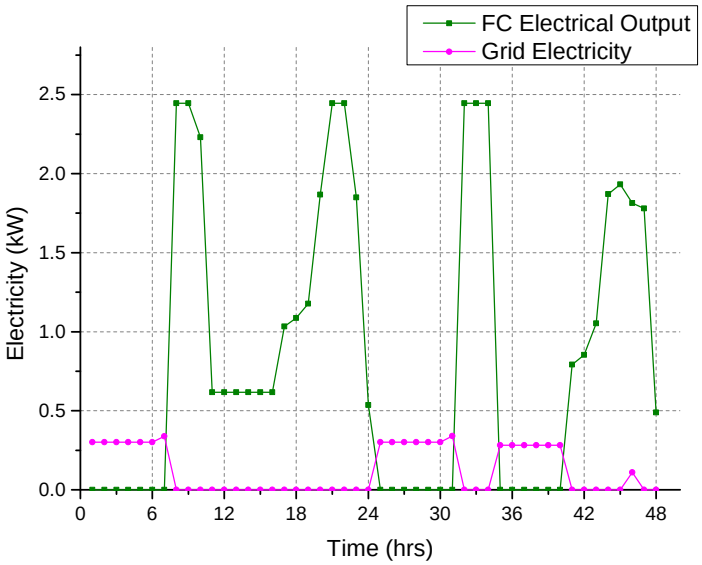

Figure 6.6.27: Graph representing the electricity output of the fuel cell micro-CHP and grid electricity for System 6

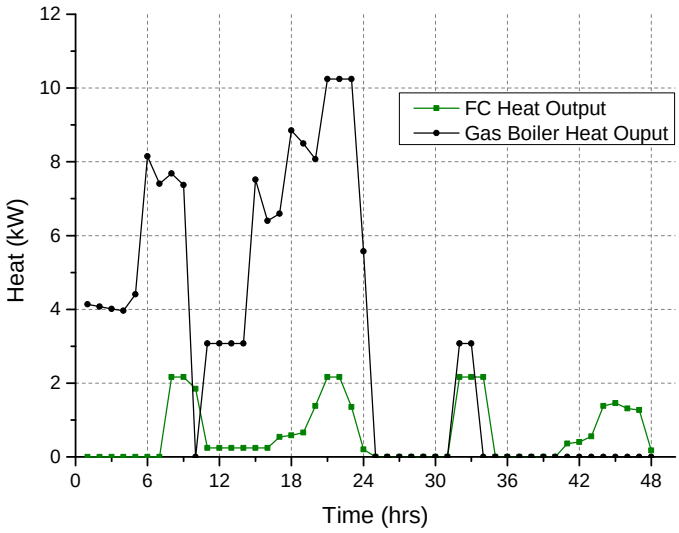

Figure 6.6.28: Graph representing the heat output of the fuel cell micro-CHP and auxiliary boiler for Case 6

Figures 6.6.25 and 6.6.29 show the effect of the storage tank: The boiler switches off between hours 25 and 48 and the majority of heat is provided by the thermal storage tank. In figure 6.6.30 it can be seen that heat stored in the tank during winter operation when the fuel cell is on, is used in the summer day to cover the demand (which is entirely for DHW). This case represents two extremes, a winter and a summer day one after the other, however it shows that heat from a period of high fuel cell utilisation can be used in periods of lower heat demand when the fuel cell is not necessarily operational.

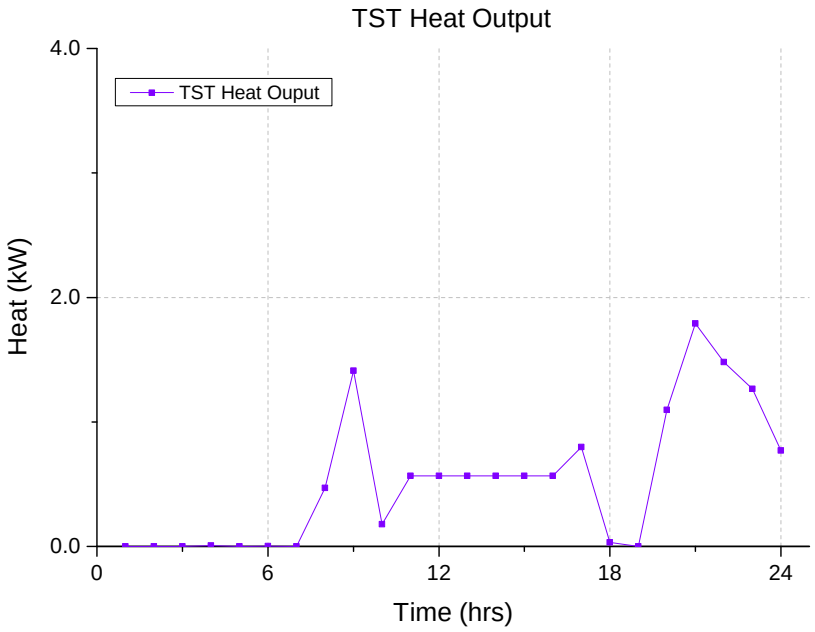

Figure 6.6.29: Graph representing the heat output from the thermal storage tank to the house for Case 6

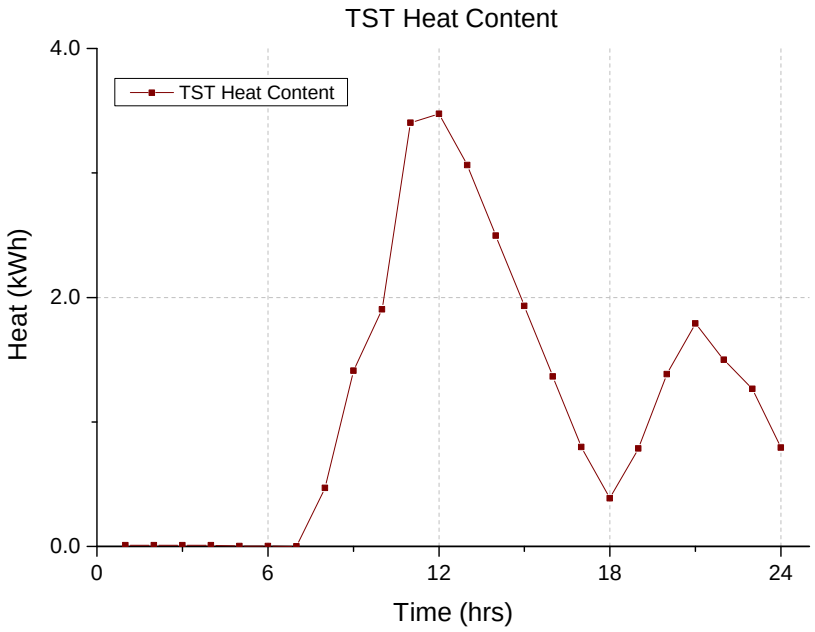

Figure 6.6.30: Graph representing the heat content of the thermal storage tank for Case 6

A comparison between Case 5 and 6 suggests that the storage tank increases the efficiency of the system allowing some of the unwanted heat of the fuel cell to be stored in the storage tank. That minimises electricity import as the fuel cell can operate for longer periods.

6.6.4 Summary of Results

Table 6.9 summarises the reduction in emissions from the systems examined.

Table 6.9: Summary of CO_2 emissions of all cases examined using model 1

	System Value	Reference Value	Reduction
Case 1	41.8 kgCO2	45.06 kgCO2	7.81%
Case 2	40.9 kgCO2	45.06 kgCO2	10.11%
Case 3	12.9 kgCO2	16.46 kgCO2	20.53%
Case 4	13.1 kgCO2	16.46 kgCO2	17.80%
Case 5	61.2 kgCO2	61.5 kgCO2	0.05%
Case 6	54.6 kgCO2	61.5 kgCO2	11.3%

Figure 6.6.31 shows the total CO_2 emissions of the designs produced by each case study broken down to the emissions caused by the various systems. The effect of the additional operation of the boiler on total emissions can be seen for cases 5 and 6.

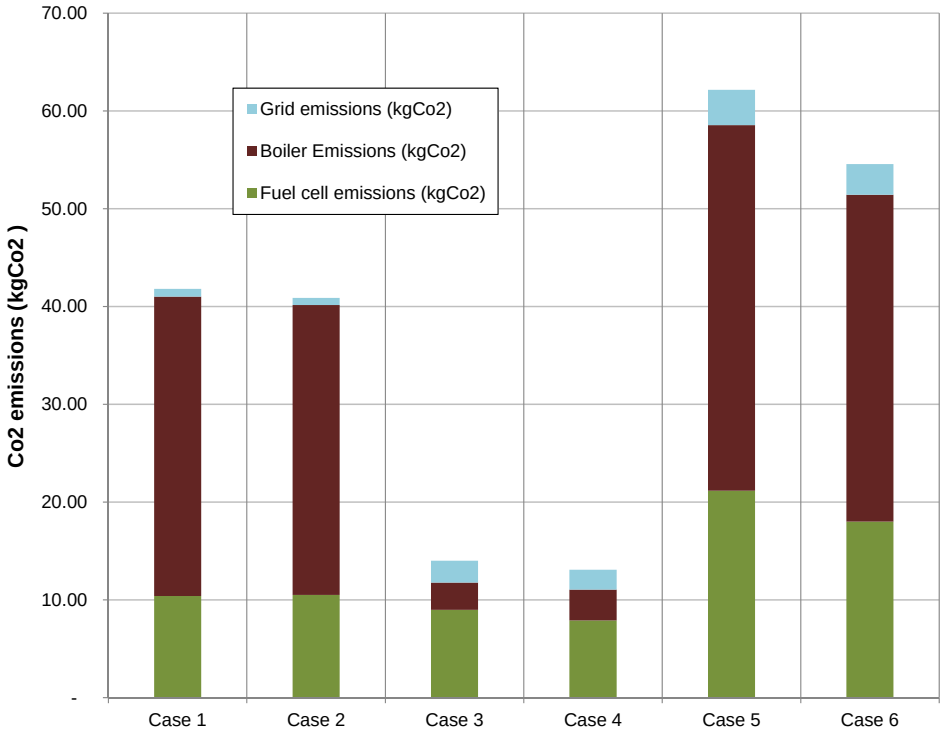

Figure 6.6.31: Graph representing the CO_2 emissions of all systems presented in Chapter 6

6.7 Discussion and Critical Analysis

In this chapter a MINLP model has been presented for evaluating a SOFC based micro-CHP design in a dwelling. The model identifies the optimal values for the maximum capacity and output of plant considering simultaneously a variety of electricity and heat sources included in the proposed design.

It has been established that a micro-CHP system when optimised on its environmental benefits can provide significant reduction in the dwelling's CO_2 emissions. This reduction can reach up to 20% depending on the design and operation. The fuel cell maximum electrical capacity ranges from 1.9-2.5 kW for all cases which is close to most existing micro-CHP products that are sized around that value. This

provides some indirect validation of the results from the industry, as the fuel cell based micro-CHP products are at the 1-3 kW capacity.

A TST can increase the energy availability of the system and reduce peaks of heat demand in winter. Including a TST in the design, allows for reduced sizing of plant as it was the case with the gas boiler in the winter day case studies. The boiler's capacity dropped from 11 kW to 8.5 kW while at the same time the hours of operation also dropped. The fuel cell system achieved longer operation and higher reductions in CO_2 emissions when storage was available. The TST allows the fuel cell micro-CHP to cover the majority of the electricity demand and to minimise electricity import from the electricity grid even when there is no heat demand by storing the recovered heat in the thermal storage tank. The effect of the TST on CO_2 emissions reduction is greater in winter than in summer. The 48 hour analysis that includes a more complete data set with winter and summer days, showed that a thermal storage tank is essential for the system to provide emissions reduction. The sizing of the boiler to cover the winter load and its operational turn down constraints cause the system to produce some additional CO_2 emissions.

The results showed that the fuel cell in some cases starts and stops twice during the examined periods (case 4, case 5, case 6). SOFCs operate at high temperatures so when an SOFC cools down to the environmental temperature it stresses the stack materials and results in degradation of the components [107]. Also, it would take some time for it to warm up again to 700 °C-100 °C [108] and restart producing electricity. The operation of SOFCs micro-CHPs fuelled by natural gas is dependent on the sufficiency of heat provided by the fuel cell to the reformer to maintain the steam reforming reaction. On start up however, when heat from the fuel cell is not available, the reformer is designed to operate on partial oxidation which is an exothermic reaction. Partial oxidation and steam reforming occur combined at the reformer from low output to full output operation [108]. Recent research is focused on lowering SOFC operating temperatures in order to reduce thermal stress and increase start-up times. Alvarez et al. studied the optimisation of a hybrid start-up process of an intermediate temperature SOFC, showing that a start-up time of 286 s can be achieved [105]. In terms of thermal management an option is to seal with insulating materials the SOFC stack and keep it within the operating temperature of the stack. Apfel et al. showed that using Microtherm, a low-conductivity material, the cool down period can be extended to days [11]. Providing an effective thermal management strategy for SOFC based micro-CHPs becomes essential to reduce thermal cycles as the number of total start-up cycles of SOFC systems should be below 100 [11]. Therefore, the results that allow the fuel cell to turn on and off

twice during a 24-hour period are still achievable as long as the stack temperature does not drop below the operating points. In terms of the system design the manufacturers would be forced to seal the stack with an advanced insulating material to allow for this type of thermal management to occur and prevent stack degradation.

Fuel cell micro-CHPs perform better in dwellings with lower heat than electricity demands due to their low heat-to-power ratio. This was demonstrated in this study as higher reductions occur at the summer case studies that heat and electricity demand are in the same order. This can be seen in table 6.9.

The methodology used in the presented work although subject to limitations (see 6.8) is a new approach in modelling micro-CHP fuel cell systems in dwellings. It considers the variability of the energy patterns of the dwelling which are produced in BIM software and the interaction with the fuel cell and its operation. It is not a technique that only maximises the fuel cell's efficiency which might not be the optimum choice for the overall CO_2 emissions of the system but considers the variation of the dwelling's energy demand.

The results obtained by using the 48 hour data set give an approximation of how the system would perform on a yearly basis, however a bigger data set would give more representative results. This is the approach followed in the analysis presented in chapter 7.

Allowing any data set (real or from building simulation) to be used in the model as input the flexibility of the process increases. This methodology is also very adaptable to adding other technologies as the models for all plant are based on efficiency equations.

6.8 Limitations of the study

This study has identified some fundamental points in the design and operation of fuel cell micro-CHPs and their interaction with the varying energy demands of a house. It has limitations as its goal is to provide a reliable tool that can be used in the early stages of the design. It is therefore not providing the actual design. The model as it has been formulated does not provide information on how the various items of plant are connected to each other but examines predetermined configurations. In addition there is no indication of system flows and temperatures. The inclusion of temperature and flow rates information for the different process streams within the fuel cell micro-CHP and the dwelling's space heating and DHW circuits could provide a complete design solution. This solution could provide information on how

each stream of heat within the fuel cell process can be used more effectively for the dwelling processes.

The results obtained for thermal storage systems assume that there is no heat loss to the surroundings. A model that would consider storage losses would result in a system that relies less on heat storage by reducing the amount of heat that gets stored in the tank. A priority would be introduced for a quick release of heat from the tank to increase efficiency as possible and reduce losses.

Another weakness of this model has to do with the hourly timesteps which affect the environmental results of the model. This however, is a weakness that is difficult to overcome when working on optimisation models that attempt to capture a whole year period. This is because increasing temporal precision will result in more complex models that are difficult to solve.

6.9 Concluding Remarks

This study has presented a micro-CHP model of a dwelling that could be used in an environmental benefit analysis. The model considers different options for satisfying the energy demand of a UK dwelling. Data sets for different scenarios were produced using BIM software and were used to determine sizing characteristics and operational profiles of all plant involved in a design based around a fuel cell micro-CHP system. Thermal energy storage was included in the model in addition to a gas boiler anda fuel cell micro-CHP. It was established that fuel cell based micro-CHP systems perform better in houses with similar electricity and heat loads. The design that produced the best results on a combined winter-summer dataset, was a fuel cell micro-CHP system coupled with a thermal energy storage tank . This combination enabled the fuel cell micro-CHP to store heat in the thermal tank when heat demand was low, so it could be used later, thus reducing the dependence on the auxiliary boiler. The results also identified a design requirement for SOFC based micro-CHP products which is the need for high quality insulation on the stack to prevent the temperature to drop below the operating temperature. Implementation of such measures could prevent thermal cycling and increase lifetime.

Chapter 7

Model 2 - An MINLP model for PEMFC based micro-CHP design in dwellings

In this chapter, an innovative methodology based around the principles of mathematical programming is proposed for the design of fuel cell micro-CHPs in dwellings. This is presented along with the fundamental basics of the model and the solution approach utilised. This study is motivated by the missing elements identified in the limitations of the previous model but also in the literature review which is a link between the heat sources and demand.

7.1 Problem Statement

The overall problem for the design of a micro-CHP in a dwelling can be stated as follows.

Given:

- A selection of heat an electricity generating plant;
- The heat and electricity demand for a dwelling;
- A low temperature hot water (LTHW) pipework network to deliver the heat demand;
- Process limitations and constraints in terms of energy generation and temperature in pipes.

Determine:

- The configuration and design between heat and electricity plant and consumption within the dwelling.
- The sizing and operational characteristics of this design.

So as to optimise the resulting CO_2 emissions from the whole dwelling energy system.

7.2 Basis for the PEMFC Model

PEMFC-based micro-CHPs deliver recoverable heat at the exit of the afterburner and at the cooling circuit of the cell. The various heat and power generation units and their interconnections influence the design and operation of the system and determine how energy demand is met. Residential energy demand varies daily and seasonally while the heat generation plant that can be used in a fuel cell micro-CHP design also has variability in temperature and operating point. Constraints related to temperatures and operational profiles imposed by heating sources and demands , should be balanced to provide a better dwelling design. As multiple heat streams exist within a fuel cell micro-CHP system and considering that they have to be integrated into the building heating services suggest that a systematic design tool can be used to improve the design of fuel cell micro-CHPs in dwellings by providing better utilisation of heat. This study presents this systematic tool which is based on an optimisation framework.

7.3 Modelling Methodology

The basic components of the model that has been implemented can be seen in Figure 7.3.1. The main points used for the model are the following:

- The fuel cell generates electricity and heat consuming H_2 reformed from natural gas in the external reformer.
- The heat required for reforming is recovered from the afterburner stream.
- Heat from the fuel cell micro-CHP unit that can be used in the dwelling is recovered by the cooling system of the fuel cell and from the afterburner exhaust stream.

- A natural gas boiler supplements the heat recovered by the fuel cell stack and afterburner to satisfy heat demand of the dwelling.
- The electricity grid supplements the electricity generated by the fuel cell to satisfy the power demand of the dwelling.
- All heat recovered from the fuel cell processes and generated by the boiler can be used in separate space heating and domestic hot water circuits via a low temperature hot water circuit.
- A thermal storage tank can store heat from either fuel cell heat sources.
- There are two low loss headers that serve heating and domestic hot water tank. Heat from all sources via the two headers serve space heating and DHW tank.

The main assumptions made in the model are:

- Natural gas used in the system is assumed to be pure CH_4.
- There is atmospheric pressure on the fuel cell processes.
- There are no heat losses or thermal stratification included in the TST model.

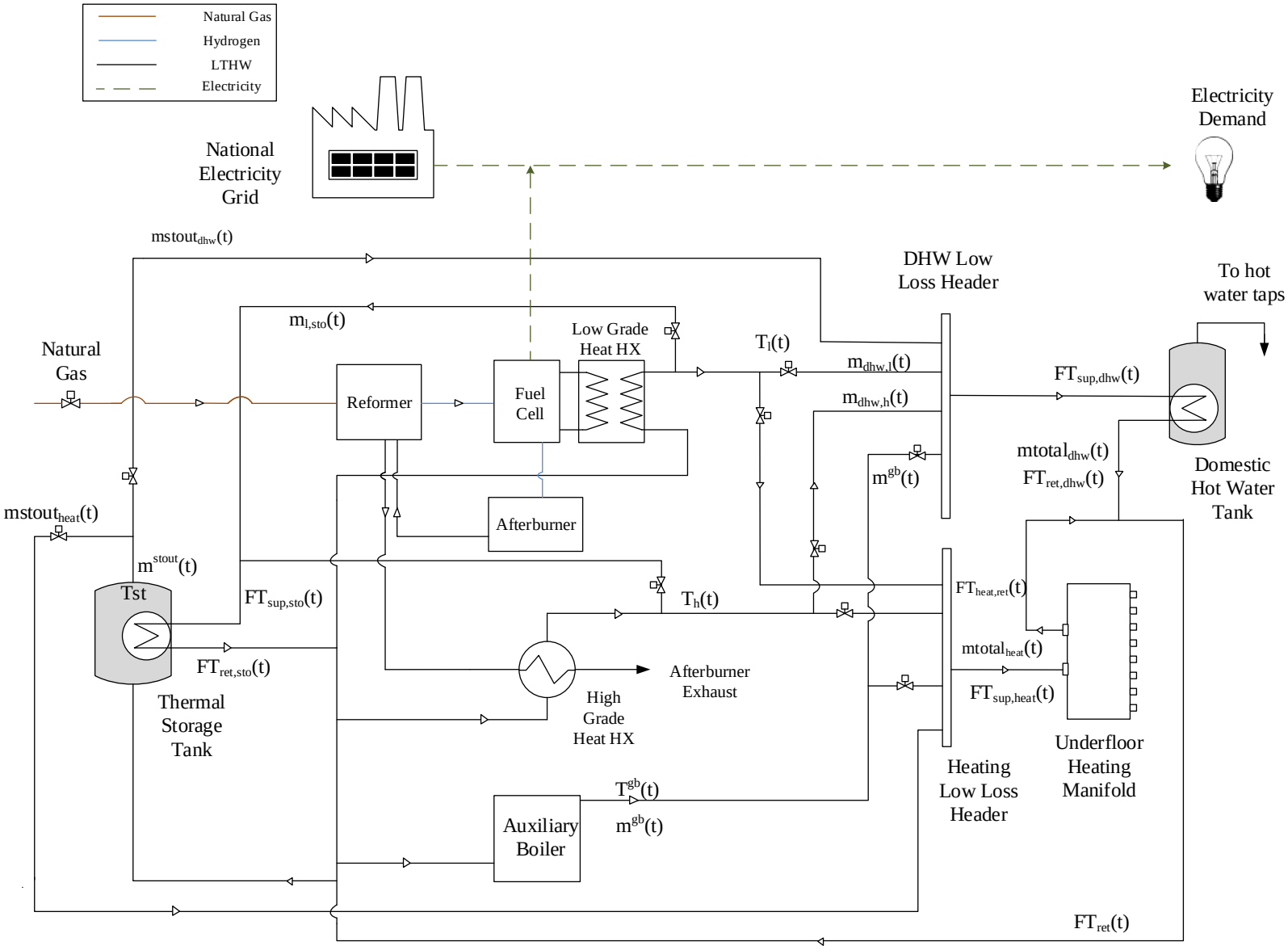

Figure 7.3.1: PEMFC based micro-CHP model schematic diagram

The aim of the model is to identify the optimal interconnections between the power and heat generation plant and the dwelling building services while optimising CO_2 emissions. It is assumed that low loss headers are used in the design which means that multiple sources can connect on them. A pipe circuit from the cooling circuit or the afterburner of the fuel cell can connect to the space heating or onto the DHW header. At the same time heat from the afterburner is used in the reforming process and the model determines how much of this heat will be left for use in the dwelling. The model also considers the temperature and flow constraints of the selected heating system.

7.3.1 Submodels

The mathematical model for the optimisation of the fuel cell micro-CHP and dwelling design is described next.

7.3.1.1 Fuel Cell Stack

The central part of the system is the fuel cell stack. Figure 7.3.2 shows a labelled diagram of the fuel cell showing incoming and outgoing flows.

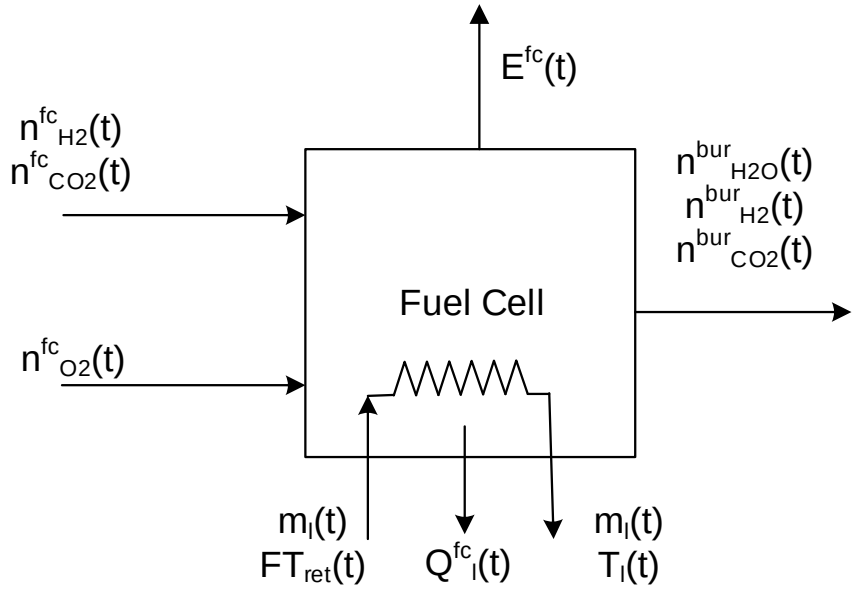

Figure 7.3.2: Schematic of the fuel cell stack showing mass and energy flows

The model for the fuel cell stack consists of the following equations:

The fuel cell electricity production $E^{fc}(t)$ as a function of the hydrogen flow rate $n^{fc}_{H2}(t)$, the fuel utilisation factor $U^{fc}(t)$, the electrical current produced by each mol of hydrogen i_{H2} [94] and the operating cell voltage $V^c(t)$, can be given by the following equation :

$$E^{fc}(t) = n^{fc}_{H2}(t) \cdot U^{fc}(t) i_{H2} \cdot V^c(t) \tag{7.3.1}$$

Heat can be recovered by the cooling circuit of the fuel cell. The amount of heat that can be recovered depends on the difference between the open circuit voltage E_{th} and the operating value.

$$Q^{fc}_l(t) = n^{fc}_{H2}(t) \cdot i_{H2} \cdot (E^{th} - V^c(t)) \tag{7.3.2}$$

, where the subscript "l" refers to the low grade heat delivered from the cooling circuit of the fuel cell. It has been assumed that all heat from the fuel cell stack can be recovered and that there is no heat lost to the surroundings.

Heat from the cooling circuit heat exchanger $Q^{fc}_l(t)$ to the dwelling satisfies equation 7.3.3. The total heat from the cooling circuit is the sum of heat delivered to all demands j.

$$Q^{fc}_l(t) = \sum_j Q_{l,j}(t) = \sum_j m_{l,j}(t) cp(T_l(t) - FT^{ret}(t)) \tag{7.3.3}$$

The fuel cell's operation is constrained by a ramp up rate of 0.25 W/s [75, 77].

$$\frac{d}{dt} E^{fc}(t) \leq ra \tag{7.3.4}$$

Degradation mechanisms such as drying or flooding of the stack are not included in the model as it has been assumed that the correct humidity level exists in the stack.

7.3.1.2 Reformer

The overall reaction at the reformer produces the hydrogen that is consumed by the fuel cell.

$$CH_4 + 2H_2O \rightarrow CO_2 + 4H_2$$

Figure 7.3.3 shows a labelled diagram of the reformer showing incoming and outgoing flows. It has been assumed that all CO is fully converted to CO_2 in the water-gas shift reaction. The unconverted carbon monoxide from the reformer can reduce the activity of the anode and lead to stack voltage reduction [129].

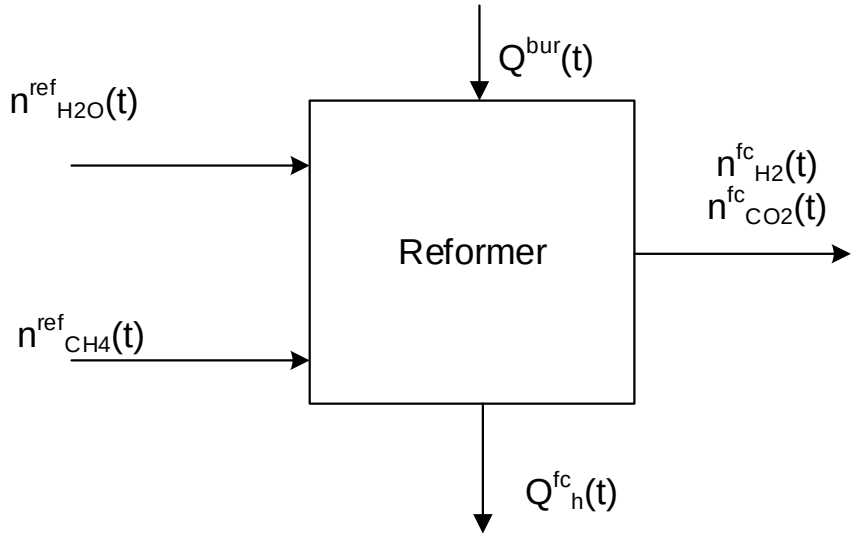

Figure 7.3.3: Schematic of the reformer showing mass and energy flows

There is a mass balance performed at the reformer where the incoming CH_4 flow is related to the resulting H_2 and CO_2 based on the overall reforming reaction:

$$n^{fc}{}_{CO2}(t) = n^{fc}{}_{CH4}(t) \tag{7.3.5}$$

$$n^{fc}{}_{CH4}(t) = \frac{n^{fc}{}_{H2}(t)}{4} \tag{7.3.6}$$

$$m^{fc}{}_{s}(t) = MW_s \cdot n^{fc}{}_{s}(t) \tag{7.3.7}$$

, where $n^{fc}{}_{s}(t)$ represents the molar flow rate at time t of species s in the fuel cell, $m^{fc}{}_{s}(t)$ the mass flow rate and MW_s the molar weight . "s" denotes species CH_4, H_2, CO_2 involved in the system. It has been assumed that all methane is converted

to hydrogen, where in reality a 100% conversion at the reformer is not possible and some methane is present in the reformate. The focus of the model is the total CO_2 emissions and these equations capture their values accurately.

7.3.1.3 Afterburner

Hydrogen that is not used in the fuel cell is combusted in the afterburner. Figure 7.3.4 shows a labelled diagram of the afterburner showing incoming and outgoing flows.

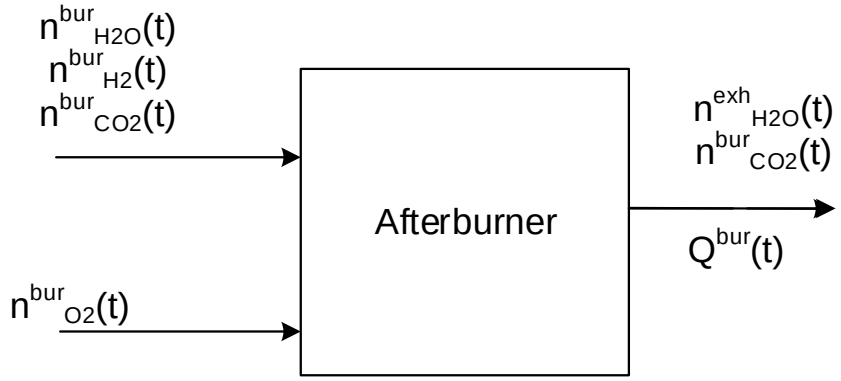

Figure 7.3.4: Schematic of the afterburner showing mass and energy flows

The amount of heat generated by combustion of hydrogen is a function of the hydrogen flow rate in the afterburner $n^{bur}_{H2}(t)$ and the calorific value of the fuel HHV_{H2} .

$$Q^{bur}(t) = n^{bur}{}_{H2}(t) \cdot HHV_{H2} \tag{7.3.8}$$

The molar flow to the afterburner is equal to the fuel that is not used in the fuel cell:

$$n^{bur}{}_{H2}(t) = (1 - U^{fc}(t))n^{fc}_{H2}(t) \tag{7.3.9}$$

The hydrogen utilisation factor is defined as the ratio between the hydrogen flow rate that reacts in the stack and the hydrogenflow input to the stack and varies in

the model between 0.6 to 0.85. Although almost 100% utilisation of hydrogen can be achieved with dry feeds of hydrogen and oxygen [126], this would require finding an alternative source for providing reforming heat such as burning natural gas.

The exhaust gases leave the combustion chamber at 700-800 °C and provide heat for the reforming process which requires high temperatures to occur [89]. The heat required for reforming is a function of methane flow rate ${n^{fc}}_{CH4}(t)$ and the energy that is required to reform one mole of CH_4 to H_2 [89].

$$Q^{ref}(t) = {n^{fc}}_{CH4}(t) \cdot q^{ref} \tag{7.3.10}$$

Useful heat $Q_h^{fc}(t)$ can be recovered from the exhaust gases after they have released heat for the reforming process at 400 °C [89] . The gases enter a heat exchanger where heat can be recovered and used in the dwelling. It has been assumed that all heat left in the afterburner exhaust stream after it leaves the reformer can be recovered.

$$Q_h^{fc}(t) = Q^{bur}(t) - Q^{ref}(t) \tag{7.3.11}$$

The remaining heat is recovered by a heat exchanger and it can be used for space heating, DHW or stored in the TST (all demands are represented by set j). This heat is modelled using Equation 7.3.12.

$$Q_h^{fc}(t) = \sum_j Q_{h,j}(t) = \sum_j m_{h,j}(t) cp(T_h(t) - FT^{ret}(t)) \tag{7.3.12}$$

At times when $Q^{bur}(t) = Q^{ref}(t)$ there is no remaining heat from the afterburner to be used in the building as all is used for reforming.

7.3.1.4 Gas Boiler

At the boiler, natural gas is combusted to produce H_2O and CO_2 based on the methane combustion reaction. In this case it has been assumed that natural gas is pure methane

$$CH_4 + 2O_2 \rightarrow CO_2 + 2H_2O$$

Figure 7.3.5 is a labelled diagram of the gas boiler showing incoming and outgoing flows.

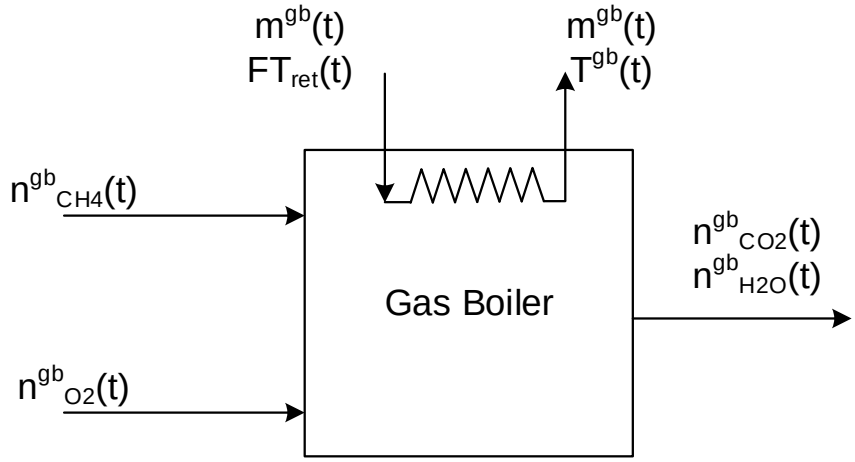

Figure 7.3.5: Natural Gas Boiler Schematic showing mass and energy flows

Mass balance is then performed in a similar way at the gas boiler resulting at the following equations

$$n^{gb}{}_{CO2}(t) = n^{gb}{}_{CH4}(t) \tag{7.3.13}$$

$$m^{gb}{}_{s}(t) = MW_s n^{gb}{}_{s}(t) \tag{7.3.14}$$

,where $n^{gb}{}_{s}(t)$ represents the molar flow rate at time t of species s in the gas boiler and $m^{gb}{}_{s}(t)$ the mass flow rate.

Boiler heat $Q_j^{gb}(t)$ to demand j is given by equation 7.3.15, where $T^{gb}(t)$ is the boiler supply temperature, cp is the specific heat capacity of water.

$$Q_j^{gb}(t) = \sum_j m_j^{gb}(t) \cdot cp \cdot (T^{gb}(t) - FT^{ret}(t)) \tag{7.3.15}$$

Boiler heat is also has to satisfy equation 7.3.16.

$$\sum_j Q_j^{gb}(t) = n^{gb}{}_{CH4}(t) \cdot HHV_{CH4} \cdot \eta^{gb} \tag{7.3.16}$$

,where η_{gb} represents the efficiency of the boiler.

Also,

$$\sum_j Q_j^{gb}(t) = r^{gb}(t) P^{gb} \tag{7.3.17}$$

, where $r^{gb}(t)$ represents the load factor and P^{gb} the maximum capacity of the gas boiler.

7.3.1.5 Thermal Storage Tank

The model for the TST builds up on the storage model presented in Chapter 6. The energy content of the storage tank E^{st} (kJ) is given by equation 7.3.18 as in Model 1.

$$E^{st}(t) = V^{st} \cdot \rho \cdot cp \cdot (T^{st}(t) - T^{emv}(t)) \tag{7.3.18}$$

Energy balance in the storage tank is given by equation7.3.19 .

$$\frac{d}{dt} E^{st}(t) = \sum_g Q_{g,sto}(t) - \sum_j {Q_j}^{stout}(t) \tag{7.3.19}$$

As there is no heat flow from the TST to the TST, for j=sto, ${Q_{sto}}^{stout}(t)$=0.

The additional elements introduced in the model relate to temperature constraints. There is a temperature limit below which the storage cannot release heat to the dwelling. A constraint of 40 °C for UFH and 60 °C for radiators has been introduced in the model before heat can be used for space heating. The constraint is 60 °C for DHW. This is to ensure that water flow from the storage is of sufficient temperature to be used in the pipe circuits that serve the demands.

This constraint was modelled using binary variable $ys_j(t)$ which is linked to both T_{st} and Q_{stout} as shown in equations 7.3.20 ,7.3.21.

$${Q_j}^{stout}(t) \leq E^{st}(t) \frac{ys_j(t)}{\delta t} \tag{7.3.20}$$

$$T_j{}^{st}(t) \geq B_j^{st}\, ys_j(t) \tag{7.3.21}$$

for $T_j^{st}(t)$, $Q_j^{stout}(t) \geq 0$.

Storage heat $Q_j^{stout}(t)$ to demand j is given by equation 7.3.22, where $m_j^{stout}(t)$ is the TST water flow rate at time t and demand j

$$Q_j^{stout}(t) = \sum_j m_j^{stout}(t) \cdot cp \cdot (T^{st}(t) - FT^{ret}(t)) \tag{7.3.22}$$

A constraint was also added to minimise the impact of the initial and final conditions with regard to the thermal mass stored in the TST. This constraint enforces the TST temperature at the last timestep to be no more than 20 °C lower than the initial value at the first timestep (7.3.23). This way the TST will not release all saved heat only because it is the last timestep and the impact on the results will be minimised.

$$T^{st}(t_f) + 20 \geq T^{st}(t_1) \tag{7.3.23}$$

, where t_f is the last timestep of the dataset and t_1 the first.

Another way to address the issue of receiving heat from the TST that cannot be accounted in the objective function (whether this is the cost or the CO_2 emissions) is to force the TST temperature at the first hour of the day to be equal to the last hour of the day for all the days of the dataset. This alternative approach has been studied and is presented in section 7.5.1.3.

No thermal losses are included in the tank model. This assumption is considered to have small effect on the model results because the datasets are small and the cumulative amount of thermal losses from the TST would not make a significant difference in the objective function or alter the results in terms of system sizing and operation. Based on the 0.0075 kWh/lday value for heat losses from hot water tanks used in IES [85], an average size TST of 200 L would require 1.5 kWh of heat from the fuel cell per day to maintain the initial TST temperature. The total annual heat loss from the TST would be then 547.5 kWh which is approximately 2.33% of the total annual combined heat demand for House A which is 23,430.11 kWh. Therefore heat for TST thermal losses was decided to be left out from the model.

Thermal stratification is also not included in the TST model. Stratification of water in a tank creates two separate water temperatures at the bottom and top of the TST. The benefit of this is that water at a higher temperature at the top can be used directly to demand, whereas water at the bottom can return to the heat source. Stratification is beneficial in solar thermal systems where water at the lower part of the TST is connected to the solar thermal collectors to extract the maximum possible heat from the heating fluid. In such systems better thermal stratification increases system performance and efficiency [57, 84]. Having a stratified tank in the model would require additional equations with regard to temperature distribution inside the tank so in order to keep the model simple, a non-stratified hot water storage tank is assumed. Celador et al. studied the effect of different modelling approaches of the TST (with or without stratification) on the economic feasibility of residential CHP plants and found differences between the results of the feasibility studies. The profits generated by the system were dependent to the TST modelling approach and the system with stratification had the shortest payback period [33]. However, as the stratification element is missing on all the case studies presented here and since the approach involves comparison between different scenarios, the main outcomes are expected not to be affected by this omission.

7.3.1.6 Pipe network and Heat Emitters

Water flows are mixed in the two headers, at the storage tank and at the return, after all flow pipework has released their heat to the demand.

Water mass balances are performed in the pipework network where different flows come together i.e.

$$m_j^{total}(t) = m_{h,j}(t) + m_{l,j}(t) + m_j^{gb}(t) + m_j^{stout}(t) \tag{7.3.24}$$

,where $m_j^{total}(t)$ is the total flow rate to each heat demand, $m_{h,j}(t)$ and $m_{l,j}(t)$ are the flow rates from afterburner heat exchanger and the fuel cell cooling circuit respectively, m_j^{gb} is the boiler flow rate and $m_j^{stout}(t)$ is the flow rate from the storage tank.

Variables $m_j^{stout}(t)$ and $m_j^{gb}(t)$ are 0 for j=sto as there is no heat flow to the TST from the boiler or TST itself.

The lower bounds for all the individual water flows are 0, as the results could propose that heat from the FC cooling circuit is only used for space heating and not for DHW.

Therefore these flows should be able to reach 0 values.

The water mass flow required for the space heating and DHW in order to maintain a 10 ^{o}C temperature difference in the demand side is calculated in each step using the following relation :

$$m_j^{total}(t) = \frac{Q_j^{req}(t)}{C_{pw} \cdot 10} \quad for\ j = HEAT, DHW \tag{7.3.25}$$

A variable flow water system has been assumed for the design which varies in each timestep providing heat to the demand. In such as system an adjustment in output requires a water flow change.

Also,

$$Q_j^{req}(t) = Q_j^{gb}(t) + Q_j^{stout}(t) + \sum_g Q_{g,j}(t) \tag{7.3.26}$$

The term $\sum_g Q_{g,j}(t)$ represents the summation of the amount of heat delivered to demand j from the g fuel cell heat exchanger.

Heat emission from the heating and DHW system also needs to satisfy the following equation:

$$Q_j^{req} = m_j^{total}(t) \cdot cp \cdot (FT_{sup,j}(t) - FT_{ret,j}(t)) \tag{7.3.27}$$

Binary variables have been used in the model in definitions of upper and lower bounds of heat output variables. Binary variables are also used in the mass balances to force the plant mass flow rates to become zero when the heat emission is zero. By using this method temperature constraints between variables are not needed. This is shown in the following equations:

$$Q_j{}^{gb}(t) \leq y_j^{gb}(t) A_j^{gb} \tag{7.3.28}$$

$$Q_j{}^{gb}(t) \geq 0.001 y_j^{gb}(t) \tag{7.3.29}$$

, where $A_j^{gb}$is the upper bound of the heat output of the boiler per demand j

Similarly, binaries $y_{gj}(t)$, are used for the fuel cell heat exchangers and for the TST output to each demand.

$$Q_{g,j}(t) \leq y_{g,j}^{fc}(t) A_{g,j}^{fc} \tag{7.3.30}$$

$$Q_{g,j}(t) \geq 0.001 y_{g,j}^{fc}(t) \tag{7.3.31}$$

,where $A_{g,j}^{fc}$ is the upper bound of the heat output of heat exchanger g to demand j. Therefore the mass balance becomes:

$$m_j^{total}(t) = y^{gb}(t) m_j^{gb}(t) + y_j^{stout}(t) m_j^{stout}(t) + \sum_g (y_{g,j}(t) m_{g,j}(t)) \tag{7.3.32}$$

7.3.1.7 Electricity Energy Balance

The electricity output of the fuel cell at time t $E^{fc}(t)$ and the electricity import from the grid at $E_g(t)$ time t have to be equal to the electricity demand $Q_{ele}^{req}(t)$ as shown in equation 7.3.33

$$Q_{ele}^{req}(t) = E^{fc}(t) + E_g(t) \tag{7.3.33}$$

7.3.1.8 Total System CO_2 emissions

The objective function that is minimised here is the total system CO_2 emissions resulting from the operation of the fuel cell and gas boiler and the imported grid electricity. For the grid electricity, emissions rates for every unit of energy have been used, as described in [50]. As mentioned earlier, many studies have chosen cost as their objective function. According to Staffell et al. though "There is considerable uncertainty in the cost targets for fuel cell CHP" [111]. This uncertainty would be carried on the results of any modelling attempt based on cost. The CO_2 emissions on the other hand, is frees of this problem as it depends on plant efficiencies and energy

balances. Therefore the CO_2 emissions as an objective function could represent with more accuracy than cost, a model that attempts to design a system such as the one shown in 7.3.1.

$$M^{fc} = \sum_t m^{fc}{}_{CO2}(t) \tag{7.3.34}$$

$$M^{gb} = \sum_t m^{gb}{}_{CO2}(t) \tag{7.3.35}$$

$$M^{el} = f_e \sum_t E^g(t) \tag{7.3.36}$$

$$min\, z = M^{fc} + M^{el} + M^{gb} \tag{7.3.37}$$

7.4 Formulation and Solution Approach

The system was modelled in GAMS 23.8. Various MINLP solvers were used on an Intel Core i5-2500 CPU, 4 GB RAM, 3.3 GHz computer.

The overall problem is formulated as mixed integer non-linear programming (MINLP) model. Binary variables are used to introduce links between variables. The resulting optimisation model is non-linear and non-convex.

The analysis is made on a 288-hour dataset of energy demands which is extracted from the 8760 hour dataset presented in chapter 5. A month, therefore is represented by 24 hours. This is a more complete dataset than the 48-hour used in the previous model as it can capture better the variation of space heating demand during the year. However, because of the use of larger dataset, the size of the problem becomes big which makes the problem difficult to solve. Trying to solve the MINLP resulted in many of the cases in no solution or into very large CPU times, therefore a two-stage solution was implemented to identify the optimal design and operation of the fuel cell micro-CHP - dwelling system. At stage 1 a simpler MINLP that does not take into account the complete pipe network and all system temperatures is solved.

Specifically equations 7.3.3, 7.3.12, 7.3.15, 7.3.22, 7.3.24, 7.3.25, 7.3.27, 7.3.32 are not included in the model at stage 1. At the same time candidate starting points for all variables are introduced to assist the solver to reach a global optimum solution. At stage 2 the complete MINLP with all equations as described above is solved. The initial solutions of stage 1 are used as good starting point for solving the complete model at stage 2. For the stage 1 the solver BARON was used and to be followed by SBB in stage 2 [67, 104].

All case studies were run using a 1% optimality limit.

The parameters and the bounds of variables are shown in Tables 7.1 and 7.2.

Table 7.1: Parameters used in model 2

Symbol	Parameter	Value	Units
Q_j^{req}(t)	Dwelling Energy Demand	Calculated using IES	kW
T^{env}	Environment Reference Temperature	10	℃
E^{th}	Theoretical fuel cell voltage	1.22	V
ra	Fuel cell ramp up	0.00025	kW/sec
ϱ	Water Density	1000	kg/m^3
f_g	Natural Gas Emission Factor [26]	0.194	kg/kWh
f_e	Grid Electricity Emission Factor [26]	0.517	kg/kWh
q^{ref}	Heat required for the reforming process	193.06	kJ/mol
i_{H2}	Electrical current of fuel cell from hydrogen flow	192.98	kAsec/mol
MW^s	Molecular Weight of species s	Varies	kg/mol
HHV^s	Higher Heating Value of species s	Varies	kJ/mol
cp	Specific Heat Capacity of Water	4.2	kJ/kgK
δt	Timestep	3600	sec
$A_j{}^{gb}$	Boiler Maximum Heat Output per demand	Varies	kW
$A_{gj}{}^{fc}$	Fuel Cell Maximum Heat Output per demand per heat exchanger g	Varies	kW
B_j^{st}	Temperature constraint for demand j	Varies	℃
$m_j^{total}(t)$	System Flow rate at time t and demand j	$Q_j^{req}(t)/(cp*10)$	kg/sec
n^{gb}	Boiler Efficiency	0.9	-

Table 7.2: Bounds used for variables in model 2. When the symbol "/" is used the values for the different heating systems used in the analysis are indicated.

Symbol	Variable	Lower Bound	Upper Bound	Units
V^{st}	Storage Tank Volume	0	0.8	m^3
$V^c(t)$	Fuel cell voltage at time t	0.6	0.75	V
$U^{fc}(t)$	Hydrogen Utilisation Factor at time t	0.6	0.85	
$FT_{sup,heat}(t)$	System Temperature at time t - Heating Supply (UFH system/radiators)	45/60	60/80	^oC
$FT_{ret,heat}$(t)	System Temperature at time t - Heating Return (UFH system/radiators)	35/50	50/70	^oC
$FT_{sup,dhw}(t)$	System Temperature at time t - DHW Supply	60	80	^oC
$FT_{ret,dhw}(t)$	System Temperature at time t - DHW Return	50	70	^oC
$T^{gb}(t)$	Boiler Temperature at time t	40	80	°C
$T_g(t)$	Heat Exchanger Temperature at grade g at time t	40	80	°C
$T^{st}(t)$	TST Temperature at time t	40	80	°C
$E^g(t)$	Grid Electricity at time t	0	5	kW
$E^{fc}(t)$	Fuel Cell Electrical Output at time t	0	5	kW
$E^{exp}(t)$	Exported Electricity to the grid at time t	0	2	kW
$Q_j^{gb}(t)$	Boiler Output at time t and demand j (House A/B)	0	10/50	kW
$r^{gb}(t)\cdot$	Load factor of Gas Boiler	0	1	-
P^{gb}	Maximum capacity of Gas Boiler	0	20 (50 for House B)	kW
$Q_{g,j}(t)$	Fuel cell heat output of g heat exchanger at time t demand j	0	5	kW

$E^{st}(t)$	Heat stored in TST	0	-[1]	kJ
$Q_j^{stout}(t)$	TST Heat Output at time t and demand j	0	-[1]	kW
$Q^{bur}(t)$	Heat generated from hydrogen combustion at time t	0	-[1]	kW
$Q^{ref}(t)$	Heat required for reforming at time t	0	-[1]	kW
$n_s^{fc}(t)$	Molar Flow Rate of species s in fuel cell at time t	0	-[1]	mol/sec
$m_s^{fc}(t)$	Mass Flow Rate of species s in fuel cell at time t	0	-[1]	mol/sec
$n_s^{gb}(t)$	Molar Flow rate of species s in gas boiler at time t	0	-[1]	mol/sec
$m_s^{gb}(t)$	Mass Flow rate of species s in gas boiler at time t	0	-[1]	mol/sec
$m_j^{stout}(t)$	TST Water Flow rate at time t and demand j	0	-[1]	kg/sec
$m_j^{gb}(t)$	Boiler Flow rate at time t and demand j	0	-[1]	kg/sec
$m_{gj}(t)$	Flow rate at fuel cell grade g at time t and demand j	0	-[1]	kg/sec
M^{fc}	CO_2 emissions caused by fuel cell	0	∞	kg
M^{gb}	CO_2 emissions caused by gas boiler	0	∞	kg
M^{el}	CO_2 emissions caused by grid electricity	0	∞	kg
M^{exp}	CO_2 emissions savings by exporting electricity to the grid	0	∞	kg
z	Total CO_2emissions	0	∞	kg

[1]Upper bounds determined by equations that calculate these variables. For example the upper bound of the fuel cell electrical output determines the upper bound of the hydrogen molar flow rate.

7.5 Modelling Results

The presentation of the results focuses on highlighting the differences in modelling the various case studies. In addition, the graphs presented in each section are not repeated throughout if the repetition is not necessary to discuss a point made. An effort has been made to include many case studies and to create a broad view of fuel cell micro-CHP design and how this can vary in different buildings and scenarios. The majority of the case studies that are presented here are for House A, the Part L dwelling. Case study 7 is for the typical UK dwelling.

7.5.1 Part L Dwelling Designed with UFH

Using the model presented above, two fuel cell micro-CHP designs are evaluated in terms of their CO_2 emissions and compared to the base case. The effect of TST in the design and operation of a Part L compliant building is tested by selecting to evaluate one design option without thermal storage (Case 1) and one with (Case 2).

7.5.1.1 Case 1

The optimum design is illustrated in Figure 7.5.1. All possible connections from the fuel cell heat exchangers are selected. The cooling circuit and afterburner are supplying heat to the space heating circuit, the DHW and to the TST. However, the amounts of heat that each source is supplying to each demand vary. The fuel cell is sized at 1.9 kWe and the boiler peaks at 5.6 kWth and 1.0 kWth for heating and DHW respectively. The total CO_2 emissions for this case are 211 $kgCO_2$.

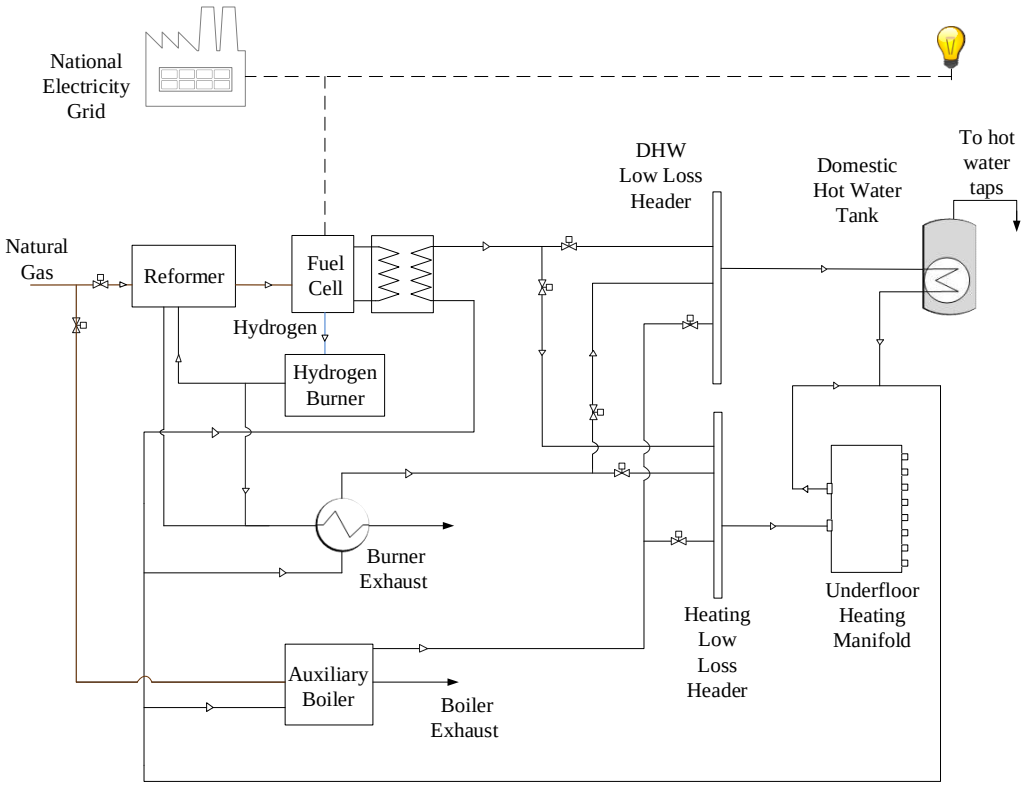

Figure 7.5.1: Schematic diagram representing the optimum design configuration for case 1

The contribution of each heat source to space heating and DHW demand is listed in Table 7.3. The fuel cell micro-CHP is serving in total the majority of the DHW demand. This can be explained by the smaller values and less variation of the DHW demand pattern compared to the heating pattern.

Table 7.3: Annual heat contribution for each source for case 1

Source	**Space Heating (%)**	**DHW(%)**
FC Cooling Circuit	15.0	48.0
Afterburner	13.0	43.0
Gas Boiler	72.0	9.0

Heating in Case 1 is satisfied from the two heat sources of the fuel cell (the high grade heat of the afterburner and the lower grade heat of the cooling circuit) and the gas boiler. This is illustrated in Figure 7.5.2 for the 288 hour dataset.

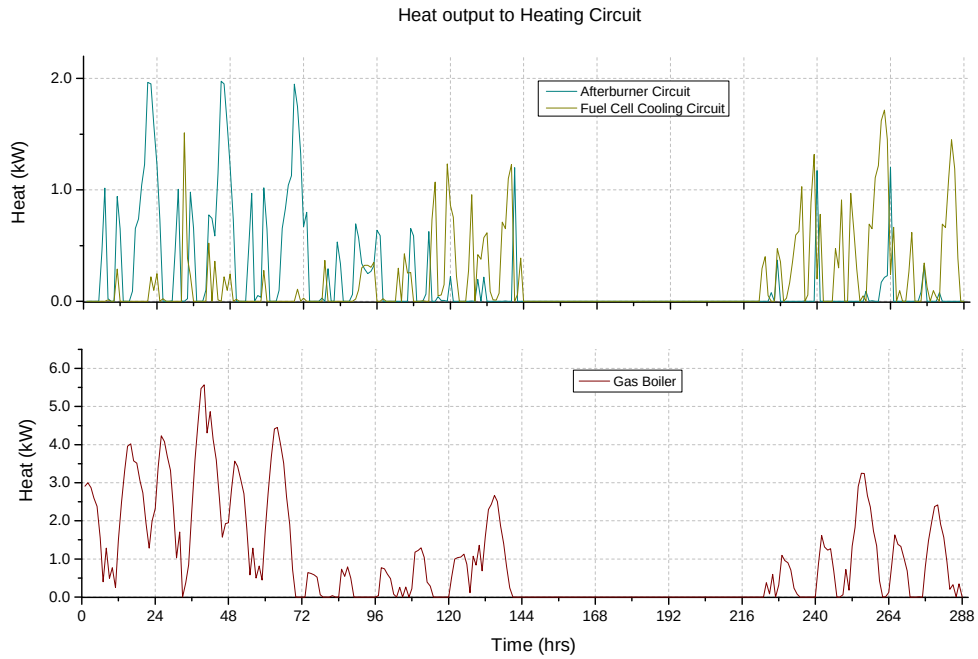

Figure 7.5.2: Graph representing how the system satisfies heating demand utilising heat from the two fuel cell heat exchangers and the natural gas boiler for Case 1

The contribution of each heat source to DHW demand is illustrated in Figure 7.5.3 for the 288 hour dataset. It is clear that the fuel cell micro-CHP is covering the majority of the DHW demand while the boiler is supplementing the fuel cell.

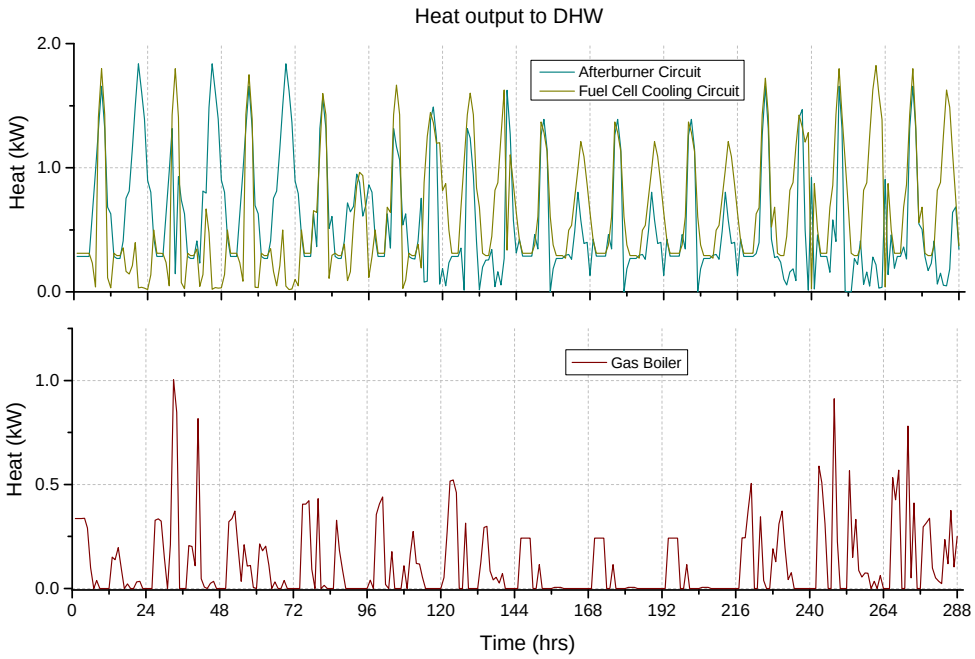

Figure 7.5.3: Graph representing how the system satisfies DHW demand utilising heat from the two fuel cell heat exchangers and the natural gas boiler for Case 1

The utilisation factor of hydrogen acts as a balancing measure for the fuel cell: when $U^{fc}(t)$ reduces, less electricity is produced at the fuel cell but more heat can be recovered from the afterburner as more hydrogen will be combusted. In the summer when less heat is required than the winter period, the utilisation factor takes values closer to its upper bound to maintain a high electricity output and to reduce heat. This can be seen in figure 7.5.4 between the hours 144 to 216 that represent the summer period.

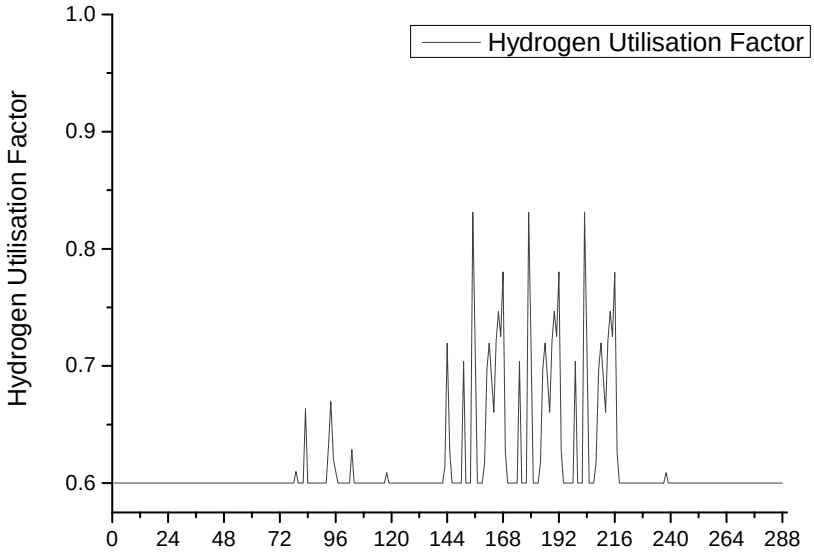

Figure 7.5.4: Graph showing the utilisation factor of hydrogen at the fuel cell for Case 1.

The variation of the total heat available from the unutilised hydrogen combusted at the afterburner and the heat recovered at the reformer is illustrated in Figure 7.5.5. The available afterburner heat at the reformer reduces in the summer, however there is a smaller decrease in the heat that the reformer is recovering. This is to maintain electricity generation to cover the majority of dwelling's demand.

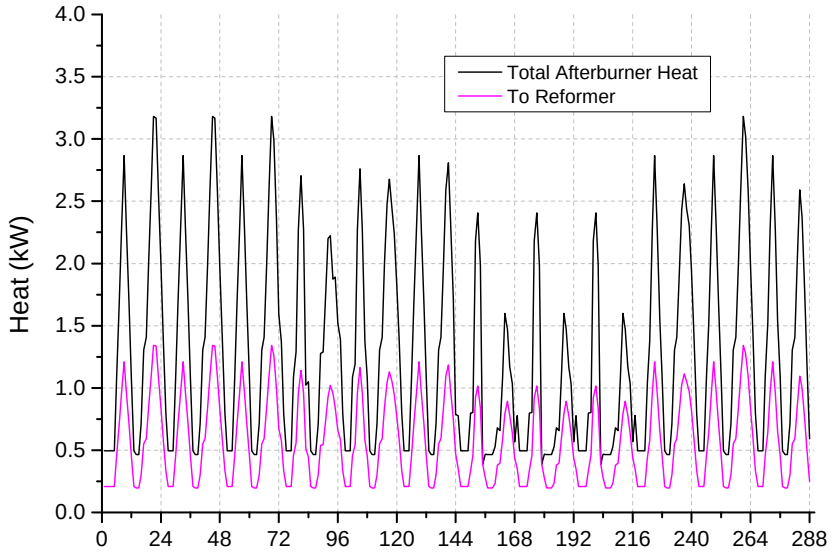

Figure 7.5.5: Graph showing the available heat from the afterburner and the recovered heat at the reformer for Case 1

In order to see the detail of the behaviour of the plant temperatures on a 24 hour part of the 288 dataset we have zoomed in. This is shown in Figure 7.5.6. The final heating flow and return temperatures can be seen in Figure 7.5.7.

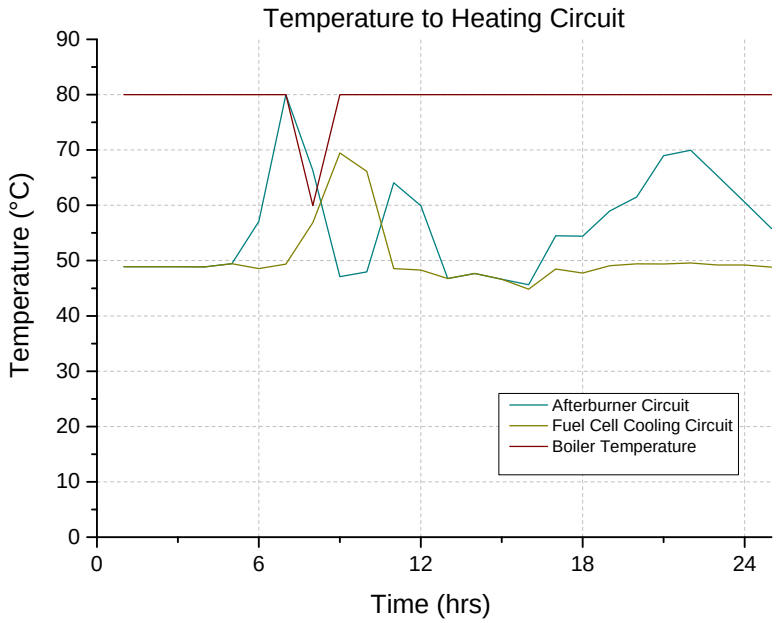

Figure 7.5.6: Graph showing the individual system temperatures over a winter 24 hour period for Case 1

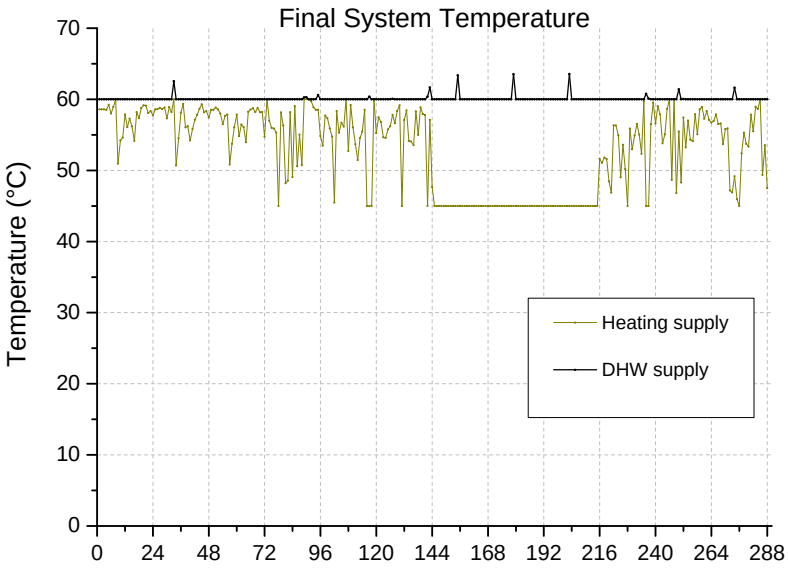

Figure 7.5.7: Graph showing the final space heating and DHW temperatures for Case 1

The final temperatures maintain a 10 °C difference throughout. In the summer, between hours 144 and 216 space heating demand is 0, so the heating supply variable takes the value of the lower bound. At the same time the flow rate to heating is 0 as it can be seen from the figure 7.5.8. The flow rate data obtained from the results help designers and manufacturers determine the maximum flows of heating and DHW circulation pumps.

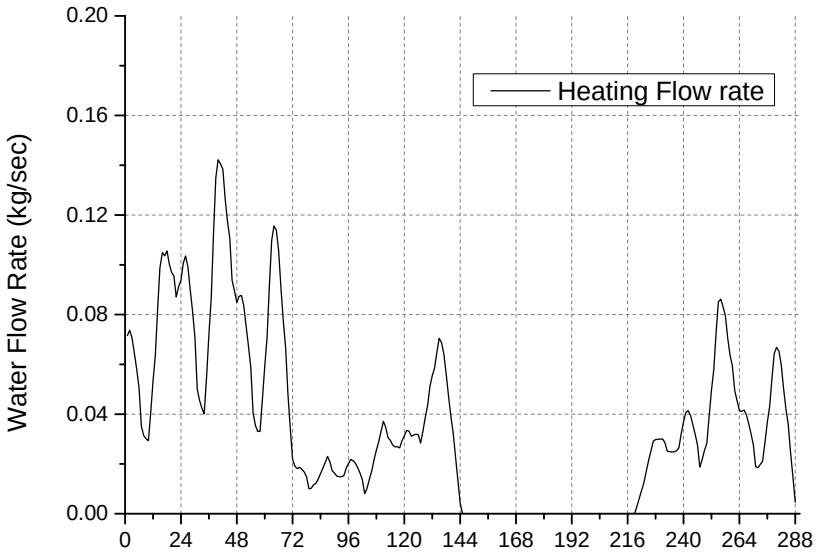

Figure 7.5.8: Graph showing the total water flow from the heating header to the UFH manifold for Case 1. The water flow is 0 in the summer months when space heating demand is 0.

The electricity generation from the fuel cell and the electricity grid input is depicted in Figure 7.5.9. At the last few hours of the dataset the fuel cell electricity drops and import from the grid increases. This is because the fuel cell is gradually ramping down to eventually stop as it approaches the final steps of the dataset. This is an issue raised in the discussion of the previous model with regard to the thermal mass of the TST and can also be seen here. It is an edge effect in the sense that the end of the dataset affects the values of the variables. This can be observed in both models and happens because the models consider only the data given and not what happens after the last timestep. However, in reality there is a continuity in any dataset whether this is 288 or 8760 hours. The impact on the results increases as the dataset becomes smaller.

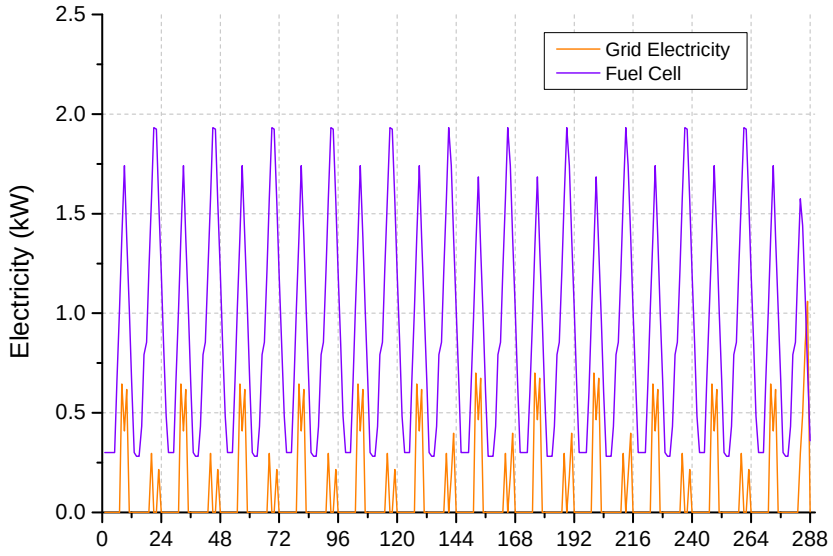

Figure 7.5.9: Graph showing the fuel cell electricity generation and the electricity from the grid for Case 1

7.5.1.2 Case 2

This case study represents a system designed with an UFH system for space heating. The difference with case study 1 is the inclusion of a TST in the design. The optimum design is graphically represented in Figure 7.5.10. The thermal storage tank is served by both the fuel cell cooling circuits and the afterburner stream and it provides heat to all possible demands, the heating circuit and domestic hot water tank. The natural gas boiler acts as a backup source of heat to both heating system and DHW circuits and is not linked to the TST as its heat is used directly from the system. All electricity is provided by the fuel cell in this case as in the inclusion of TST in the design allows the fuel cell to operate constantly and store the excess heat in the tank. However in reality there is always a connection between the grid and the dwelling, but it shows that a system such as this one could be considered for stand-alone independent systems. The fuel cell is sized at 2.2 kWe and the boiler peaks at 5.3 kWth and 2.7 kWth for heating and DHW respectively. The TST is sized at 140 L. The total CO_2 emissions for this case are 197 $kgCO_2$.

The contribution of each heat source to space heating and DHW demand is listed in Table 7.4. The fuel cell micro-CHP is again serving in total the majority of

the DHW demand which has lower values and less variation compared to the space heating demand. The total heat output of the fuel cell micro-CHP system have been increased approximately 7% compared to case 1.

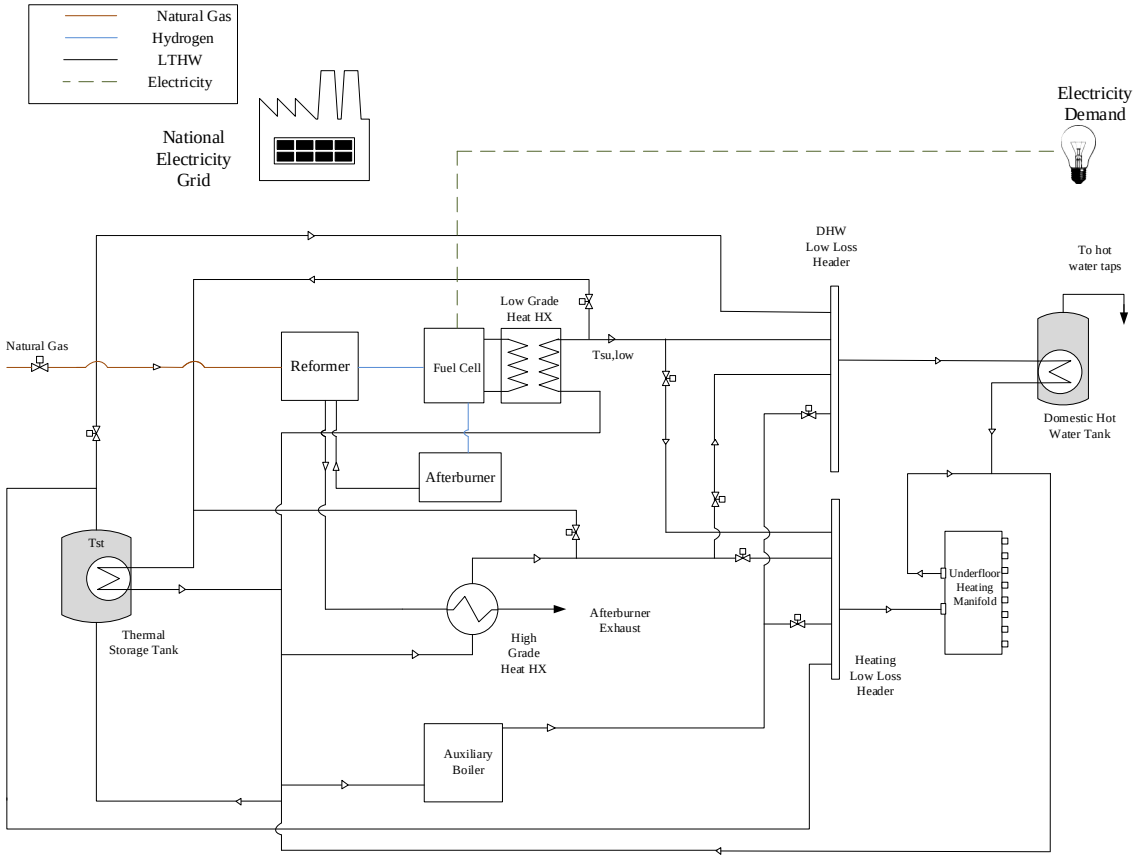

Figure 7.5.10: Schematic diagram representing the optimum design configuration for case 2 showing the TST in addition to the other units and its connections to the system

Table 7.4: Annual heat contribution for each source for case 2

Source	**Space Heating (%)**	**DHW(%)**
FC Cooling Circuit	17	36
Afterburner	13	30
Gas Boiler	60	24
TST	4	10

Figure 7.5.11 shows the electricity generation of the fuel cell system. In this case the operation of the fuel cell is following the electricity demand and there is no import from the grid.

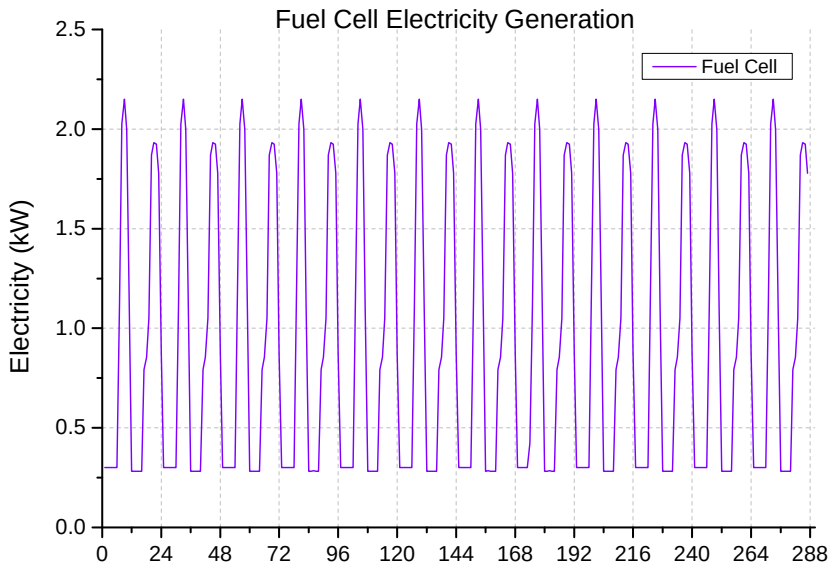

Figure 7.5.11: Graph representing the electricity output of the fuel cell micro-CHP for Case 2

Heat from the cooling circuit and the afterburner of the fuel cell is used for heating, DHW and for charging the TST. The heat that they deliver to the dwelling on a winter day can be seen in Figure 7.5.12 (for timesteps 1-24 of the 288 dataset) and on a summer day on Figure 7.5.13 (for timesteps 145-169). A presentation of the whole 288 dataset although possible would result in a very congested graph, therefore a separate winter and summer graph are created. Both graphs demonstrate that the demand is covered by a combination of heat sources giving flexibility to the system by storing heat in the TST and allowing the fuel cell to cover the whole electricity demand.

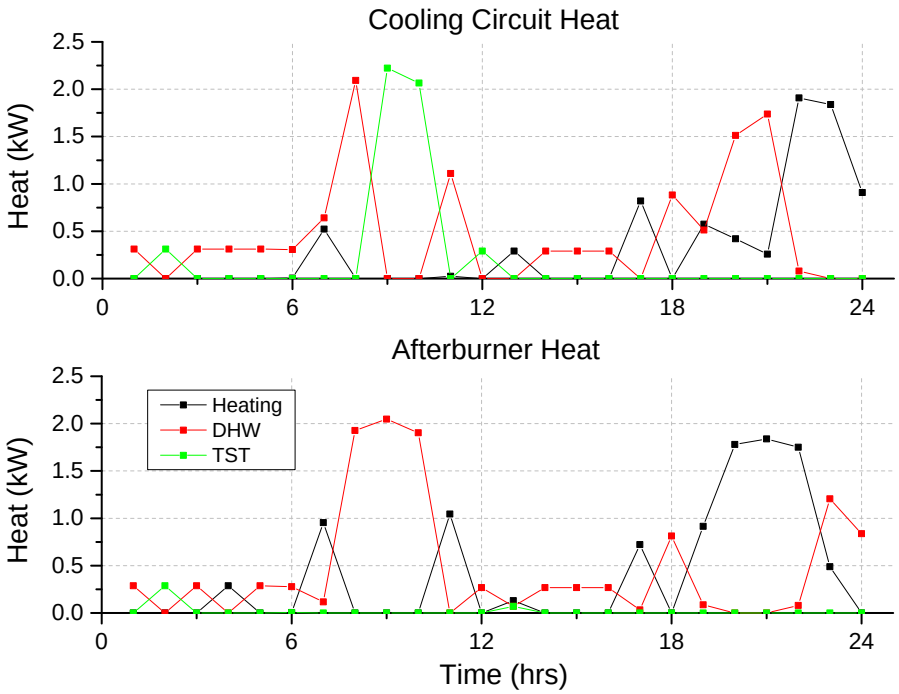

Figure 7.5.12: Graph representing the heat extracted from the fuel cell and where this heat is delivered in the dwelling on a winter day for Case 2

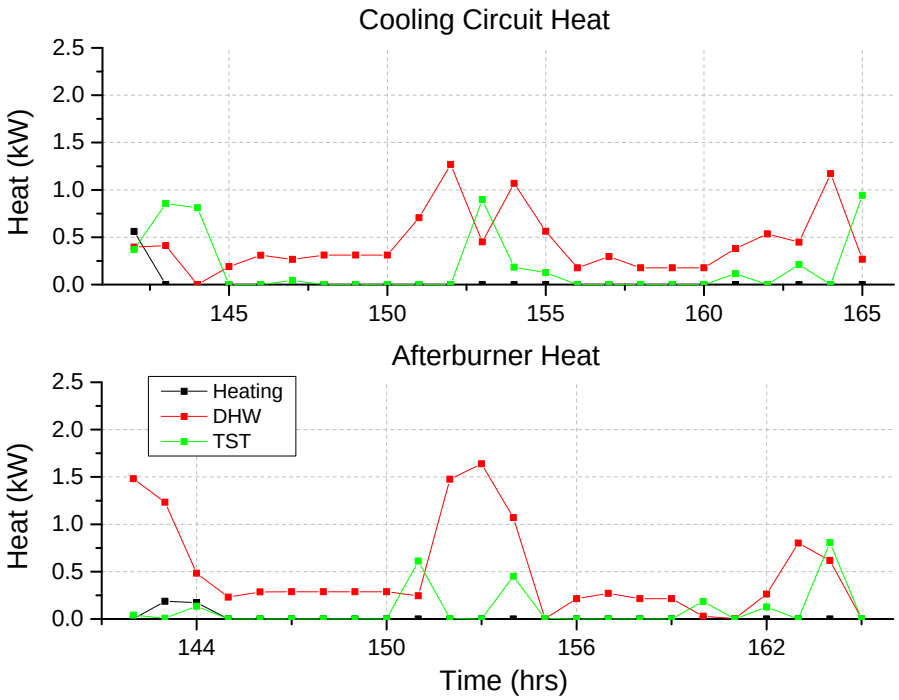

Figure 7.5.13: Graph representing the heat extracted from the fuel cell and where this heat is delivered in the dwelling on a summer day for Case 2

The heat delivered and received from the thermal storage during the whole 288 hour dataset is shown in Figure 7.5.14. The negative sign is indicative of the fact that heat is being removed from the tank.

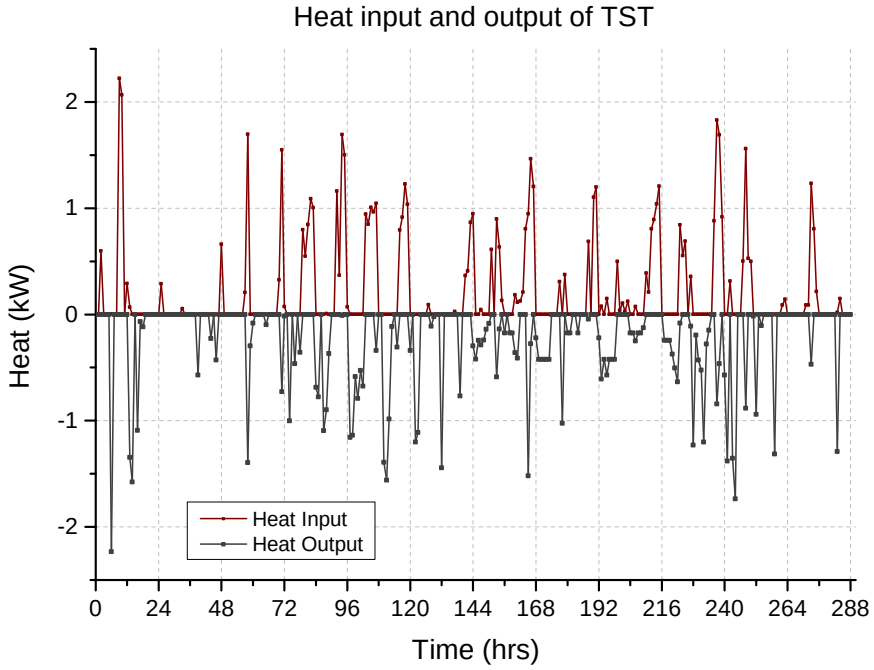

Figure 7.5.14: Graph representing the heat input and output of the TST for Case 2

The temperature of the storage tank has been assumed to be at 60 °C initially and has to be above 40 at the end. The optimum volume of the storage tank is 140 L. The upper bound was selected to be 800 L. However the low volume of the storage tank compared to its upper bound ensures that water above the 45 °C heating threshold would be more easily available in the TST. 800 litres of water would require more fuel cell heat to be raised to 45 °C . Its variation over the 288 timesteps can be seen in Figure 7.5.15.

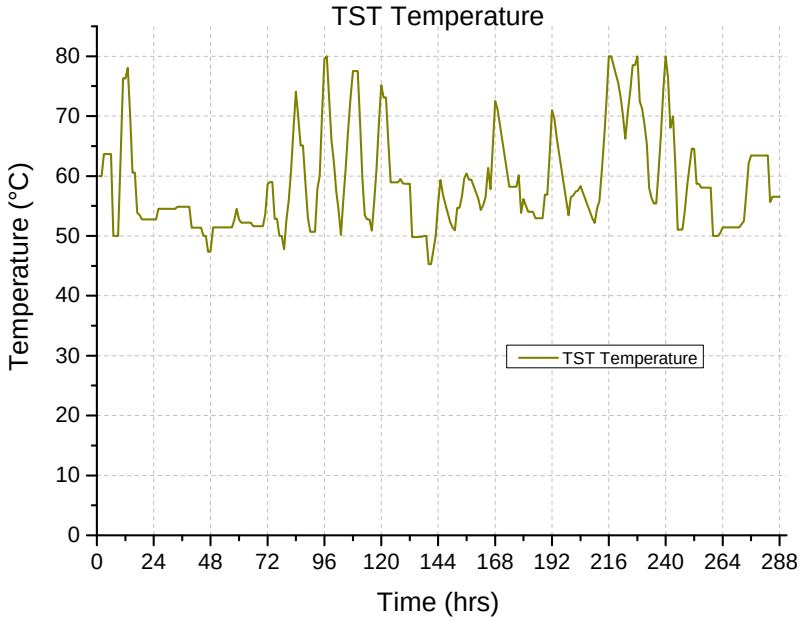

Figure 7.5.15: Graph representing the variation of water temperature in the TST for Case 2

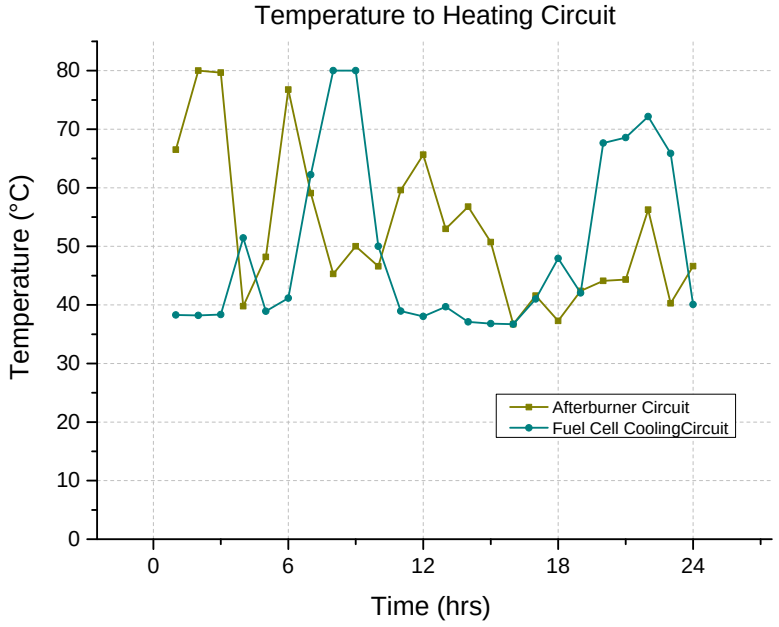

Figure 7.5.16: Graph showing the individual system temperatures over a winter 24 hour period for Case 2

The supply temperatures of heating and DHW circuits can be seen in Figure 7.5.17. The temperatures peak at periods of higher heating and DHW demand respectively following the daily activities of the house.

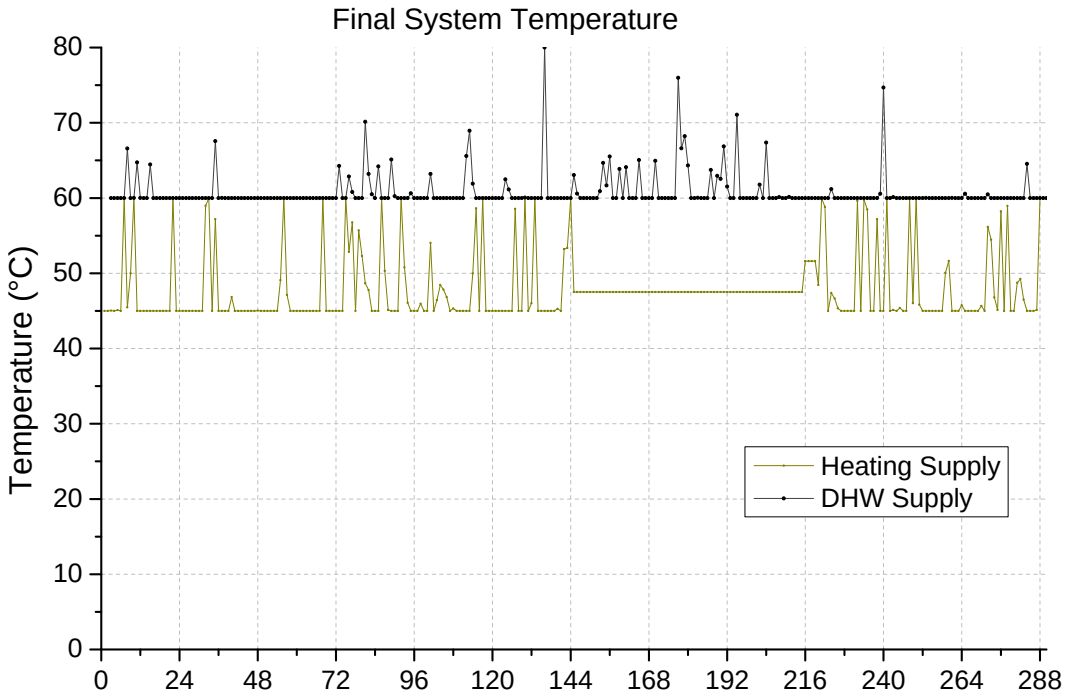

Figure 7.5.17: Graph showing the final total system temperatures for space heating and DHW over a 288 hour period for Case 2

7.5.1.3 Variation 1 - The effect of applying a different temperature constraint on the storage model

In this case study the exact same system is evaluated as in Case 2 with the difference being a constraint in the TST model. Here the TST temperature at the first hour of the day is forced to be equal to the last hour of the day for all the days of the dataset. This case will be referred to as Case 2b. In this case the maximum fuel cell capacity has been sized at 2.2 kW and the gas boiler peaks at 6 kW and 2.7 kW for heating and DHW respectively. The size of the TST has been calculated at 138 L which is slightly smaller than before. The total CO_2 emissions have been increased compared to Case 2 to 203 $kgCO_2$ however there are still lower than case 1, the case with no TST.

A summary of the annual heat contribution of each source can be seen in Table 7.5.

The total heat from the TST to the heating and DHW has been decreased compared to Case 2 to only 4% in heating and 3% in DHW. Naturally, the gas boiler's total heat contribution to both heating and DHW has been increased compared to Case 2.

Table 7.5: Annual heat contribution for each source for Case 2b

Source	**Space Heating (%)**	**DHW(%)**
FC Cooling Circuit	10	34
Afterburner	4	9
Gas Boiler	82	54
TST	4	3

This case study compared to case 2 relies more on the gas boiler for heat production while the fuel cell operates at a higher average utilisation factor and voltage to favour electricity production. However because the fuel cell overall is used less than before there is some grid electricity imported to satisfy demand.

Figure 7.5.18 shows the variation of the TST temperature. It can be seen that at the end of each day the temperature is equal to the start of the day. In the figure it is also shown that the otherwise wasted summer heat is stored in the TST increasing water temperature. The temperature in the TST increases above 50 °C in the summer when heat from the fuel cell that is not needed in the system is stored in the TST.

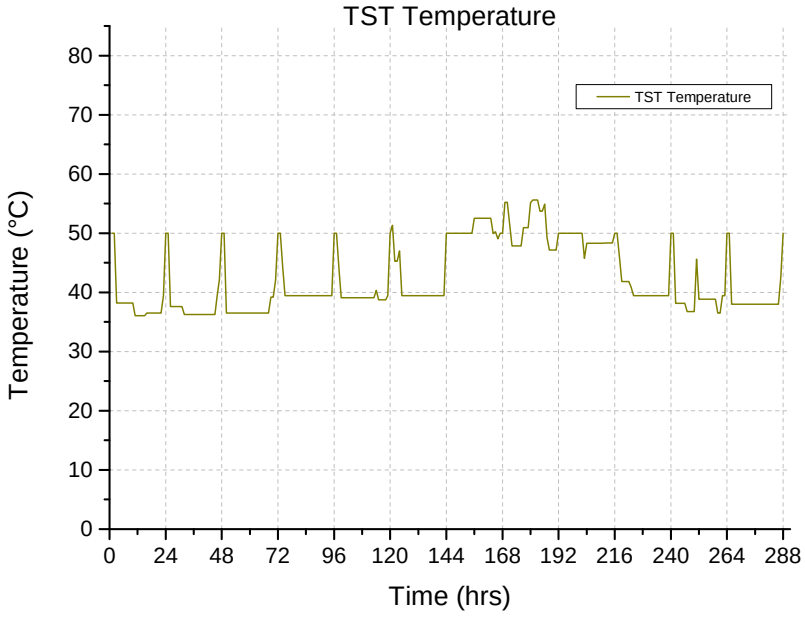

Figure 7.5.18: Graph representing the variation of water temperature in the TST for Case 2b

7.5.1.4 Comparative Results

Table 7.6 summarises the basic characteristics of the three designs and of the variation. The reductions in CO_2 emissions from the base case varybetween 27% and 32% respectively. The variation of case 2, case 2b which includes a different approach in modelling the TST, results in a very similar system to case 2 but with different operation pattern. The base case emissions are derived from the reference building presented in chapter 5.

Table 7.6: Summary of results for cases l and 2

	CO_2 emissions (kgCO_2)	**Reduction (%)**	**Boiler CO_2 emissions (kgCO_2)**	**Fuel Cell CO_2 emissions (kgCO_2)**	**Grid Electricity CO_2 emissions (kgCO_2)**
Base Case	289	-	161	-	128
Case 1	211	27.0	60	135	16
Case 2	197	31.8	54	143	0
Case 2b	203	29.9	103	98	1

Comparing the cases presented here, the main points are the following:

Table 7.7: Overview of system characteristics for cases 1 and 2

	Maximum Boiler Load Heating (kW)	**Maximum Boiler Load DHW (kW)**	**Maximum FC Electrical Capacity (kW)**	**TST Volume** (m^3)
Base Case	6.0	2.8	-	-
Case 1	5.6	1.0	1.9	-
Case 2	5.3	2.7	2.2	0.140
Case 2b	6	2.7	2.2	0.138

- Case 2 covers electricity by using the fuel cell with no electricity input from the grid compared to case 1 where a small amount of electricity is imported. The fuel cell in case 2 is allowed to operate for more hours and satisfy the entire electricity demand while the heat that it generates can be stored in the TST. This gives the system an additional flexibility that case 1 does not have.

- The system temperatures are lower values for case 2. This can be seen in Figures 7.5.6, 7.5.7, 7.5.16, 7.5.17 and also in Figure 7.5.19 that represents the temperature at the point where the flows from the heating and DHW come together.

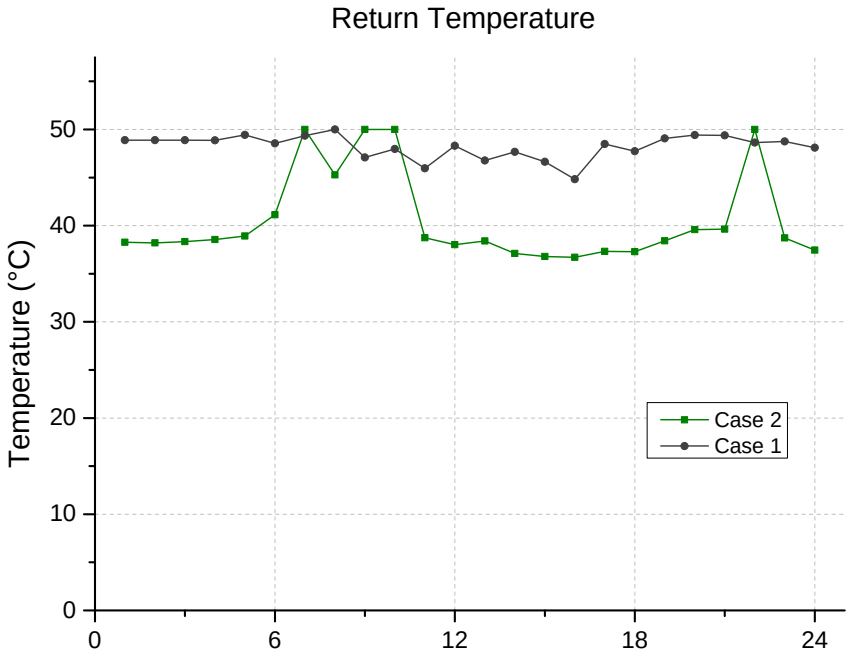

Figure 7.5.19: Graph showing the total return system temperatures over a winter 24 hour period for Cases 1 and 2

The total boiler CO_2 emissions are reduced in Case 2 which together with the higher sizing of the fuel cell indicates that case 2 relies more on the fuel cell to cover energy demand. Figure 7.5.20 shows the variation of the total boiler load for the whole 288 period. It can be seen that the boiler in Case 1 is operating in the summer hours (144 to 216), whereas the boiler in case 2 has turned off.

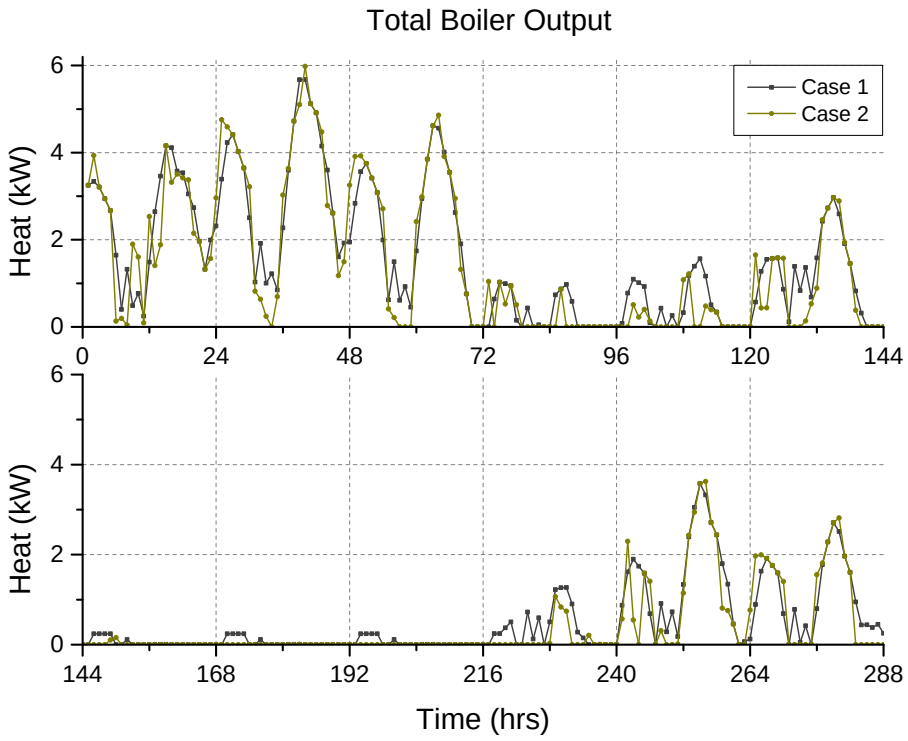

Figure 7.5.20: Graph showing the total boiler operation over the whole year period for Cases 1 and 2

7.5.2 Part L Dwelling Designed with Radiators

In this case study the design of a fuel cell micro-CHP system will be evaluated in a dwelling with a radiator system. As highlighted in section 2.9, different heat emitters require different water temperatures and flow rates to efficiently deliver the heat output.

In terms of modelling this case study uses the same model principles of section 7.3, however the temperature bounds have been changed to allow for the higher temperatures of the radiator system. The fuel cell is assumed to operate at 80 ^{o}C to be able to supply an temperature of the same order at the cooling circuit. Similarly with cases 1 and 2, Cases 3 and 4 differ on the inclusion of TST in the design. The results are also compared against the findings of section 7.5.1 focusing on discussing the differences between the design outcomes.

7.5.2.1 Case 3

The optimum design and the connections from each heat exchanger to heating and hot water demands are illustrated in Figure 7.5.21. The fuel cell is sized at 2.5kWe and the boiler at 6.2 kWth and 1.5 kWth for heating and DHW respectively. All possible heat sources are contributing to satisfying space heating and DHW demand.

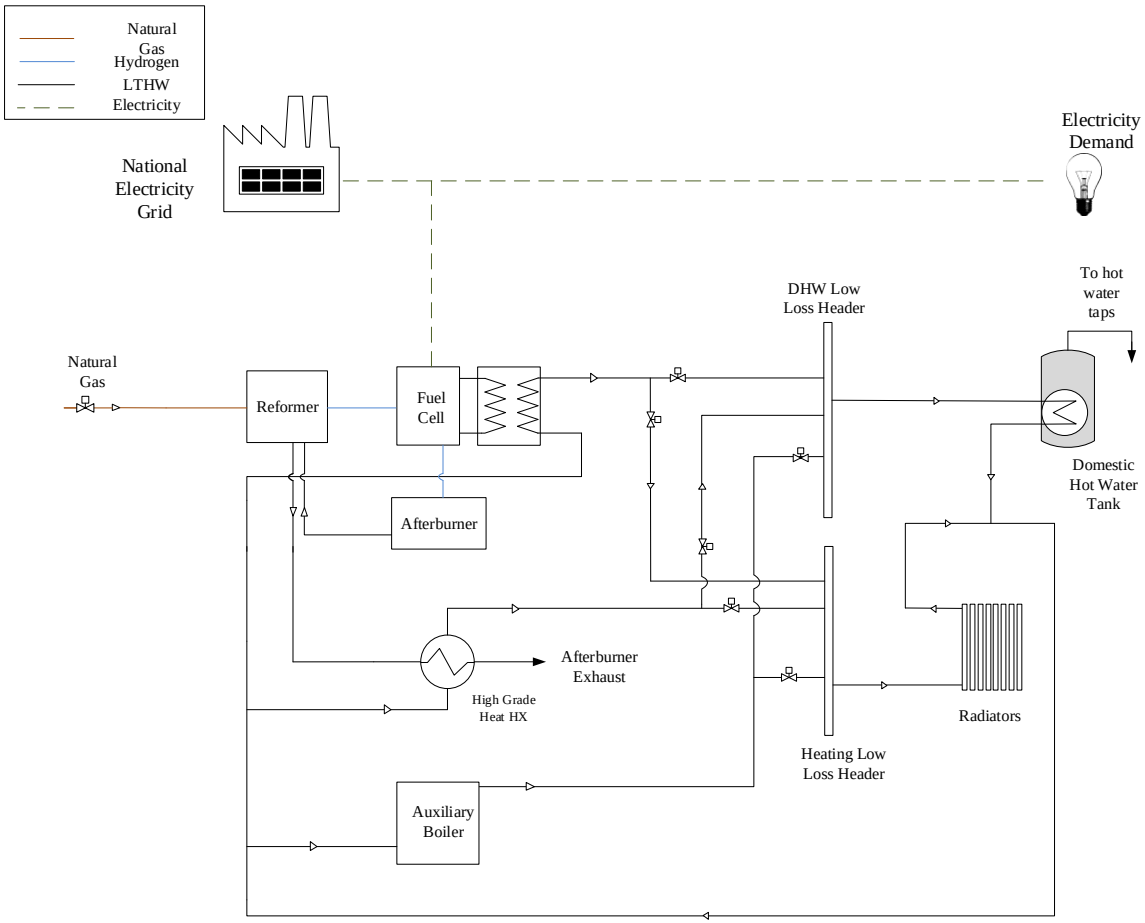

Figure 7.5.21: Schematic diagram representing the optimum design configuration for case 3

The contribution of each heat source to space heating and DHW demand is listed in Table 7.8. The fuel cell micro-CHP is serving in total 80% of the DHW demand.

Table 7.8: Annual heat contribution for each source for case 3

Source	**Space Heating (%)**	**DHW(%)**
FC Cooling Circuit	13.0	50.0
Afterburner	9.0	30.0
Gas Boiler	78.0	20.0

The higher pipe temperatures of the heating system are the characteristic of this case study. This is best illustrated in Figure 7.5.22 which zooms in again on the 288 dataset to show the pipe temperature leaving the fuel cell cooling circuit and the afterburner heat exchanger for the first 48 hours of the 288 data set. Figure 7.5.23 shows the resulting final supply and return pipe temperature at the heating and DHW circuits. The final temperatures in both circuits follow a 10 °C temperature difference while the flow rate varies to satisfy the demand.

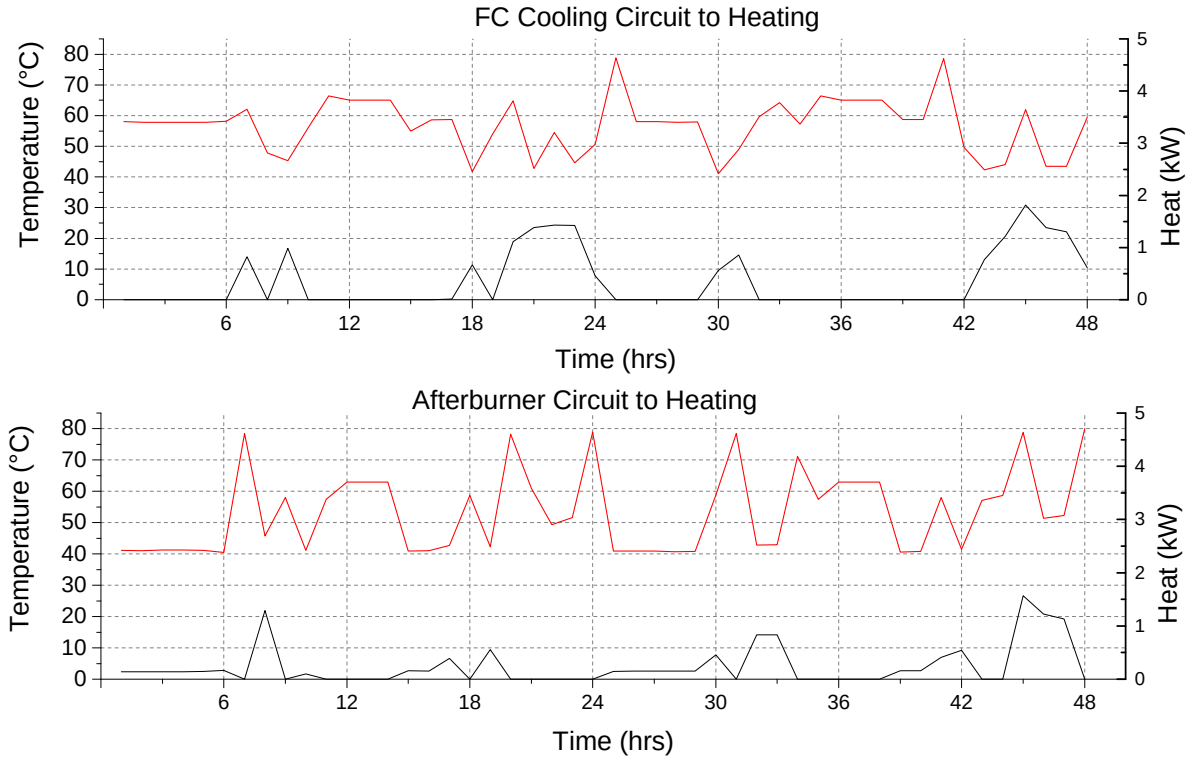

Figure 7.5.22: Graph showing the supply temperatures of the fuel cell cooling circuit and afterburner heat exchangers over a period of 48 hours for Case 3. Additionally the heat output of each heat exchanger to space heating is shown on the right axis

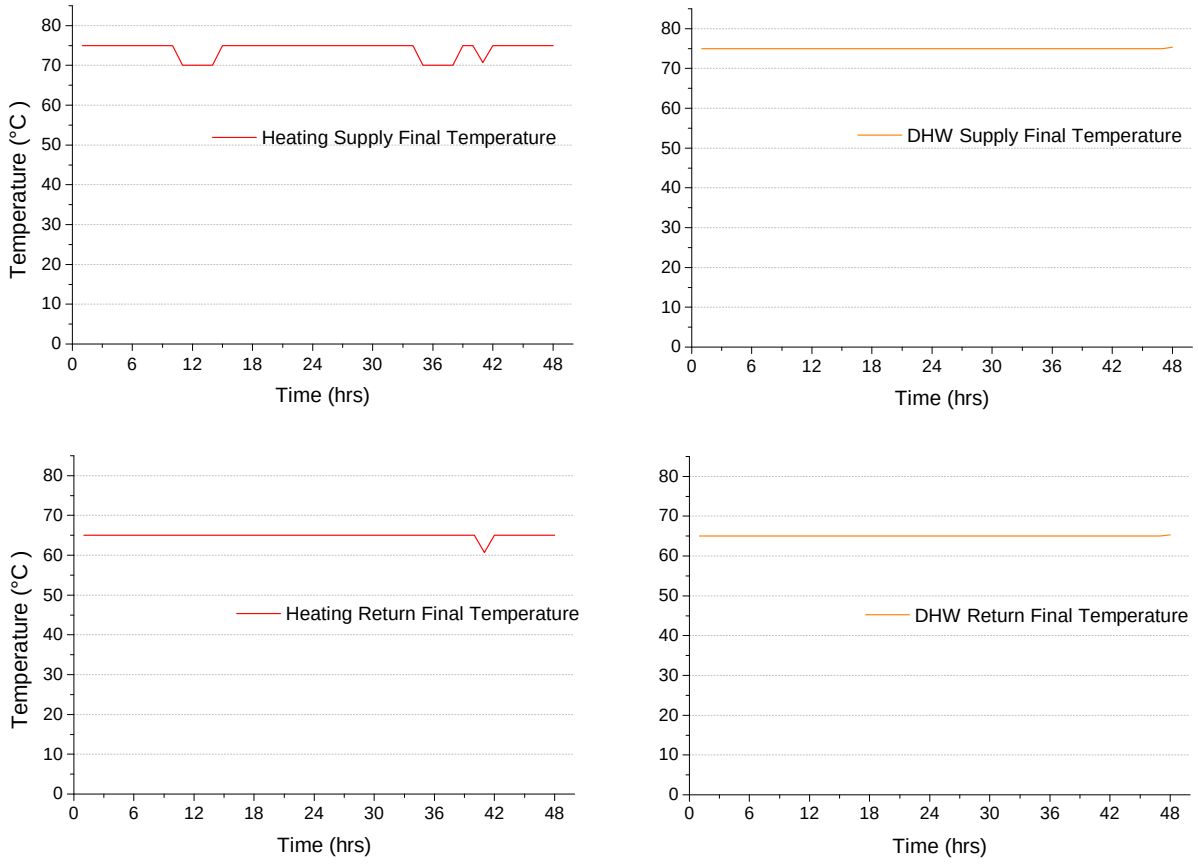

Figure 7.5.23: Graph showing the total system temperatures over the first 48 hour period for Case 3. At times of 0 demand, the temperature variable takes also the 0 value as it can be seen for the space heating supply and return temperature.

The total water flow rates follow the heat demand patterns as shown in Figure 7.5.24. At times of no space heating demand, the flow rate takes the 0 value.

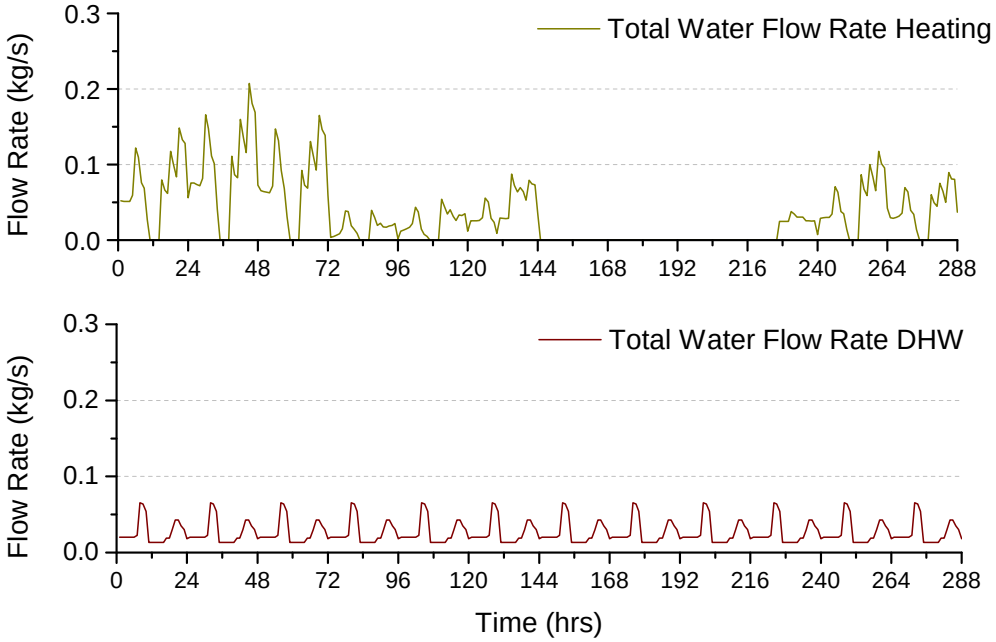

Figure 7.5.24: Graph showing total water flow rates over the whole 288 hour period for Case 3

7.5.2.2 Variation 2 - The effect of the minimum modulation of the gas boiler

This variation of case 3 explores the effect of relaxing the minimum modulation or load factor of the gas boiler down from 0.3, to 0, 0.1, 0.2. The average load factor and the results in terms of CO_2 emissions are listed in Table 7.9. The total emissions of each system increase as the minimum modulation increases. The overall configuration is identical as Case 3 with the fuel cell micro-CHP and the auxiliary gas boiler serving both space heating and DHW. There is no TST.

The operation from case to case differs in the following way: Generally the fuel cell micro-CHP is preferred as it produces both electricity and heat. For heat demands that the fuel cell cannot cover due to capacity limitations, the gas boiler is used. In the cases with high modulation limit this means that higher amounts of heat will be generated as a minimum and therefore for these cases it is not advantageous for the objective function, to use the fuel cell as its heat would not be used or stored at all at the absence of a TST. So, as the modulation increases, there is an increased electricity input from the grid.

Table 7.9: CO_2 emission of each system after altering the minimum modulation level of the gas boiler

Minimum Load Factor	**Average Load Factor**	CO_2 **Emissions (kg**CO_2**)**
0	0.14	.202
0.1	0.21	.203
0.2	0.20	.205
0.3 (Case 3)	0.21	.209

The variation of the load factor of the gas boiler is shown in figure 7.5.25. Systems with higher modulation limit are not capable to reduce the output of the gas boiler to match a low heat demand. This can be seen in the summer period between timesteps 144-216 where the gas boiler in the upper graph of figure 7.5.25 can operate at low capacity and provide the required output. This cannot be done for cases 0.2 and 0.3 that are shown in the bottom graph which shows that the boiler is not supplying any heat to the system.

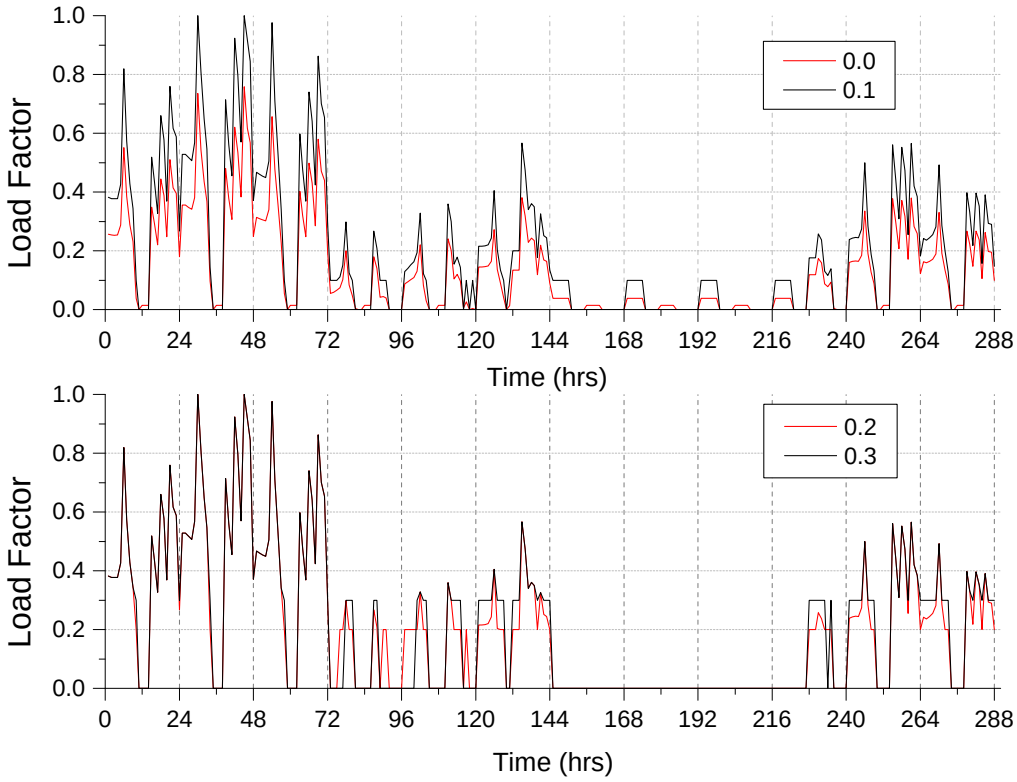

Figure 7.5.25: Graph showing the load factor of the gas boiler over the whole 288 hour period for all cases after altering the minimum modulation limit

7.5.2.3 Case 4

The design and performance of a system comprised of a fuel cell micro-CHP, a gas boiler and a TST coupled with radiators for heat emitters is evaluated in this example. The addition of TST in this system compared to case 3 gives a system designed with a larger fuel cell sized at 3.6 kW. A TST sized at 115 L provides heat to the system, reducing the operation of the gas boiler and allowing the fuel cell to cover most of the electricity demand minimising electricity import from grid.

In this optimum design, space heating and DHW demand are covered by all possible sources, the fuel cell cooling circuit, the afterburner, the gas boiler and the TST.

Table 7.10 shows the annual contribution of each heating source to satisfying demand. The fuel cell totally covers 72% of space heating and 69% of DHW demand and at the same time the whole electricity demand.

Table 7.10: Annual heat contribution for each source for case 4

Source	**Space Heating (%)**	**DHW(%)**
FC Cooling Circuit	37.0	31.0
Afterburner	35.0	38.0
Gas Boiler	27.0	29.0
TST	1.0	2.0

Figure 7.5.26 zooms in the whole dataset to show the electricity generation of the fuel cell on a winter and on a summer day. The fuel cell covers the entire electricity demand of the dwelling. As the electricity is generating electricity in the summer when space heating demand is low, all heat is used for DHW as it can be seen in Figure 7.5.29.

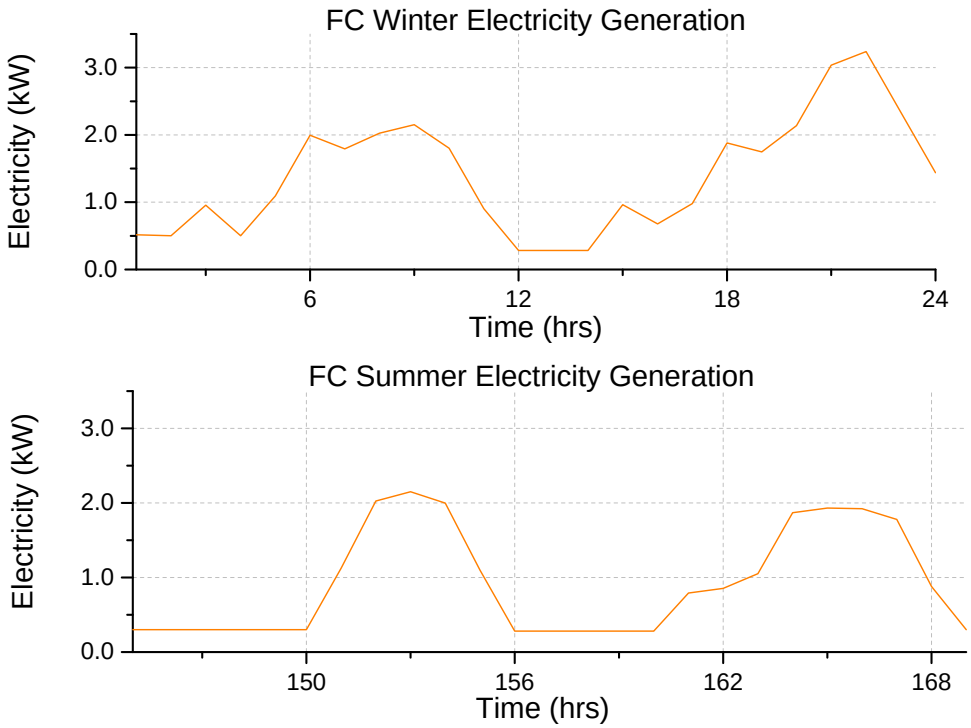

Figure 7.5.26: Graph representing the electricity generation of the fuel cell on a winter and on a summer day for Case 4

Figure 7.5.27 shows the total heat of the afterburner stream and the amount released for the reforming process. The remaining afterburner heat is then used in the building for space heating, DHW or gets stored in the TST.

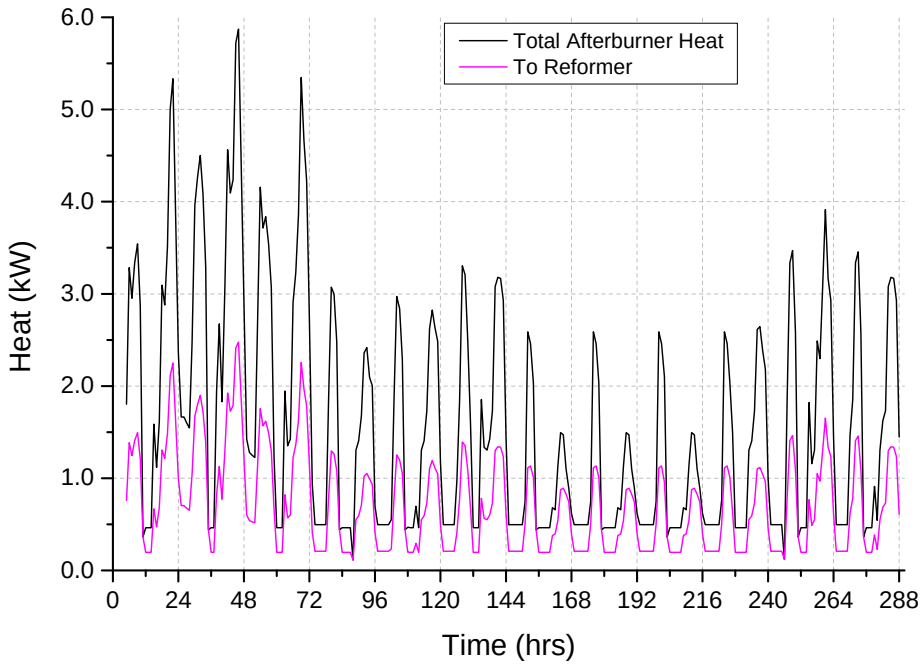

Figure 7.5.27: Graph representing the heat extracted from the afterburner and the heat recovered from the reformer for Case 4

Figures 7.5.28 and 7.5.29 show the annual contribution of each heating source to space heating and DHW respectively. They show that the boiler's contribution to heat demand is kept low as it is covered mostly by the fuel cell. It can be seen that heat from the two different heat sources of the fuel cell is used to cover the space heating and DHW demand of the house.

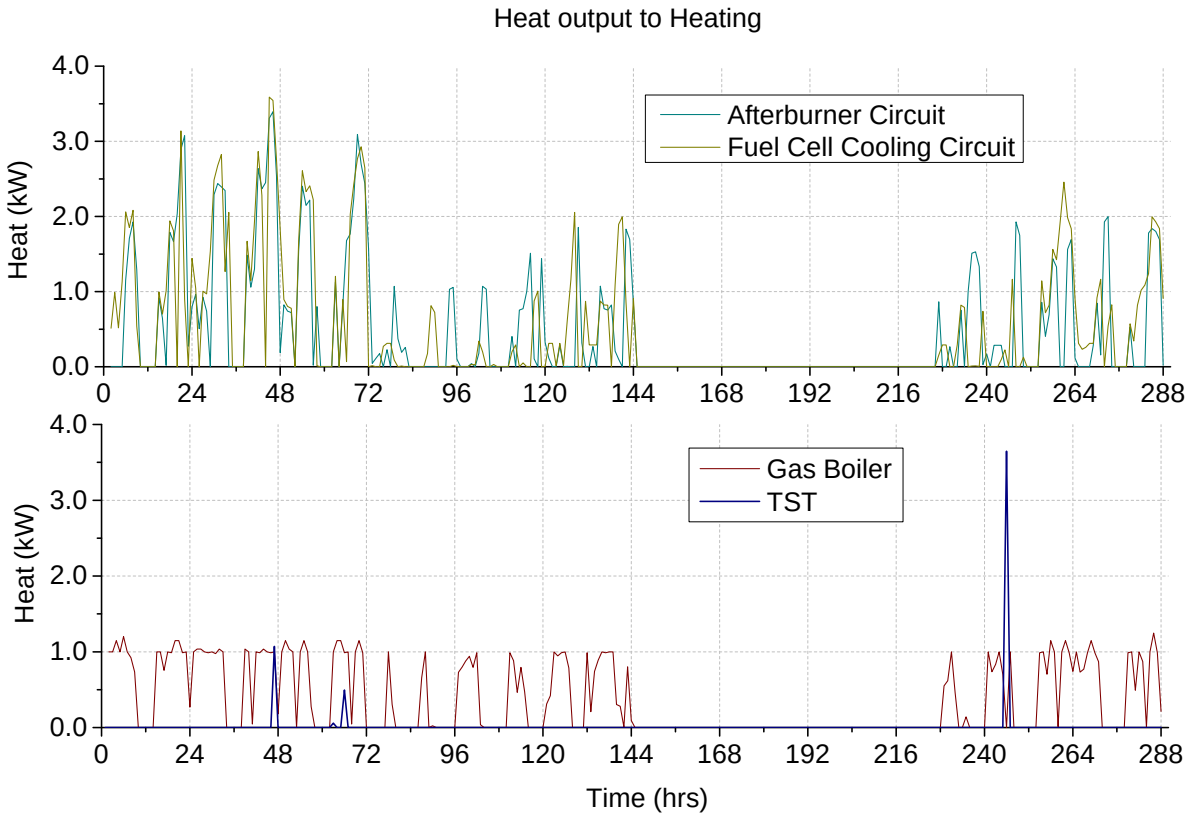

Figure 7.5.28: Graph representing the heat output of each plant delivered to the space heating circuit on an annual basis for Case 4. The graph shows the output of the gas boiler is supplementary to the fuel cell which is sized to cover most heat demand

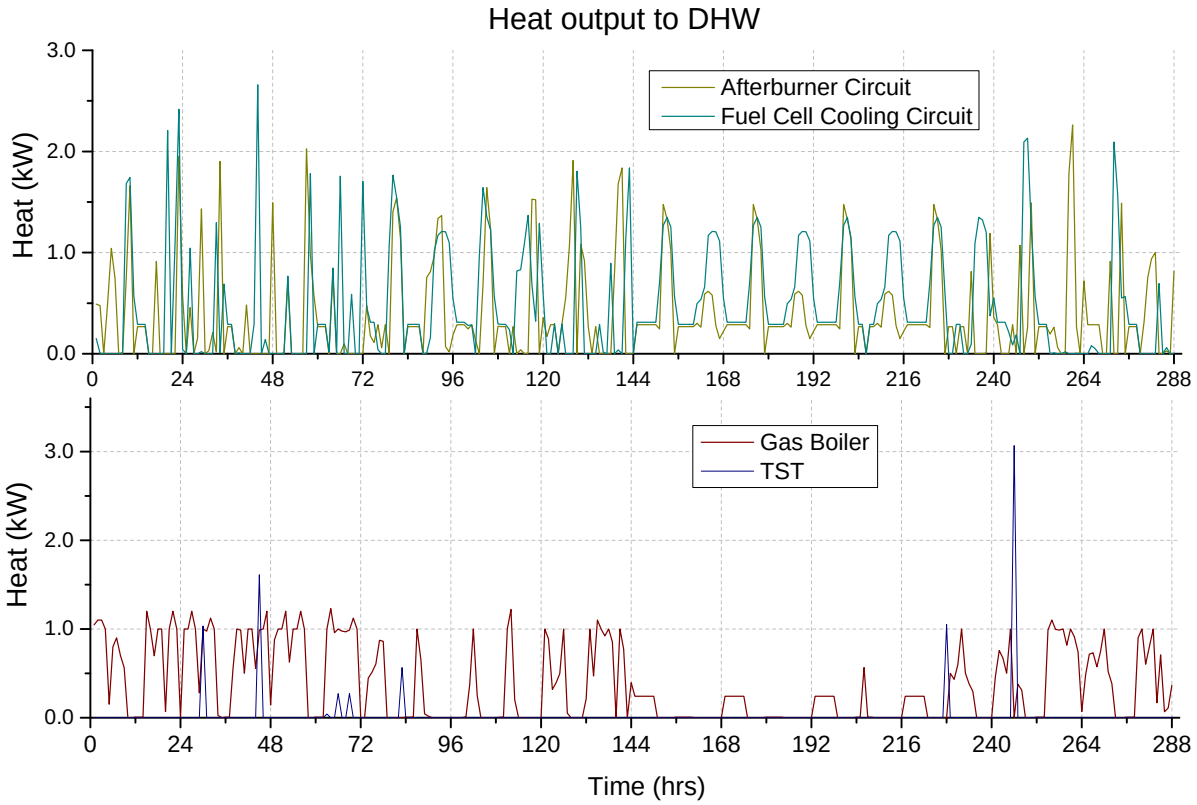

Figure 7.5.29: Graph representing the heat output of each plant delivered to the DHW circuit on an annual basis for Case 4

The increased capacity of the fuel cell compared to cases 1&2 is a result of the more rapid space heating demand pattern of the radiator system. The average value of the hydrogen utilisation factor for the whole 288 hour dataset is 0.63 which favours heat production compared to electricity. This is also supported by an average value for voltage of 0.64 V which is closer to the lower bounds of the variables and allows the fuel cell to produce more heat at both heat exchangers.

Figures 7.5.30 and 7.5.31 are snapshots of Figures 7.5.28 and 7.5.29 show the heat output of the fuel cell cooling circuit and afterburner for each demand for a winter (1-24) and a summer day (145-168).

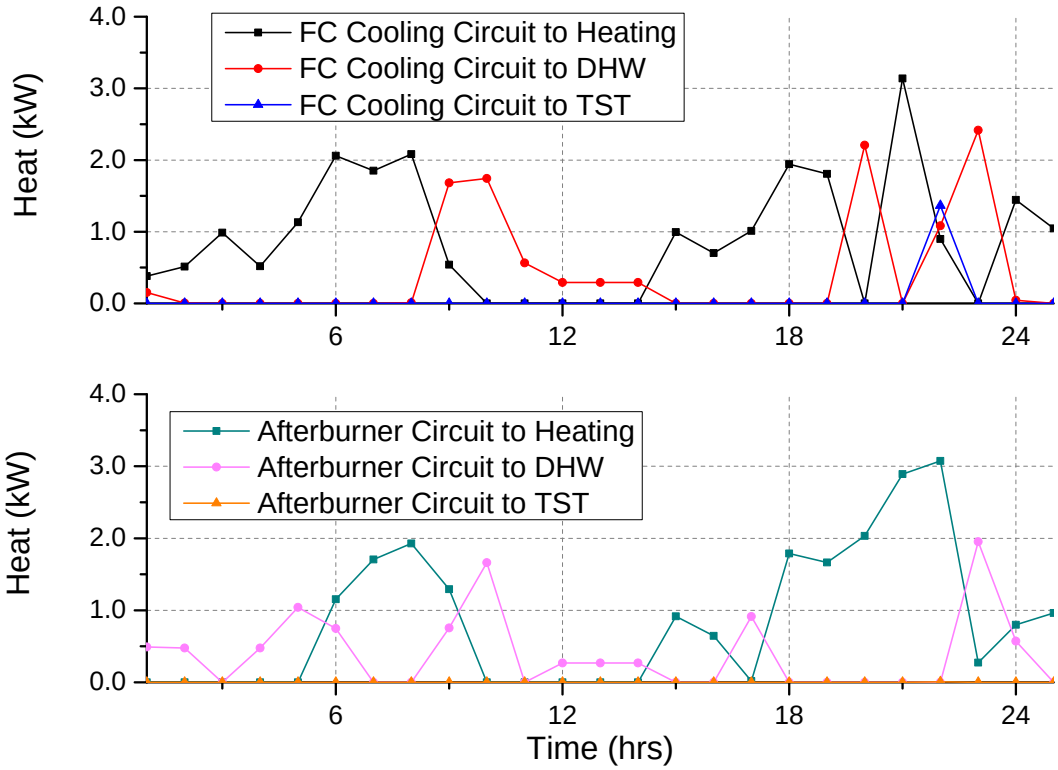

Figure 7.5.30: Graph representing the heat extracted from the fuel cell and where this heat is delivered in the dwelling on a winter day for Case 4

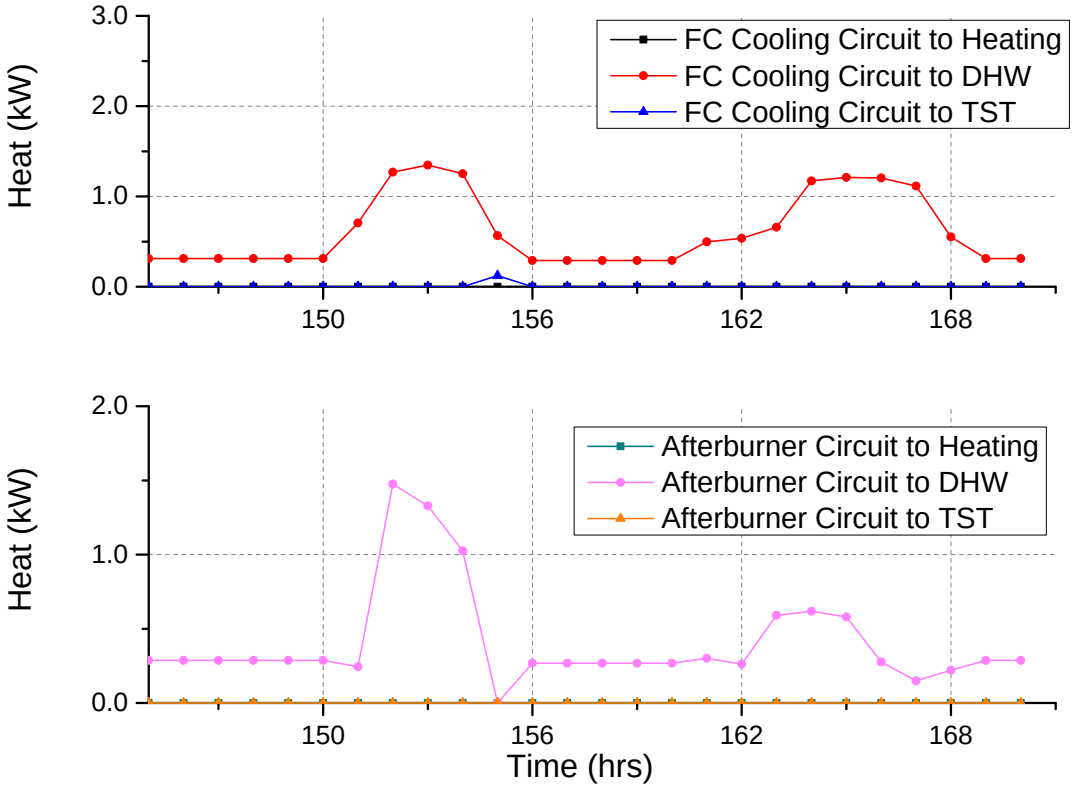

Figure 7.5.31: Graph representing the heat extracted from the fuel cell and where this heat is delivered in the dwelling on a summer day for Case 4

Heat input and output of the TST can be seen in Figure 7.5.32. The total contribution of the TST in the whole heat demand combined is only 3%. This shows that for the case of a fuel cell sized to cover a big portion of space heating and DHW demand, the TST acts supportively ensuring that water is maintained at the high temperature at all times to be used when needed in the dwelling. The TST is not used as much as for the case of UFH system presented in case 2 because the higher temperature required for radiators is more difficult to achieve.

The model at this case study has opted for a TST that is not used much. The design engineer looking at these results should make a decision with regard to the TST being required in the design.

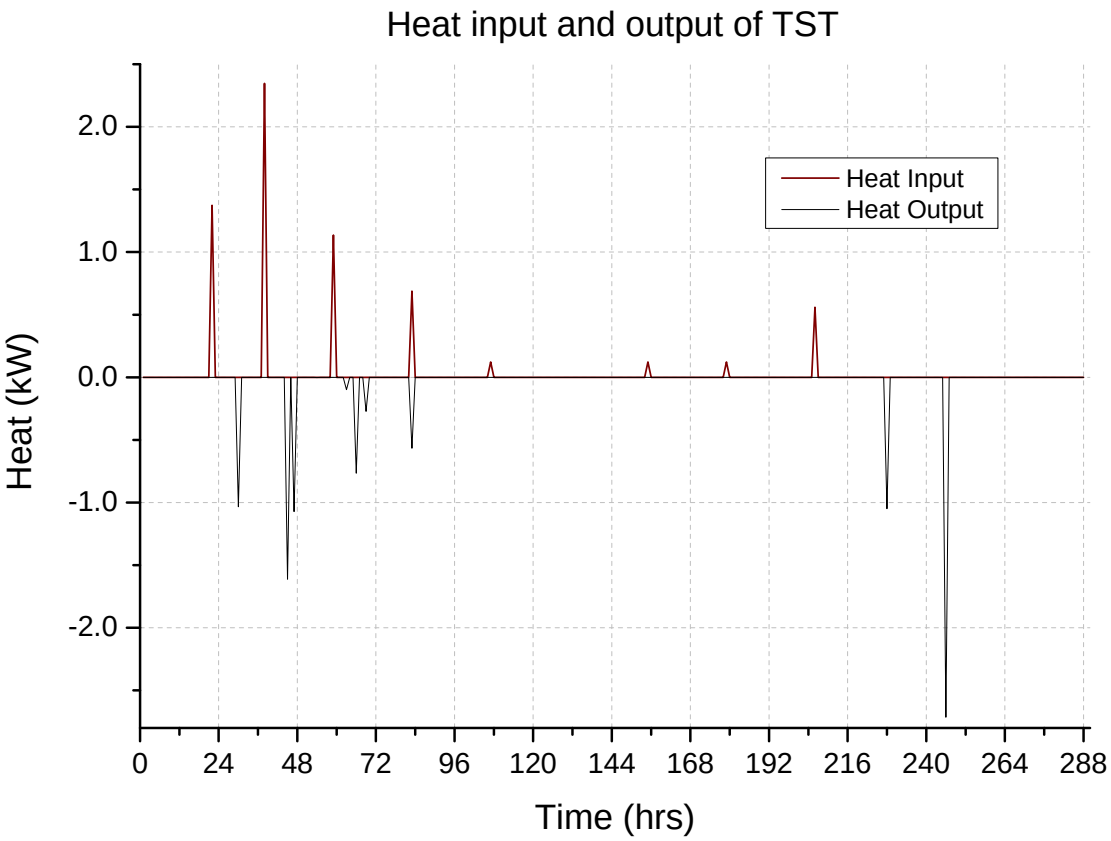

Figure 7.5.32: Graph representing the heat input and output of the TST for Case 4

Figure 7.5.33 shows the variation of TST temperature throughout the 288 hours. From the graph the reader can see the effect of not modelling any heat losses at the TST. If losses were added to the TST model, two possible things could have happened: either the TST would not be used as much because of the loss of efficiency or any heat stored would be used in the subsequent timesteps.

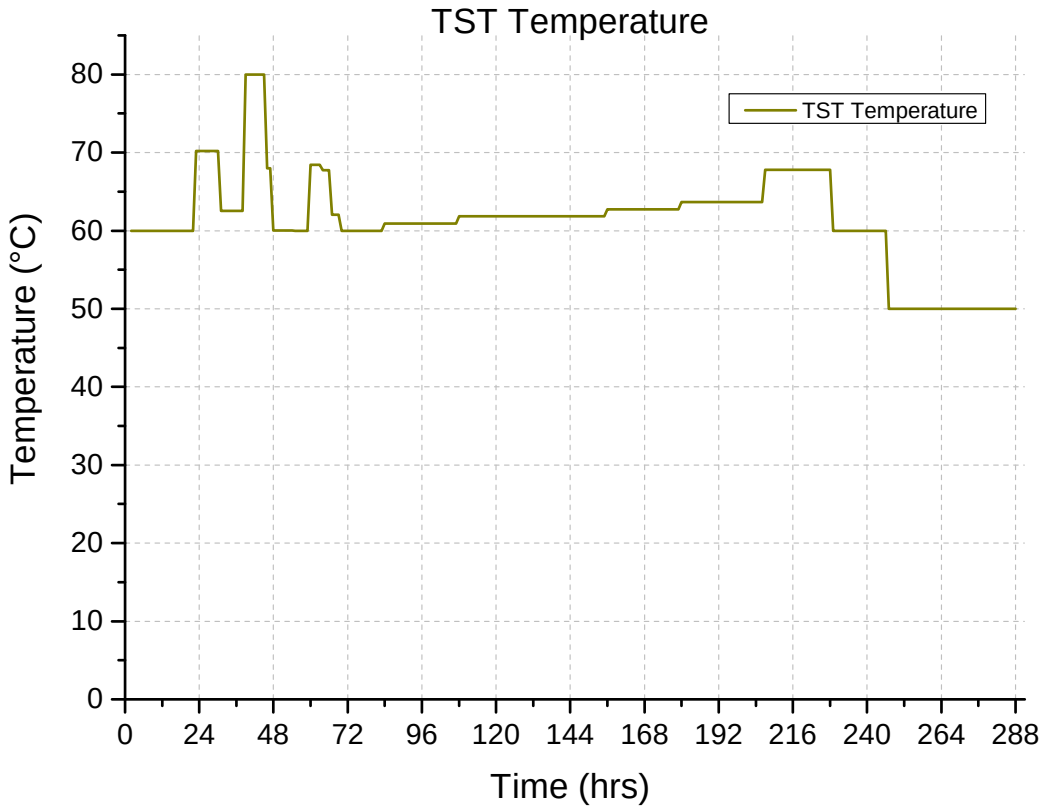

Figure 7.5.33: Graph representing the variation of water temperature in the TST for Case 4

In order to show the relation between the heat recovered from the fuel cell's cooling circuit and afterburner, to the water temperature in the pipe networks, figures 7.5.34 and 7.5.35 are used. At times of no heat output, e.g. between 144 to 220, the supply stream temperature of the the fuel cell heat exchanger takes a constant value of 50°C; as the heating flow rate at these timesteps is 0, the temperature variables take the values that were used for initialisation.

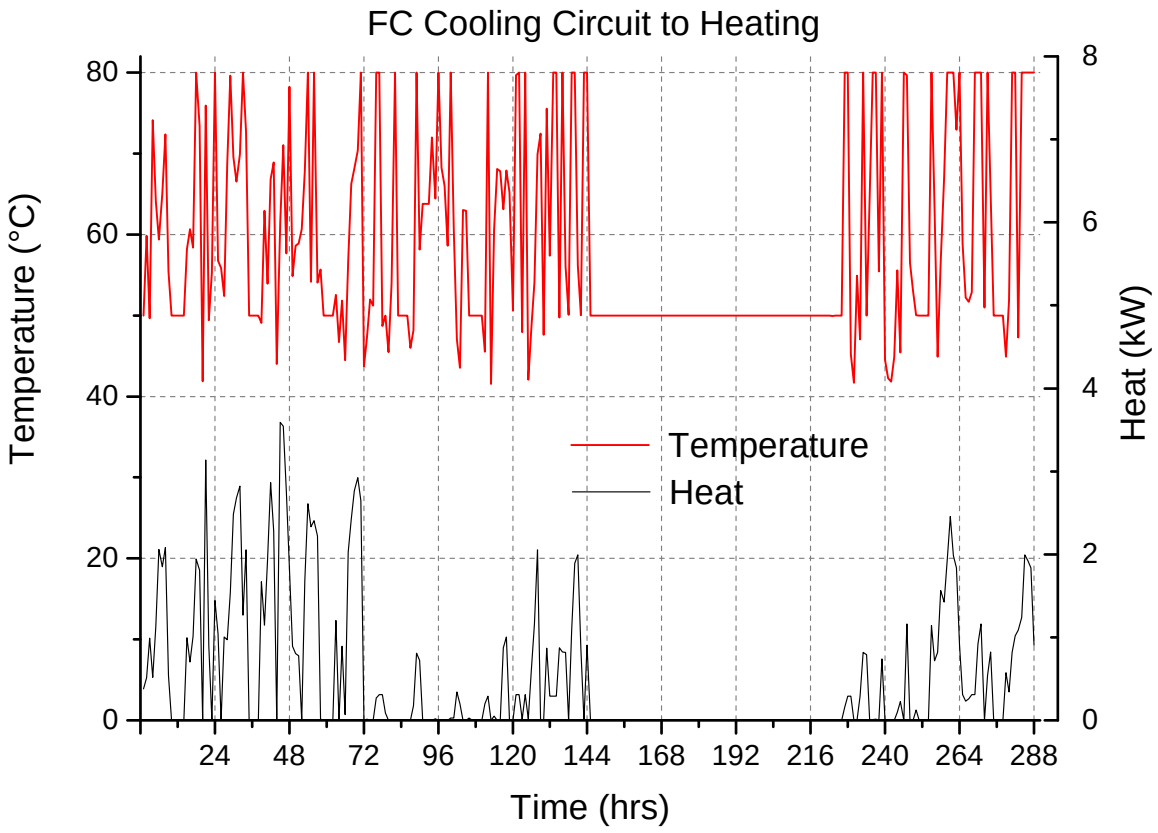

Figure 7.5.34: Graph representing the supply temperature and heat released from the fuel cell cooling circuit to the space heating pipe circuit for Case 4.

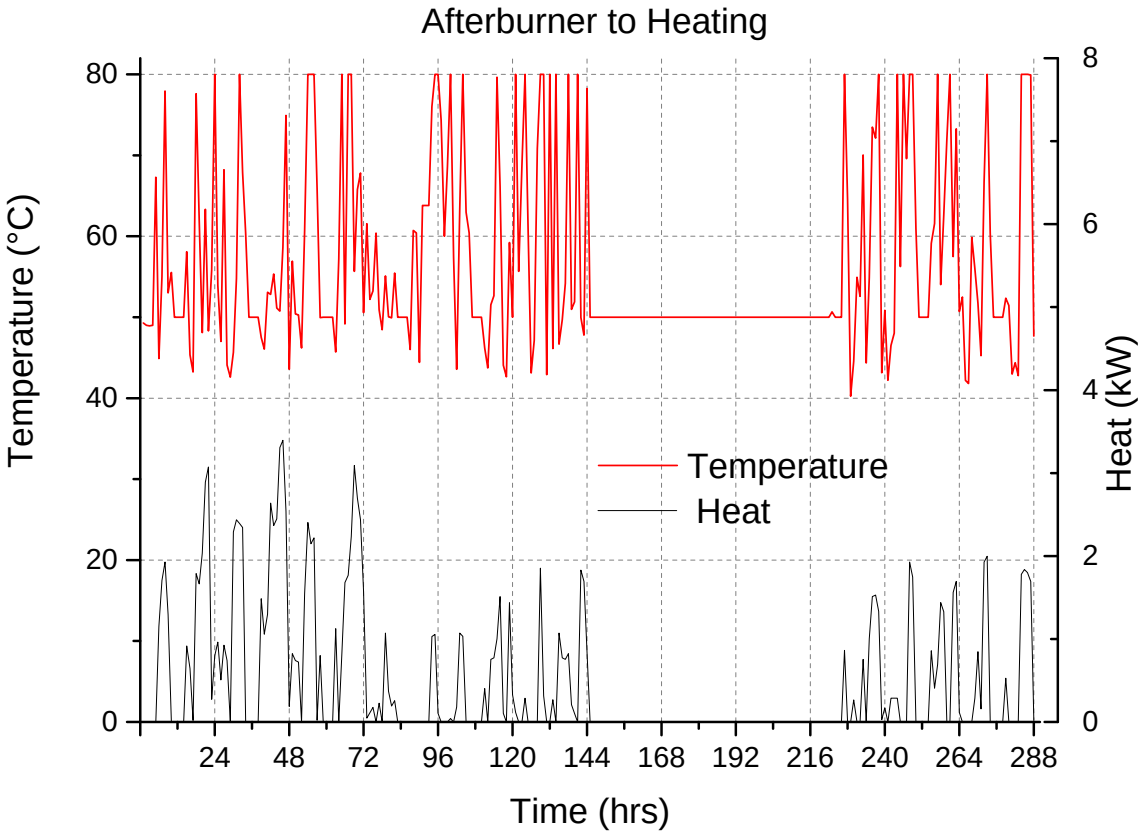

Figure 7.5.35: Graph representing the supply temperature and heat released from the afterburner circuit to the space heating pipe circuit for Case 4.

7.5.2.4 Comparative Results

Table 7.11 summarises the basic characteristics of Cases 3 and 4 against the base case. There is an approximate 29% in CO_2 emissions from the base case for both cases presented in 5.2.1.2 which is similar to the reduction calculated for case 1 against the base case. However, system design is different with higher temperatures and boiler sizing. This might suggest that the overall reduction in CO_2 emissions is guaranteed regardless of the emitter selection and system temperature, on the basis that all plant can satisfy the temperature and ramp up constraints.

Table 7.11: Summary of results for cases 3 and 4

	CO_2 emissions (kgCO_2)	Reduction (%)	Boiler CO_2 emissions (kgCO_2)	Fuel Cell CO_2 emissions (kgCO_2)	Grid Electricity CO_2 emissions (kgCO_2)
Base Case	292	-	164	-	128
Case 3	209	28.4	82	125	2
Case 4	209	28.4	42	166	1

Table 7.12: Overview of system characteristics for cases 3 and 4

	Maximum Boiler Load Heating (kW)	Maximum Boiler Load DHW (kW)	Maximum FC Electrical Capacity (kW)	TST Volume (m^3)
Base Case	8.7	2.8	-	-
Case 3	6.2	.1.5	2.5	-
Case 4	1.1	1.2	3.6	0.115

7.5.3 Part L Dwelling - Electricity Exporting Scenarios

There is a lot of interest lately on the effects of exporting energy from domestic properties and specially when they are supported by schemes such as the feed-in-tarrifs. In this case study the design of a fuel cell micro-CHP system will be evaluated in a dwelling that uses the fuel cell to export electricity to the grid.

The building is served by UFH. In terms of modelling this case study uses the same principles of section 7.3, however the electricity generated by the fuel can either be used in the building or exported to the grid. The electricity exported in the grid reduces generation at the electricity stations, therefore reduces emissions from the grid. The analysis is based on an emissions and not cost basis, as prices for exporting electricity to the grid vary significantly; a fact which introduces uncertainty on the results.

A new variable has been introduced ($E^{exp}(t)$) which represents the exported electricity per time step. The changes that had to be implemented in the model involve a new electricity balance equation (equation 7.5.1) and an addition on the equation that calculates the total CO_2 emissions (equation 7.5.2).

$$E^{exp}(t) + E^{fc}(t) = n^{fc}_{H2}(t) \cdot i_{H2} \cdot V^c(t) \tag{7.5.1}$$

$$M^{el} = f_e \sum_t (E^g(t) - E^{exp}(t)) \tag{7.5.2}$$

The model favours the export of electricity to the grid as it not only reduces the total system emissions but also generates heat that can be used in the building. Therefore different examples were run where the bounds of variable $E^{exp}(t)$ where gradually increased from 0.5 kW to 2.0 kW using 0.5 kW steps considering the fact that a domestic fuel cell will not be sized higher than 3-4 kW.

7.5.3.1 Case 5

Case 5 represents the design without TST and has the same connections from plant to demand as case 1 (Figure 7.5.1). The fuel cell is sized to cover the electricity demand of the house but also the exported electricity.

Table 7.13 lists the basic sizing values for each subcase.

Table 7.13: Overview of system characteristics for case 5

Limit on exported electricity (kW)	**Maximum Boiler Load Heating (kW)**	**Maximum Boiler Load DHW (kW)**	**Maximum FC Electrical Capacity (kW)**	CO_2 **emissions (kg**CO_2**)**
0.5	4.1	1.1	2.7	152
1.0	3.3	1.1	3.2	109
1.5	2.2	1.2	3.7	69
2.0	2.0	0.5	4.2	30

Figure 7.5.36 shows a summary of the results for the four different subcases that are created by varying the limit for exporting electricity. The larger the limit becomes, the total system emissions reduce which is an effect of the lower emissions per unit of energy of the fuel cell compared to grid electricity. The boiler emissions also reduce at higher limits of exported electricity as the majority of the heating load is covered by the fuel cell's increased heat output. For the case of the 2 kW exporting limit the emissions become very low representing an approximate 90% reduction from the reference building showing the potential of fuel cells for exporting electricity and balancing the grid.

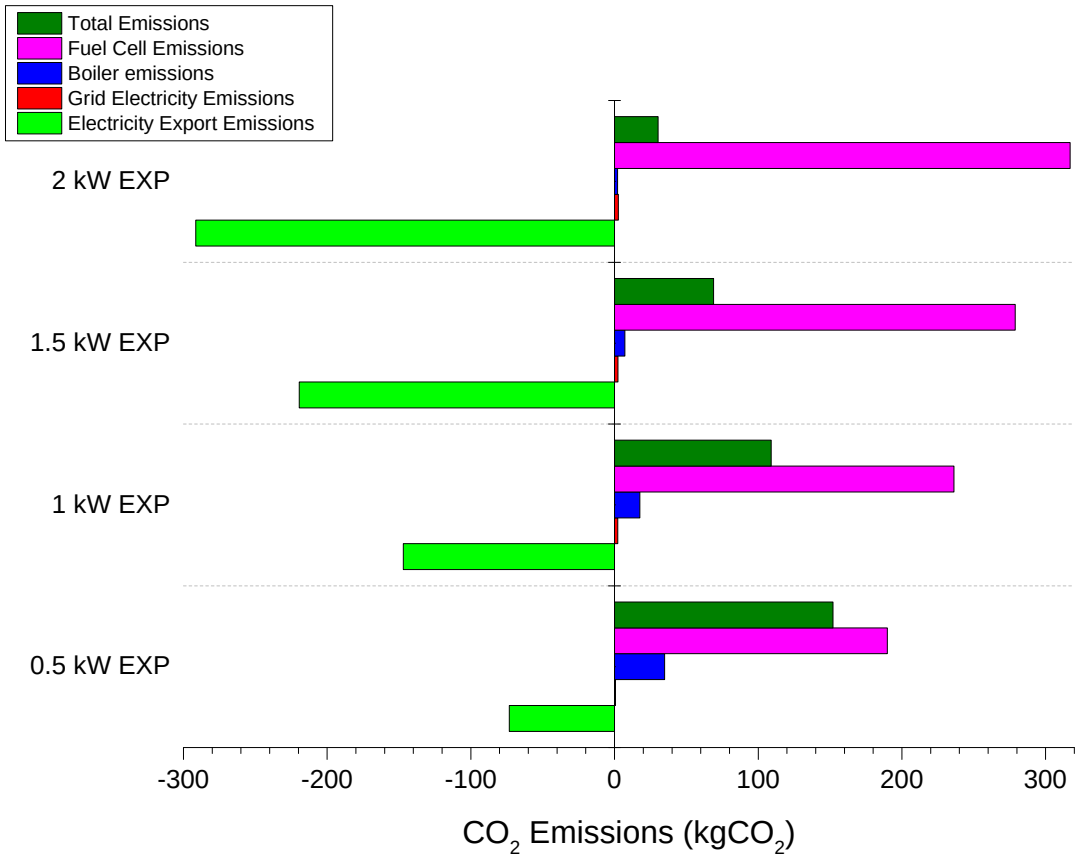

Figure 7.5.36: Breakdown of emissions caused by altering the limit of exported electricity to the grid for case 5. Emissions reduce as the limit increases

7.5.3.2 Case 6

The case that incorporates a TST the extreme case of 2 kW exporting limit was looked at as it represented the case with the highest savings. The inclusion of thermal storage in Case 6 gives an approximate 8% reduction of total emissions compared to case 5. For the 2 kW limit on electricity export the emissions reduce from 30.4 kgCO_2 to to 28.0 kgCO_2 with the main system characteristics shown on Table 7.14.

Table 7.14: Overview of system characteristics for case 6

Limit on exported electricity (kW)	**Maximum Boiler Load Heating (kW)**	**Maximum Boiler Load DHW (kW)**	**Maximum FC Electrical Capacity (kW)**	**TST Volume** (m^3)	CO_2 **emissions** (kgCO_2)
2.0	0.8	0.2	4.2	0.343	28.0

The fact that the fuel cell's increased electrical and heat capacity is used directly in the dwelling, has the effect of low heat input from the fuel cell to the storage tank by the system. In addition the average utilisation factor of hydrogen reaches 0.74 and the voltage 0.73 V, values that promote electricity generation. The input to the TST occurs primarily in the summer months when space heating demand is low. Figure 7.5.37 shows the heat input and output of the TST for Case 6. It demonstrates that the initial heat of the TST which is caused by an assumed initial temperature delivers heat to the dwelling in the first steps, then in the summer hours there is a charging period which is then followed by additional heat delivery to the system.

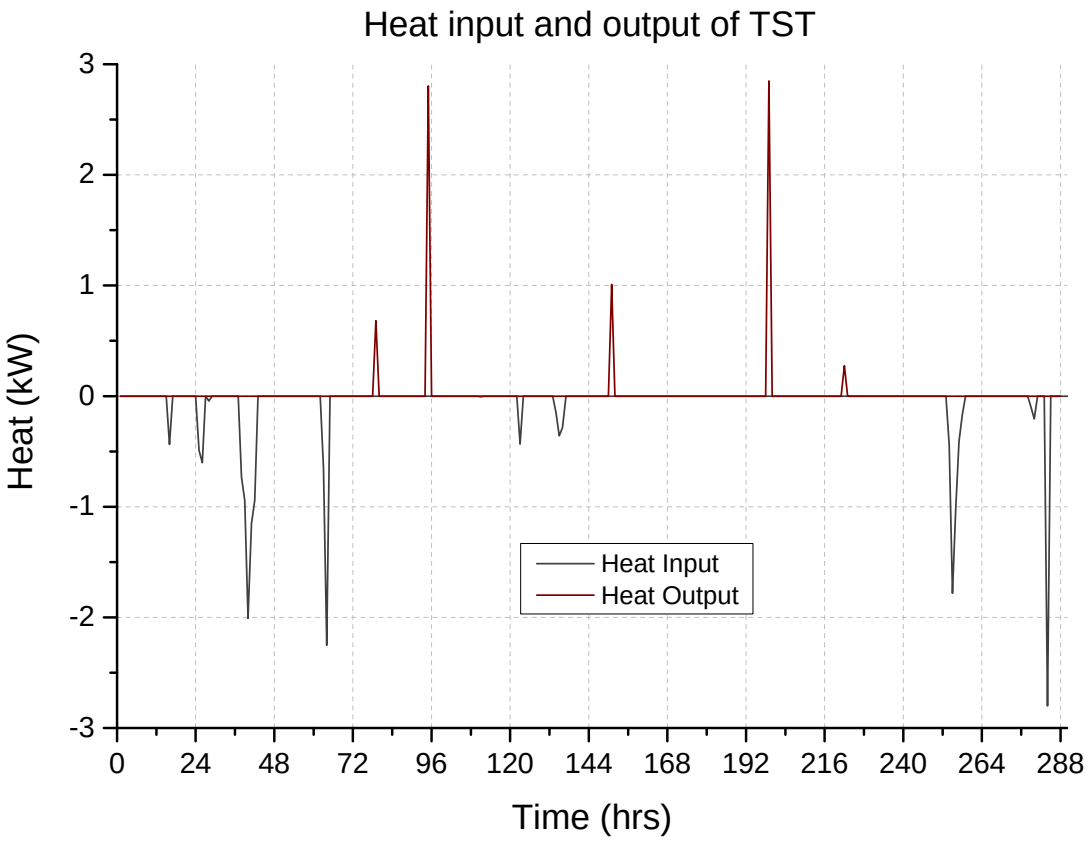

Figure 7.5.37: Graph representing the heat input and output of the TST for Case 6.

7.5.4 House B -Typical UK Dwelling

7.5.4.1 Case 7

Simple changes on the model allow for different data to be used as input. In this case the data generated and presented in section 5.2.2 for a typical UK dwelling, have been used to identify the design of a fuel cell micro-CHP in a dwelling with higher space heating demand than before. In terms of modelling changes, the bounds of variables that represent heat delivery to the space heating circuit had to be adjusted to allow for the increase in heating demand. In this case the design includes a TST as an option; it has been established from the previous examples that it allows the fuel cell to operate longer and adds flexibility to the system. The analysis presented here is made for the case of a radiator heating system.

Table 7.15 shows the annual contribution of each heating source to satisfying demand. The two fuel cell heat exchangers cover almost 10% of space heating and 57% of DHW demand and at the same time the majority of the electricity demand (99.3%). The optimum sizing of the fuel cell is in 2.2 kWe and of the gas boiler 32.8 kW. It can be seen from the table below that the fuel cell is mainly providing heat to the DHW circuit; this could be happening for two reasons; firstly the space heating demand can go as high as 44 kW, a figure that the fuel cell can cover only a small part of and secondly there is a fluctuation from timestep to timestep that can reach 19 kW (in cases when heating is turned on for the first time in the morning). Therefore, the fuel cell is mainly used in the DHW circuit which peaks at around 3 kW and has smaller variations. The total emissions reduction from the reference building reaches 20% at 456 $kgCO_2$. This reduction is lower than the fuel cell micro-CHP designs of the Part L building for all the non-exporting electricity case studies confirming some of the findings of model 1 and of the literature review for the suitability of fuel cells in dwellings with low heat-to-power demand ratio.

Table 7.15: Annual heat contribution from each source for case 7

Source	**Space Heating (%)**	**DHW(%)**
FC Cooling Circuit	4	35
Afterburner	6	22
Gas Boiler	8	39
TST	1	4

The contribution of each source to heating and DHW on an annual basis can be seen in Figures 7.5.38 and 7.5.39 respectively.

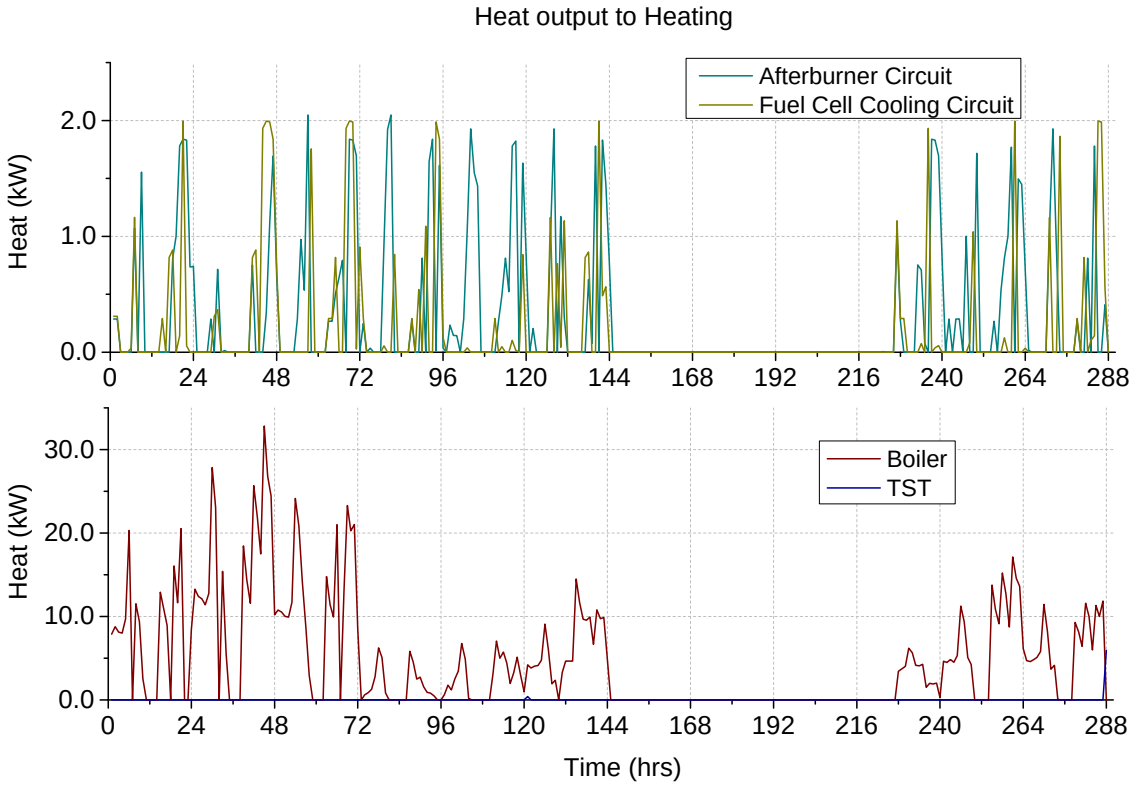

Figure 7.5.38: Graph representing the heat output of each plant delivered to the space heating circuit on an annual basis for Case 7. The graph shows the output of the fuel cell is supplementary to the gas boiler which is sized to cover most heat demand.

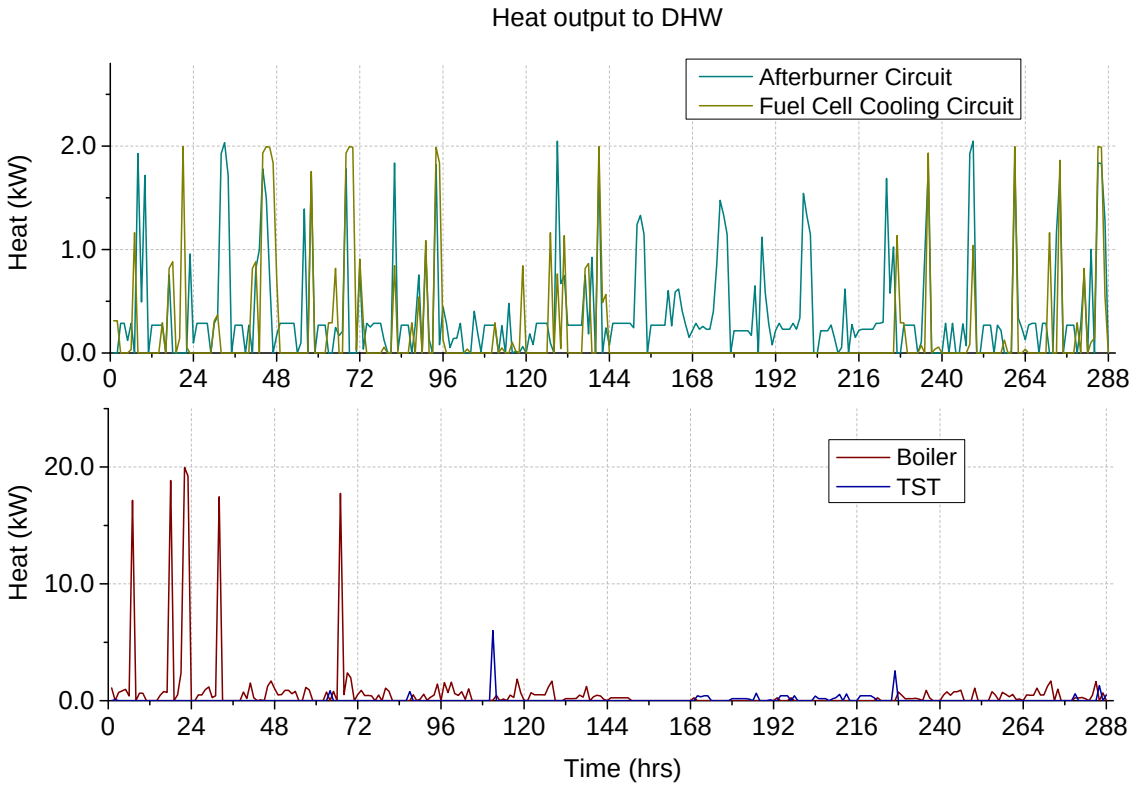

Figure 7.5.39: Graph representing the heat output of each plant delivered to the DHW on an annual basis for Case 7.

The volume of the TST is 110 L and the annual variation of TST temperature can be seen in Figure 7.5.40.

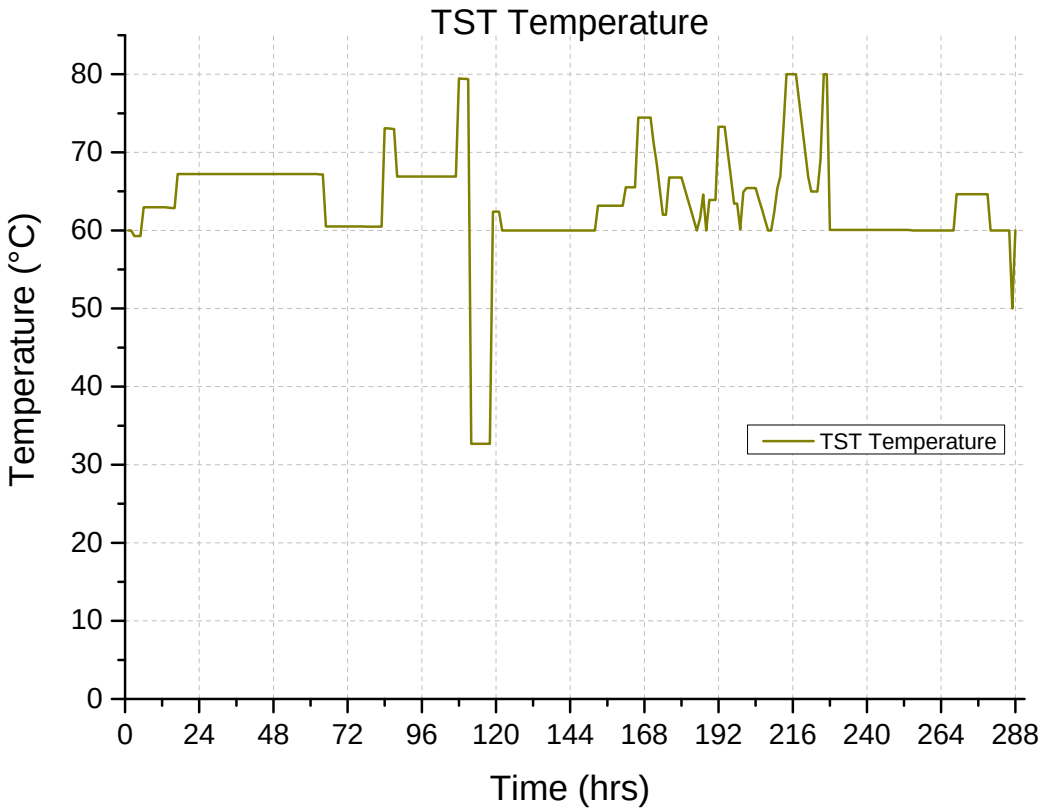

Figure 7.5.40: Graph representing the variation of water temperature in the TST for Case 7

7.6 Discussion and Critical Analysis

In this chapter a MINLP model has been presented for optimising the design of a integrated system comprised of a PEMFC based micro-CHP and a dwelling's heating system. The model identifies optimal ways of utilising available heat from the fuel cell's different heat exchangers at varying temperatures. It designs the pipe network that delivers heat to the dwelling to satisfy heat demand calculating mass flow rates and pipe temperatures. It is a tool that can be used with little alterations in many case studies for many buildings and technologies.

Decisions on variable constraints and assumptions have been made to construct the model and these affect the results in many ways. For instance, the upper bound of the fuel cell electrical capacity was set at 5 kW and although most products for

domestic micro-generation applications are sized at smaller capacity, this allows the model to provide unconstrained results for this variable. This is true for case 4 where a higher capacity than most cases 3.6 kW fuel cell has been selected. Similarly, the method for modelling the TST tank also determines how much it is being used. The variation of Case 2 that was run with a different modelling approach presents a system that relies more on the boiler and uses less the TST. Also, the constraint imposed on the minimum modulation of the gas boiler defines the system operation as it was shown in 7.5.2.2.

The concept of using data from BIM software as input of the models provides benefits compared to other studies which don't use building data at all [90] or use assumed figures for energy demand per season [13]. The use of simulated data of two extremes in terms of energy demand provides a defined basis for understanding the results.

The choice of objective function defines the results of the model. In this case the results obtained minimise CO_2, while many researchers have selected to minimise cost. In terms of system sizing the optimum electrical capacity of the fuel cell is generally higher than most studies in literature and that can be considered an effect of the choice of the objective function. Hawkes et al. calculated an optimum fuel cell capacity between 0.9 kW and 1.3 kW by using cost as the objective function [73]. In terms of system operation and energy outputs, Napoli et al. performed both energy and economic analysis for fuel cell micro-CHP systems and found out that following the electrical demand profile is preferable in terms of energy and cost, as it increases the independence of the systems from the grid [93]. This is something that is demonstrated here as well as for most configurations examined, the fuel cell operation is electricity led with the majority of electricity (above 90% for all cases) covered by the fuel cell. The electrical led mode is easier to be followed by the fuel cell compared to the thermal because of its lower primary energy consumption. The thermal load profile is generally higher compared to the fuel cell capacity as also discussed by [93]. However case 4 which is a dwelling heated by radiators showed that a fuel cell sized higher compared to all other (non-exporting electricity) case studies can satisfy a big portion of the space heating demand. Generally for all configurations the fuel cell micro-CHP has the priority in operation and all the other systems around it run supportively. The UK Good Practice Guide 388 Combined heat and power for buildings suggests that regardless of the connection method, the CHP should operate as the lead boiler in order to maximise its operating hours. [1]. This is something shown in the results especially for the systems with TST which extend the fuel cell's operating hours.

The comparison between the system design for slower heating systems such as UFH

and for systems with radiators suggests that the fuel cell system can handle easier the smooth demand pattern of the UFH system and covers a higher percentage of the demand. This is because of the ramp up rate constraints of the fuel cell and of the amount of heat demand which becomes higher than the fuel cell capacity.

Thermal storage increases predicted CO_2 savings compared to the cases without storage. Its inclusion in the design and the correct sizing reduces the use of gas boiler and grid electricity allowing the fuel cell to operate more hours. When the thermal and electrical demand profiles follow different patterns, the additional heat produced by the fuel cell can be stored in a thermal storage tank. Storage tanks of larger volume are preferred on low temperature UFH systems while smaller tanks that be charged and achieve a higher 60-80^{o}C temperature are preferred for radiator systems. Barbieri et al. [18] makes a similar point concluding that the effect that the size of the thermal energy storage has on the system, is not linearly correlated to the power of the fuel cell but it is system specific. Bianchi et al. concludes that "...the analysis of the energy performance shows that CHP units, with an appropriately sized thermal storage system, can cover the overall thermal energy demand with a primary energy saving index ranging from about 15–45%, depending on the CHP technology."[23]. This is true for all case studies with more than 25% emissions reductions from the reference cases. The optimum size of plant however has also space constraints that can influence the decision of inclusion of a fuel cell micro-CHP into a dwelling, aside from any environmental or cost benefits. A bigger plant room than typically required for conventional systems is needed to accommodate the micro-CHP unit, the auxiliary boiler, the TST and all supportive systems.

The utilisation factor of hydrogen and voltage can act as a controlling measure of the fuel cell: when U^{fc} and voltage reduce, less electricity is produced at the fuel cell and more heat can be recovered from the afterburner as more hydrogen will be combusted. In the summer when less heat is required than the winter period, the utilisation factor takes values closer to its higher bound to maintain a high electricity output and to the reduce heat output.

In cases of high electricity demand covered by the fuel cell micro-CHP, there is surplus thermal energy which can be recovered in the TST. This generates the potential to increase the efficiency of the system as boiler use will be reduced. The exporting electricity case studies show that the electricity exported to the grid has a high impact on the results, both in terms of outputs and sizing of plant, in allexporting limits. This can be justified by the effect of exporting electricity on the objective function which is significant.

Barbieri [19] in a study that examined various micro-CHP technologies concluded

that the suitability of a micro-CHP technology in a dwelling increases when the power to heat ratio of the unit fits the power to heat ratio of the demand. This point is confirmed in this study as the case study that presented the typical UK dwelling appears to have lower reduction in emissions compared to the case studies for House A. The influence of the energy efficiency of the house on system performance has been studied by Gandiglio et al. [68]. In their study, in a high efficiency building, the PEMFC stack cogeneration heat can satisfy the thermal load required for the household. On the contrary PEMFC stacks on lower class buildings are able to provide only 20% of the required thermal power. Similar findings occur in case 7 on a typical UK dwelling where the fuel cell stack is only able to provide a 10% of the space heating demand.

The minimum modulation limit of plant has been found to affect the total system operation and emissions. Different boiler manufacturers produce models with different characteristics and a boiler that has a low modulation limit can increase predicted CO_2 savings by being able to generate the exact amount of heat required in an instance.

The higher heating value has been used for this model to represent the heat generated from combustion of methane in the case of the gas boiler and hydrogen in the case of the fuel cell micro-CHP afterburner. However this assumption is not accurate for all timesteps as it depends on the system return temperature. According to the micro-CHP accelerator report by Carbon Trust "a condensing boiler will only operate in condensing mode with a water return temperature of 57ºC or below and needs this to fall nearer to 50ºC for significant condensation" [32]. For the majority of the cases examined the average return temperature of the system is below 60 °C, so both systems will have a good enough representation of the extra energy from condensing the generated exhaust gases vapour.

Stack degradation which occurs for a fuel cell at a rate of 1–2 μV·h can increase with load cycling, start–stop cycles, low humidity at the stack, temperatures above 90 °C and lack of fuel in the anode [41]. In all cases presented here, the fuel cell operates at all times, generating the majority of electricity, so there are no start-stop cycles and no fuel starvation of the stack. The summer heat demand for DHW is the reason these problems are avoided as the fuel cell micro-CHP heat can be used for hot water generation.

The extra level of detail compared to other similar studies that becomes available as the model's output is the temperature and flow rates at the heat exchangers of the fuel cell micro-CHP system. This allows manufacturers and designers to size the micro-CHP heat exchangers. Also with the available information on temperature and flow

rates, the heating and DHW network pipework can be sized and an approximation of the circulation pump's capacity can be obtained. This information will help building services designers choose the finalised pipework circuits. These circuits may include compensated heating circuits: The decision to include a three port valve in the heating circuit after the main heating header is something that can be determined because the exact variation of flow temperature is known.

The fuel cell stack temperature defines the cooling water temperature which will be used in the dwelling. In the few studies in literature that the heating system temperature constraints are taken into account, the stack and exhaust temperatures are assumed to be constant at a certain level. Gandiglio et al. have assumed a stack temperature and afterburner exhaust of 62 °C and 120 °C respectively [68]. The model in this thesis uses an optimisation framework and allows a varying temperature at the cooling and afterburner exhaust circuits obtained at the results. The varying flow rate and temperature at the heating and DHW circuits define the amount of heat that can be captured.

The novelty of this model is that it considers the plant and house as one and optimises the whole system designing plant and heating pipework. The inclusion of temperature and flow rates for the different process streams within the fuel cell micro-CHP and the dwelling's space heating and DHW circuits provide a design solution.

7.7 Limitations of the study

An element that the model lacks is the consideration of the policy drivers and subsequent cost reductions behind the commercialisation of the fuel cell micro-CHP. The feed-in-tarrifs and the impact of different support schemes can contribute on improving the cost of micro-CHP units. These drivers can be integrated in the model by introducing a cost function as the objective function.

Another limitation of this study is related to the temporal precision of the model which is in hourly timesteps. The minute by minute variability of power and heat demand cannot be captured in hourly data, therefore the results carry the assumption of a constant load within this hourly timestep. The peaks in energy demand that occur usually for a short amount of time are averaged in the 1-hour period. A model based on a 5-minute timestep run for a few hours would capture the variations in electricity and heat demand that occur in this shorter period. The fuel cell micro-CHP and all plant would have to respond to these demands and that could uncover their limitations in terms of ramping up or down. In timesteps that e.g. a 50%

increase in the electricity demand occurs that cannot be satisfied by the fuel cell, grid electricity will be used. This element cannot be captured by models using hourly timesteps. A small case study on 5-minute timesteps could be run on selected designs after the entire 288-hour model has been run, as a robustness test. Despite this limitation, the benefit of a yearly dataset is that it can capture the seasonal variation of all demands and deliver a design that can satisfy them.

The same limitations discussed for the TST model presented in Chapter 6 occur here because no heat losses are considered in the TST and in pipework. In addition, the effect of the initial energy levels of the TST in the results was raised as an issue that was addressed in different ways in the model.

7.8 Concluding Remarks

In this Chapter, a MINLP model formulation has been presented for designing a fuel cell micro-CHP in dwellings optimising the resulting CO_2 emissions from the whole dwelling energy system. The model considers the variability of the different heating systems and their temperature constraints while at the same time it utilises different sources of heat from the fuel cell heat exchangers and other plant of the design to match thermal demand.

Chapter 8

Conclusions and Future Directions

The aim of this thesis was to provide tools for designing fuel cell micro-CHP systems for domestic applications. Towards that goal, a number of mathematical models were developed and their results were presented in the previous chapters. In the following section, the main contributions of the thesis are summarised followed by new directions for future work.

8.1 Summary of Contribution

This thesis focused on the optimisation of fuel cell micro-CHP systems design in dwellings. In Chapter 1, some basic background information were presented followed by the aims and objectives of this project. In Chapter 2 the context of the project was presented focusing on the UK energy market, fuel cell design and products, the built environment and finally the design of heating systems.

In Chapter 3, current approaches in the area of fuel cell micro-CHP modelling were highlighted. Most current models of fuel cell micro-CHP in dwellings ignore the building side of the system when evaluating the performance of the system or conducting a techno-economical assessment. An element missing from existing models in literature is related to the temperature constraints of the various heat sources and distribution systems and how these can be integrated into a reliable system that can satisfy the varying energy demand of a dwelling. At the same time as fuel cells do not represent a technology that is established in the micro-generation market, their potential savings in the domestic energy sector are not very well understood yet. Based on the findings of the literature, chapter presented the options of heat recovery in fuel cells. It mentioned the need for a systematic modelling tool for

designing such systems. There is potential for energy savings from understanding and applying the results of optimisation models that consider the various heat exchangers of the fuel cell micro-CHP and the building services of the dwelling. The next chapter presented the modelling process in BIM software that provided energy demand data for a dwelling and also the reference building that all the models can be compared against. In Chapter 6 a MINLP model that optimises CO_2 emissions and gives information on plant and operation, sufficient for an quick evaluation of a fuel micro-CHP design in dwellings was presented. The model's formulation was improved using linear approximation techniques and it was solved for different case studies.

Next, in Chapter 7 a MINLP model was presented that can handle multiple heat sources and demands and provide a design that integrates the temperature and water flow constraints of a dwelling's heating system with the heat streams within the fuel cell processes while optimising the system's CO_2 emissions. Seven case studies that attempt to capture a variety of designs and examples from the building stock were presented while the results were discussed and compared with current literature.

The results for both models confirm that a fuel cell micro-CHP system can reduce CO_2 emissions and satisfy household heat and electricity demand. The predicted emissions reduction compared to the reference building vary from 20% to approximately 32%. Modelling the flow and temperatures in the heat exchangers allows a design based on the selected heating system. The correct design of the fuel cell thermal management system ensures that heat from the fuel cell stack and the fuel processing system can be used effectively.

8.2 Implications for fuel cell micro-CHP system design

The main findings of this thesis in terms of system design and operation can be summarised as follows:

1. The thermal management strategy and the stack temperature of a SOFC based micro-CHPs defines the number of start-up cycles. These cycles should be kept to the minimum to prevent stack degradation. In terms of system design for SOFC fuel cell micro-CHP that would mean that an advanced insulating material should be used to seal the stack.

2. The fuel cell micro-CHP system will be used more and will cover a higher percentage of the demand when combined with an UFH system. The more

irregular demand pattern of a radiator heating system compared to UFH and the ramp up rate constraints of the fuel cell affect the amount of heat that can be recovered from the fuel cell micro-CHP.

3. A better system and heat exchanger design is possible by using the findings of the model in terms of pipework configuration, flow rates and temperature.

4. The inclusion of a thermal storage tank in a design that includes a fuel cell micro-CHP, whether it is a SOFC or a PEMFC, increases the energy availability and results in longer fuel cell operation and higher reductions in CO_2 emissions.

5. The size of the TST is related to the type of heating system chosen. Heating systems with higher temperature demands require water at similar temperatures to be stored in the TST to be able to utilise the heat. Therefore such systems combine with smaller TSTs to make sure the TST temperature can be maintained at a higher level using less energy from the fuel cell micro-CHP.

6. The hydrogen utilisation factor of the fuel cell and the stack voltage can be used to affect the ratio of heat and power generated from the fuel cell micro-CHP depending on heat demand.

7. Auxiliary boiler modulation limit affects the predicted CO_2 emissions of the system and this should be taken into consideration when designing such systems.

8. Systems designed to have the option of exporting electricity to the grid will favour fuel cells of higher capacity to maximise the exported electricity.

9. Fuel cell micro-CHP produces greater CO_2 savings in dwellings with lower heat-to-power demand ratio.

8.3 Recommendations for future work

There are a number of possible future directions related to the modelling of fuel cell micro-CHPs in buildings and in particular to this model.

This optimisation framework can be expanded to consider additional technologies that can be used in buildings. Hybrid systems such as a fuel micro-CHP coupled with ground source heat pumps can be modelled. Different prime movers such as Stirling engines and internal combustion engines can be added to drive the micro-CHP. As each one of them have different heat to power ratios, the resulting design would be interesting to evaluate.

An economic evaluation can be incorporated in the objective function by just adding an approximate capital cost of each unit and using current operating costs for gas and electricity. The accuracy of this would be improved when more precise costs can be obtained for fuel cell micro-CHP products.

In the thesis all results obtained are produced from mathematical modelling and are tested against current literature. Data from field trials as the ones described earlier could be used as input in the model. In such way the model can be improved based on real data.

Bibliography

[1] Action Energy. *UK Good Practice Guide GPG388: Combined heat and power for buildings*, 2004.

[2] A. Adam, E.S. Fraga, and D. J.L. Brett. Options for residential building services design using fuel cell based micro-CHP and the potential for heat integration. *Applied Energy*, 138:685 – 694, 2015.

[3] A. Adam, E.S. Fraga, and D.J.L. Brett. Modelling and optimisation in terms of CO_2 emissions of a solid oxide fuel cell based micro-CHP system in a four bedroom house in London. *Energy Procedia*, 42:201 – 209, 2013. Mediterranean Green Energy Forum 2013: Proceedings of an International Conference MGEF-13.

[4] P. Aguiar, D.J.L. Brett, and N.P. Brandon. Feasibility study and techno-economic analysis of an SOFC/battery hybrid system for vehicle applications. *Journal of Power Sources*, 171(1):186–197, 2007.

[5] P. Aguiar, D.J.L. Brett, and N.P. Brandon. Solid oxide fuel cell/gas turbine hybrid system analysis for high-altitude long-endurance unmanned aerial vehicles. *International Journal of Hydrogen Energy*, 33(23):7214 – 7223, 2008.

[6] AIMMS. *AIMMS 4.13, AIMMS B.V., Haarlem, The Netherlands, 2015; software available at http://www.aimms.com/.*

[7] S.M.C. Ang, D.J.L. Brett, and E.S. Fraga. A model for the multi-objective optimisation of a polymer electrolyte fuel cell micro-combined heat and power system. In *20th European Symposium om Computer Aided Process Engineering*, 2010.

[8] S.M.C. Ang, D.J.L. Brett, and E.S. Fraga. A multi-objective optimisation model for a general polymer electrolyte membrane fuel cell system. *Journal of Power Sources*, 195:2754 – 2763, 2010.

[9] S.M.C. Ang, D.J.L. Brett, I. Staffell, A.D. Hawkes, E.S. Fraga, N.J. Samsatli, and N.P Brandon. Design of fuel-cell micro-cogeneration systems through modeling and optimization. *Wiley Interdisciplinary Reviews: Energy and Environment*, 1(2):181–193, 2012.

[10] S.M.C. Ang, E.S. Fraga, N.P. Brandon, N.J. Samsatli, and D.J.L. Brett. Fuel cell systems optimisation methods and strategies. *International Journal of Hydrogen Energy*, 36:14678 – 14703, 2011.

[11] H. Apfel, M. Rzepka, H. Tu, and U. Stimming. Thermal start-up behaviour and thermal management of sofc's. *Journal of Power Sources*, 154(2):370 – 378, 2006. Selected papers from the Ninth Ulm Electrochemical Days.

[12] Arki Consulting & Development. *GAMS/SBB Poster accessed from http://www.gams.com/presentations/postersbb.pdf on 19 August 2012.*

[13] A. Arsalis, M. P. Nielsen, and S. K. Kaer. Modeling and off-design performance of a 1 kWe HT-PEMFC-based residential micro-CHP system for Danish single-family households. *Journal of Energy*, 36:993 – 1002, 2011.

[14] A. Arsalis, M. P. Nielsen, and S. K. Kaer. Modeling and optimization of a 1 kWe HT-PEMFC-based micro-CHP residential system. *International Journal of Hydrogen Energy*, 37(3):2470 – 2481, 2012. 2010 {AIChE} Annual Meeting Topical Conference on Hydrogen Production and Storage Special Issue.

[15] A. Arsalis, M. P. Nielsen, and S.K. Kaer. Modeling and parametric study of a 1 kWe HT-PEMFC-based residential micro-CHP system. *International Journal of Hydrogen Energy*, 36:5010 – 5020, 2011.

[16] G. R. Ashari, M. A. Ehyaei, A. Mozafari, F. Atabi, E. Hajidavalloo, and S. Shalbaf. Exergy, economic, and environmental analysis of a PEM fuel cell power system to meet electrical and thermal energy needs of residential buildings. *Journal of Fuel Cell Science and Technology*, 9, 2012.

[17] E. S. Barbieri, F. Melino, and M. Morini. Influence of the thermal energy storage on the profitability of micro-CHP systems for residential building applications. *Journal of Applied Energy*, 97:714–722, 2012.

[18] E. S. Barbieri, F. Melino, and M. Morini. Influence of the thermal energy storage on the profitability of micro-CHP systems for residential building applications. *Applied Energy*, 97(0):714 – 722, 2012. Energy Solutions for a

Sustainable World - Proceedings of the Third International Conference on Applied Energy, May 16-18, 2011 - Perugia, Italy.

[19] E.S. Barbieri, P.R Spina, and M. Venturini. Analysis of innovative micro-CHP systems to meet household energy demands. *Journal of Applied Energy*, 97:723–733, 2012.

[20] L. Barelli, G. Bidini, F. Gallorini, and A. Ottaviano. An energetic exergetic analysis of a residential CHP system based on PEM fuel cell. *Journal of Applied Energy*, 88:4334 – 4342, 2011.

[21] L. Barelli, G. Bidini, F. Gallorini, and A. Ottaviano. Dynamic analysis of PEMFC-based CHP systems for domestic application. *Journal of Applied Energy*, 91:13–28, 2012.

[22] Baxi Innotech. *Baxi Innotech - Gamma 1.0 Status and Outlook. http://www.iphe.net/docs/Events/Japan_3-11/2%20Klose_Baxi_IPHE.pdf accessed on 16 February 2016.*

[23] M. Bianchi, A. De Pascale, and P.R. Spina. Guidelines for residential micro-CHP systems design. *Journal of Applied Energy*, 97:673–685, 2012.

[24] M. Bianchi, A. De Pascale, and F. Melino. Performance analysis of an integrated CHP system with thermal and electric energy storage for residential application. *Applied Energy*, 112(0):928 – 938, 2013.

[25] P. Biddulph, V. Gori, C.A. Elwell, C. Scott, C. Rye, R. Lowe, and T. Oreszczyn. Inferring the thermal resistance and effective thermal mass of a wall using frequent temperature and heat flux measurements. *Energy and Buildings*, 78:10 – 16, 2014.

[26] BRE. *SAP 2009 The Government's Standard Assessment Procedure for Energy Rating of Dwellings*, 2009.

[27] BRE. *SAP 2012 The Government's Standard Assessment Procedure for Energy Rating of Dwellings 2012 Edition*, 2012.

[28] D.J.L. Brett, A. Atkinson, D. Cumming, E. Ramírez-Cabrera, R. Rudkindkin, and N.P. Brandon. Methanol as a direct fuel in intermediate temperature solid oxide fuel cells with copper based anodes. *Chemical Engineering Science*, 60(21):5649 – 5662, 2005.

[29] A. Brooke, D. Kendrick, A. Meeraus, and R. Raman. *GAMS - A User's Guide. GAMS Development Corporation.* 2008.

[30] BSRIA. *BSRIA Rules of thumb - guidelines for building services BG 9/2011 by Glenn Hawkins*, 5th edition.

[31] Buffer-Tank.co.uk. Buffer-Tank.co.uk. Available from: http://buffer-tank.co.uk/ accessed on 16 September 2012.

[32] Carbon Trust. *Micro-CHP Accelarator - Final Report*, 2011.

[33] A. Campos Celador, M. Odriozola, and J.M. Sala. Implications of the modelling of stratified hot water storage tanks in the simulation of {CHP} plants. *Energy Conversion and Management*, 52(8-9):3018 – 3026, 2011.

[34] Ceramic Fuel Cells. BlueGen Unit. Available from: http://www.bluegen.de/de/start/ accessed on 5 January 2016.

[35] Ceramic Fuel Cells. *Ceramic Fuel Cells Media Release.*, 2010. Available from http://www.cfcl.com.au/archive/ accessed on 10 October 2012.

[36] Chartered Institution of Building Services Engineers. *CIBSE Guide B1: Heating*, 2002.

[37] Chartered Institution of Building Services Engineers. *CIBSE Guide A: Environemental Design*, 2006.

[38] Chartered Institution of Building Services Engineers. *CIBSE AM14: Non-domestic hot water heating systems*, 2010.

[39] Copper Development AssociationI. *Copper in Domestic Heating Systems : TN39*, 1988.

[40] Crest Nicholson. *Crest Nicholson Press Release 02.07.2012 available at https://www.crestnicholson.com/news/corporate/2012/crest-nicholson-leads-the-industry-by-deploying-the-uks-first-fuel-cell-in-a-new-build-home accessed on 15 February 2014.*

[41] F. A. de Bruijn, V. A. T. Dam, and G. J. M. Janssen. Review: Durability and degradation issues of pem fuel cell components. *Fuel Cells*, 8(1):3–22, 2008.

[42] Department for Communities and Local Government. *English Housing Survey Households Annual report on England's households 2012-13*, 2014.

[43] Department of Energy and Climate Change. Department of Energy and Climate Change. Available from: http://www.decc.gov.uk/en/content/cms/statistics/publications/flow/flow.aspx accessed on 20 December 2012.

[44] Department of Energy and Climate Change. Department of Energy and Climate Change. Available from: http://www.decc.gov.uk/en/content/cms/statistics/publications/flow/flow.aspx accessed on 20 December 2014.

[45] Department of Energy and Climate Change. *Digest of United Kingdom Energy Statistics 2011*, 2011.

[46] Department of Energy and Climate Change. *Energy consumption in the United Kingdom*, 2011.

[47] Department of Energy and Climate Change. *Microgeneration Strategy*, 2011.

[48] Department of Energy and Climate Change. *Digest of United Kingdom Energy Statistics 2014*, 2014.

[49] Department of Energy and Climate Change. *Energy consumption in the United Kingdom*, 2014.

[50] Department of Food and Rural Affairs. *Government GHG Conversion Factors for Company Reporting: Methodology Paper for Emission Factors*, 2013.

[51] P.E. Dodds, I. Staffell, A.D. Hawkes, F. Li, P. Grünewald, W. McDowall, and P. Ekins. Hydrogen and fuel cell technologies for heating: A review. *International Journal of Hydrogen Energy*, 40(5):2065 – 2083, 2015.

[52] V. Dorer, R. Weber, and A. Weber. Performance assessment of fuel cell micro-cogeneration systems for residential buildings. *Energy and Buildings*, 37:1132 – 1146, 2005.

[53] T.F. Edgar, D.M. Himmelblau, and L.S. Lasdon. *Optimization of Chemical Processes*. McGraw-Hill Higher Education, tenth edition, 2001.

[54] Ene.field. *Ene.field available at http://enefield.eu/ accessed on 20 March 2016.*

[55] Ene.field. *http://enefield.eu/category/news/reports/ accessed on 25 April 2016.*

[56] Energy Saving Trust. Energy Saving Trust. Available from http://www.energysavingtrust.org.uk/Generating-energy/Choosing-a-renewable-technology/Micro-CHP-micro-combined-heat-and-power accessed on 10 September 2012.

[57] D. Erdemir and N. Altuntop. Improved thermal stratification with obstacles placed inside the vertical mantled hot water tanks. *Applied Thermal Engineering*, 100:20 – 29, 2016.

[58] ESP-R. *ESP-R available at http://www.esru.strath.ac.uk/Programs/ESP-r.htm accessed on 10 March 2016.*

[59] European Comission. *Energy Efficiency Plan 2011*, 2011.

[60] European Parliament. *Directive 2002/91/EC of the European Parliament and of the Council on the Energy Performance of Buildings*, 2002.

[61] European Parliament. *Directive 2003/87/EC of the European Parliament and of the Council of 13 October 2003 establishing a scheme for greenhouse gas emission allowance trading within the Community and amending Council Directive 96/61/EC*, 2002.

[62] European Parliament. *Directive 2004/8/EC of the European Parliament and of the Council on the promotion of cogeneration based on useful heat demand in the internal energy market and amending Directive 92/42/EE*, 2004.

[63] R.M. Felder and R.W. Rousseau. *Elementary Principles of Chemical Processes.* Third edition, 2005.

[64] A. Fragaki and A.N. Andersen. Conditions for aggregation of CHP plants in the UK electricity market and exploration of plant size. *Applied Energy*, 88(11):3930 – 3940, 2011.

[65] Fuel Cell Europe. Available from: http://www.fuelcelleurope.org/index.php?m=7&sm=44 accessed on 12 September 2012.

[66] Fuel Cell Today. *The Fuel Cell Industry Review 2013*, 2013.

[67] GAMS Development Corp. *GAMS - The Solver Manuals*, 2014.

[68] M. Gandiglio, A. Lanzini, M. Santarelli, and P. Leone. Design and optimization of a proton exchange membrane fuel cell CHP system for residential use. *Energy and Buildings*, 69:381 – 393, 2014.

[69] P. Ghadimi, S. Kara, and B. Kornfeld. The optimal selection of on-site CHP systems through integrated sizing and operational strategy. *Applied Energy*, 126(0):38 – 46, 2014.

[70] G. Gigliucci, L. Petruzzi, E. Cerelli, A. Garzisi, and A. La Mendola. Demonstration of a residential CHP system based on PEM fuel cells. *Journal of Power Sources*, 131(1-2):62 – 68, 2004.

[71] A. Hawkes and M. Leach. Impacts of temporal precision in optimisation modelling of micro-combined heat and power. *Energy*, 30(10):1759 – 1779, 2005.

[72] A. Hawkes, I. Staffell, D. Brett, and N.P. Brandon. Fuel cells for micro-combined heat and power generation. *Energy and Environmental Science*, 2:729–744, 2009.

[73] A.D. Hawkes, P. Aguiar, B. Croxford, M.A. Leach, C.S. Adjiman, and N.P. Brandon. Solid oxide fuel cell micro combined heat and power system operating strategy: Options for provision of residential space and water heating. *Journal of Power Sources*, 164:260 – 271, 2007.

[74] A.D. Hawkes, P. Aguiar, C.A. Hernandez-Aramburo, M.A. Leach, N.P. Brandon, T.C. Green, and C.S. Adjiman. Techno-economic modelling of a solid oxide fuel cell stack for micro combined heat and power. *Journal of Power Sources*, 156:321 – 333, 2006.

[75] A.D. Hawkes, D.J.L. Brett, and N.P. Brandon. Fuel cell micro-CHP techno-economics: Part 1 model concept and formulation. *International Journal of Hydrogen Energy*, 34:9545 – 9557, 2009.

[76] A.D. Hawkes, D.J.L. Brett, and N.P. Brandon. Fuel cell micro-CHP techno-economics: Part 2 model application to consider the economic and environmental impact of stack degradation. *International Journal of Hydrogen Energy*, 34:9558 – 9569, 2009.

[77] A.D. Hawkes and M.A. Leach. Cost-effective operating strategy for residential micro-combined heat and power. *Energy*, 32:711 – 723, 2007.

[78] US Environemntal Protection Agency Combined Heat and Power Partnership. *Catalog of CHP Technologies.* 2015.

[79] Heating and Ventilating Contractors Association (HVCA). *Domestic Central Heating Installation Specification*, 2004.

[80] A. Hesaraki, A. Ploskic, and S. Holmberg. Integrating low-temperature heating systems into energy efficient buildings. *Energy Procedia*, 78:3043 – 3048, 2015. 6th International Building Physics Conference, {IBPC} 2015.

[81] HM Government. *Building Regulations 2000, Conservation of Fuel and Power in new dwellings, 2010 Edition*, 2010.

[82] HM Government. *Climate Change Act 2008*, 2010.

[83] HM Government. *Domestic Building Services Compliance Guide 2010 Edition*, 2010.

[84] K.G.T. Hollands and M.F. Lightstone. A review of low-flow, stratified-tank solar water heating systems. *Solar Energy*, 43(2):97 – 105, 1989.

[85] IES. *Integrated Environmental Solutions. Apache View User Guide. Available from http://www.iesve.com/downloads/help/Thermal/ApacheView.pdf accessed on 15 February 2016.*

[86] IES. *Integrated Environmental Solutions. APlocate: Location and Weather User Guide Available from http://www.iesve.com/downloads/help/ve2014/Thermal/APLocate.pdf accessed on 15 February 2016.*

[87] IES. *Integrated Environmental Solutions http://www.iesve.com/ accessed on 01 January 2016.*

[88] R.M.H. Khorasany, A.S. Alavijeh, E. Kjeang, G.G. Wang, and R.K.N.D. Rajapakse. Mechanical degradation of fuel cell membranes under fatigue fracture tests. *Journal of Power Sources*, 274:1208 – 1216, 2015.

[89] J. Larminie and A. Dicks. *Fuel Cell Systems Explained.* Wiley, second edition, 2003.

[90] V. Liso, A.C. Olesen, M.P Nielsen, and S.K. Kær. Performance comparison between partial oxidation and methane steam reforming processes for solid oxide fuel cell (SOFC) micro combined heat and power (CHP) system. *Energy*, 36(7):4216 – 4226, 2011.

[91] Mathworks. *MATLAB and Statistics Toolbox Release 2012b, The MathWorks, Inc., Natick, Massachusetts, United States.*

[92] M.R., S.M.T. Bathaee, and M.A. Golkar. Dynamic modeling and nonlinear control of fuel cell vehicles with different hybrid power sources. *International Journal of Hydrogen Energy*, 2016.

[93] R. Napoli, M. Gandiglio, A. Lanzini, and M. Santarelli. Techno-economic analysis of PEMFC and SOFC micro-CHP fuel cell systems for the residential sector. *Energy and Buildings*, 103:131 – 146, 2015.

[94] U.S. Department of Energy. *Fuel Cell Handbook.* 2004.

[95] S.D. Oh, K.Y. Kim, S.B. Oh, and H.Y. Kwak. Optimal operation of a 1-kW PEMFC-based CHP system for residential applications. *Applied Energy*, 95:93 – 101, 2012.

[96] D.R. Oughton and S.L. Hodkinson. *Faber and Kell's Heating and Air-Conditioning of Buildings*. Elsevier Ltd, tenth edition, 2008.

[97] F. Palazzi, N. Autissier, F.M.A. Marechal, and D. Favrat. A methodology for thermo-economic modeling and optimization of solid oxide fuel cell systems. *Applied Thermal Engineering*, 27:2703 – 2712, 2007.

[98] A. Pascale, C. Ferrari, F. Melino, M. Morini, and M. Pinelli. Integration between a thermophotovoltaic generator and an organic rankine cycle. *Applied Energy*, 97(0):695 – 703, 2012. Energy Solutions for a Sustainable World - Proceedings of the Third International Conference on Applied Energy, May 16-18, 2011 - Perugia, Italy.

[99] S. Pellegrino, A. Lanzini, and P. Leone. Techno-economic and policy requirements for the market-entry of the fuel cell micro-chp system in the residential sector. *Applied Energy*, 143:370 – 382, 2015.

[100] K. Qiu and A.C.S. Hayden. Integrated thermoelectric and organic rankine cycles for micro-CHP systems. *Applied Energy*, 97(0):667 – 672, 2012. Energy Solutions for a Sustainable World - Proceedings of the Third International Conference on Applied Energy, May 16-18, 2011 - Perugia, Italy.

[101] K. Qiu and A.C.S. Hayden. Implementation of a TPV integrated boiler for micro-CHP in residential buildings. *Applied Energy*, 134(0):143 – 149, 2014.

[102] G.L. Race. *How to design a heating systen*. Chartered Institution of Building Services Engineers. CIBSE Knowledge Series.

[103] S.M. Rakhtala and E. Shafiee Roudbari. Fuzzy pid control of a stand-alone system based on pem fuel cell. *International Journal of Electrical Power and Energy Systems*, 78:576 – 590, 2016.

[104] N. V. Sahinidis. *BARON 14.3.1: Global Optimization of Mixed-Integer Nonlinear Programs,* User's Manual, 2014.

[105] A.J Santis-Alvarez, M. Nabavi, N. Hild, D. Poulikakos, and W.J. Stark. A fast hybrid start-up process for thermally self-sustained catalyticn-butane reforming in micro-sofc power plants. *Energy Environ. Sci.*, 4:3041–3050, 2011.

[106] O.A. Shaneb and P.C. Taylor. An evaluation of integrated fuel cell and energy storage systems for residential applications. In *Upec:2009 44th International Universities Power Engineering Conference*, 2009.

[107] S.C Singhal. Solid oxide fuel cells for stationary, mobile, and military applications. *Solid State Ionics*, pages 405 – 410, 2002.

[108] S.C. Singhal and K. Kendall. *High Temperature Solid Oxide Fuel Cells: Fundamentals, Design and Applications*. Els, 2003.

[109] I. Staffell, D. Brett, N. Brandon, and A. Hawkes. A review of domestic heat pumps. *Energy Environ. Sci.*, 5:9291–9306, 2012.

[110] I. Staffell and R. Green. The cost of domestic fuel cell micro-CHP systems, discussion paper. 2012.

[111] I. Staffell, R. Green, and K. Kendall. Cost targets for domestic fuel cell CHP. *Journal of Power Sources*, 181:339 – 349, 2008.

[112] Stelrad Radiators. Stelrad Radiators. Available from: www.stelrad.com accessed on 15 September 2012.

[113] Sulzer Hexis. Galileo 1000N Unit. Available from: http://www.hexis.com/en/galileo-1000-n accessed on 5 January 2016.

[114] G. Taljan, G. Verbic, M. Pantos, M. Sakulin, and L. Fickert. Optimal sizing of biomass-fired organic rankine cycle CHP system with heat storage. *Renewable Energy*, 41:29 – 38, 2012.

[115] K. Tapia-Ahumada, I.J. Pérez-Arriaga, and E.J. Moniz. A methodology for understanding the impacts of large-scale penetration of micro-combined heat and power. *Energy Policy*, 61:496 – 512, 2013.

[116] TAS. *TAS available at http://www.edsl.net/main/Default.aspx accessed on 02 March 2016.*

[117] D. Tempesti, G. Manfrida, and D. Fiaschi. Thermodynamic analysis of two micro-CHP systems operating with geothermal and solar energy. *Applied Energy*, 97:609–617, 2012.

[118] B. Timurkutluk, C. Timurkutluk, M.D. Mat, and Y. Kaplan. A review on cell/stack designs for high performance solid oxide fuel cells. *Renewable and Sustainable Energy Reviews*, 56:1101 – 1121, 2016.

[119] TRNSYS. *TRNSYS available at http://sel.me.wisc.edu/trnsys/faq/faq.htm accessed on 02 March 2016.*

[120] U.S. Department of Energy. *Fuel Cell Technologies Market Report 2014*, 2014.

[121] U.S. Energy Information Administration. *International Energy Outlook 2013*, 2013.

[122] U.S. Environmental Protection Agency, Combined Heat and Power Partnership. *Technology Characterization: Fuel Cells*, 2015.

[123] Viessman. *Low Loss Header installation manual*, 2010.

[124] Wavin, Underfloor Heating Division. Available from: http://thermoboard.wavin.com accessed on 15 September 2012.

[125] H.R. Wilk. Integrated fuel cell energy systems for building applications 48 months of experience with SOFC and PEMFC systems. Technical report, Energie AG OÖ, 2005.

[126] C.H. Woo and J.B. Benziger. PEM fuel cell current regulation by fuel feed control. *Chemical Engineering Science*, 62(4):957 – 968, 2007.

[127] Worcester-Bosch. *Worcester-Bosch Product Manual. https://www.worcester-bosch.co.uk/support/manuals-and-brochures accessed on 15 March 2016.*

[128] X. Yu, M.R. Starke, L.M. Tolbert, and B. Ozpineci. Fuel cell power conditioning for electric power applications: a summary. *Electric Power Applications, IET*, 1(5):643–656, Sept 2007.

[129] F. Zenith. Reducing fuel cell degradation in micro combined heat and power systems. *IFAC-PapersOnLine*, 48(8):445 – 450, 2015.

[130] G. Zhang and S.G. Kandlikar. A critical review of cooling techniques in proton exchange membrane fuel cell stacks. *International Journal of Hydrogen Energy*, 37(3):2412 – 2429, 2012.

[131] L. Zhang, J. Jiang, H. Cheng, Z. Deng, and X. Li. Control strategy for power management, efficiency-optimization and operating-safety of a 5-kw solid oxide fuel cell system. *Electrochimica Acta*, 177:237 – 249, 2015. International Conference on Electrochemical Energy Science and Technology (EEST2014).

List of Communications

1. A. Adam, E.S. Fraga, and D.J.L. Brett. Modelling and optimisation in terms of CO_2 emissions of a solid oxide fuel cell based micro-CHP system in a four bedroom house in London. Energy Procedia, 42:201 209, 2013. Mediterranean Green Energy Forum 2013: Proceedings of an International Conference MGEF-13.

2. A. Adam, E.S. Fraga, and D.J.L. Brett. Modelling and optimisation of a solid oxide fuel cell based micro-CHP system in a four bedroom house in London in present and future energy scenarios. FutureBuild 2013 proceedings. University of Bath.

3. A. Adam, E.S. Fraga, and D. J.L. Brett. Options for residential building services design using fuel cell based micro-CHP and the potential for heat integration. Applied Energy, 138:685-694, 2015.

Appendix A

Reference House Architectural Drawings

Architectural drawings were produced for the reference building. These are presented in this section.

SCALE
1:50@A3

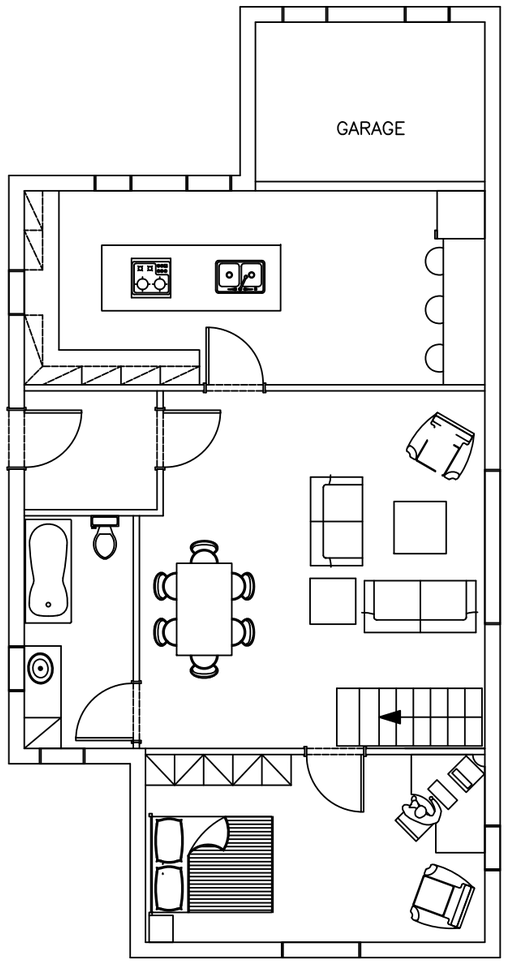

GROUND FLOOR

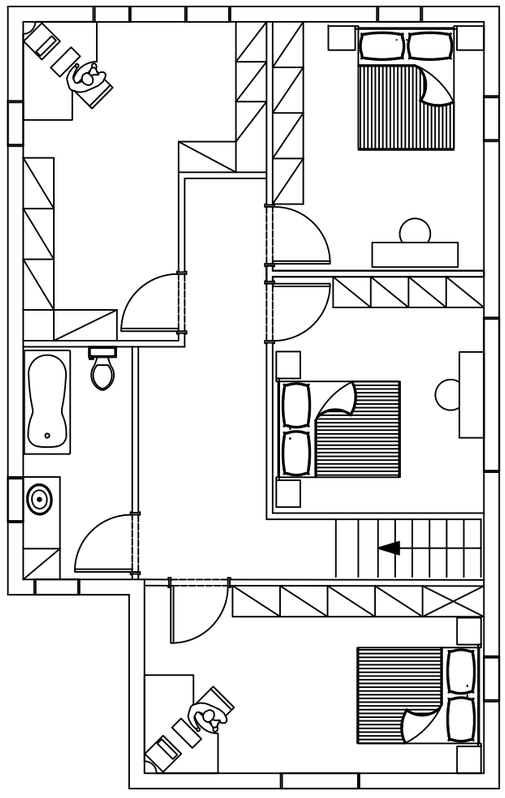

FIRST FLOOR

PRODUCED BY AN AUTODESK EDUCATIONAL PRODUCT

PRODUCED BY AN AUTODESK EDUCATIONAL PRODUCT

PRODUCED BY AN AUTODESK EDUCATIONAL PRODUCT